Rheological Properties of Tailor-Made Metallocene and Ziegler-Natta Based Controlled Rheology Polypropylenes

by

Shouliang Nie

A thesis

presented to the University of Waterloo

in fulfillment of the

thesis requirement for the degree of

Master of Applied Science

in

Chemical Engineering

Waterloo, Ontario, Canada, 2015

Author's declaration:

I hereby declare that I am the sole author of this thesis. This is a true copy of the thesis, including any required final revisions, as accepted by my examiners.

I understand that my thesis may be made electronically available to the public.

Shouliang Nie

ABSTRACT

Controlled rheology polypropylenes (CRPP) have been produced industrially by peroxide induced degradation in post-polymerization reactive extrusion (REX) operations. This has been well developed for commodity Ziegler-Natta based polypropylene (ZN-PP) resins, resulting in materials with controlled rheological properties with accompanying narrower molecular weight distribution (MWD). In this work, this methodology has been tested on both metallocene based polypropylenes (mPP), which have a narrow MWD initially, and ZN-PP resins at various peroxide concentrations. The differences in their degradation process as well as the properties of the resulting CRPPs were compared.

A previously developed kinetic model was used to simulate the degradation process at various peroxide concentrations. Modelling results for a mPP and a ZN-PP with similar molecular weight indicated that the MWDs of both materials approached "most probable distribution" (PDI=2) as expected, due to the random nature of the scission reactions involved. However, unlike the ZN-PP resin for which the polydispersity was sharply decreased, the MWDs of CRPPs from mPP was almost unchanged with a PDI of about 2. This indicated that polypropylenes from the two types could be used to produce CRPPs with specified/targeted MW and MWD patterns and therefore special properties.

Two groups of tailor-made CRPPs were produced using mPP and ZN-PP. One group had similar MW but different MWDs and another group had similar melt flow rate (MFR). In particular, the zero-shear viscosity and rheological polydispersity, which were obtained through oscillatory

shear rheometry, were successfully applied to monitor the MW level and the MWD of the products.

The two series of materials were also submitted to extrusion tests using a single screw extruder equipped with a capillary die. Based on the extrusion results, with respect to the CRPPs of similar MW, materials of broader MWD, thus stronger shear-thinning at high shear rate, resulted in slower increase of extrusion pressure with apparent shear rate. The shear rate of the onset of extrudate melt-fracture, which coincided with previous studies of polypropylenes extrusion, was higher for broader MWD material. With respect to the CRPPs with similar MFR, a metric commonly used for grade inspection in industry, their extrusion behaviours were nearly identical.

ACKNOWLEDGEMENTS

I would like to express my deep and sincere gratitude to my supervisor, Professor Costas Tzoganakis, for his guidance, insight and encouragement throughout the course of the work. I have indebted a lot to him for his kind teaching with his in-depth knowledge and his concern and support for my life in Canada.

I would like to thank Professors Alexander Penlidis and Neil McManus for patient reading, correcting the manuscript of the thesis to assure the expression in it more accurate. In addition, as the oral defence examiner, their comments and critique are very valuable and inspiring for me.

My gratitude to the dear members in Polymer Processing Lab, Dr. Mo Meysami, Dr. Prashant Mutyala, Tadayoshi Matsumura, Ankita Sakia, Umar Farooq, for their generous assistant in the lab. In particular, I thank Dr. Shuihan Zhu and Dr. Yasaman Amintowlieh for their patient training of the experiments and share their solid research knowledge. Thank my friends for their discussion for my experiment results especially Dr. Hui Wang, Priscilla Lai. Gratitude also extends to the Department of Chemical Engineering, especially Bert Habicher for his excellent precise machining work. Thank Dr. Allen Wang from NOVA Chemicals for the GPC test.

Finally, I thank my girlfriend, my whole family for their unconditional support, encouragement and love.

Dedicated to my grandfather, Xing-Gui Nie.

For his upright, fortitude, wisdom and enlightment.

TABLE OF CONTENTS

LIST OF FIGURES

LIST OF TABLES

NOMENCLATURE

A	collision frequency factor, s^{-1}
a	parameter in equation (6.7), dimensionless
D	orifice diameter of die, mm
E_a	activation energy, J/mol
f	initiator efficiency, dimensionless
G'	storage/elastic modulus, Pa
G"	loss/viscos modulus, Pa
G*	complex modulus, Pa
G_c	crossover modulus, Pa
G_{ref}	reference modulus, Pa
H(λ)	relaxation spectrum function, Pa
[I]	initiator concentration, mol/L
$[I]_0$	initial initiator concentration, mol/L
k	termination constant in equation (4.2), $m^3/(mol \cdot s)$
k_d	peroxide decomposition rate constant, s^{-1}
k_{tc}	combination termination constant, $m^3/(mol \cdot s)$
k_{td}	disproportionation termination constant, $m^3/(mol \cdot s)$
L	length, mm
L/D	length diameter ratio, dimensionless
m_0	molar mass of the monomer, g/mol
M_n	number average molecular weight, g/mol
M_w	weight average molecular weight, g/mol
n	polymer chain length
	or power law index, dimensionless
P	pressure, psi
ΔP	pressure drop, psi
[Pn]	concentration of polymer chain, mol/L
Q	volumetric flow rate, m^3/s

R universal gas constant = 8.314 J/(K·mol)

or radius, mm

T temperature, K if not specify

t time, s

$t_{1/2}$ half-life time, s

Greek letters:

α half entrance angle, degree

$\dot{\gamma}$ shear rate, s^{-1}

$\dot{\gamma}_{app}$ apparent shear rate, s^{-1}

$\dot{\gamma}_{w}$ shear rate at wall, s^{-1}

δ phase angle, degree

η' dynamic viscosity, Pa·s

η* complex viscosity, Pa·s

η_0 zero shear viscosity, Pa·s

η_∞ infinite shear viscosity, Pa·s

η_{app} apparent shear rate, Pa·s

λ relaxation time, s

$\lambda_{1\sim3}$ parameters in equation (4.2), dimensionless

ξ reaction conversion, %

ρ_p density of polymer, kg/m^3

σ shear stress, Pa

σ_w shear stress at die wall, Pa

τ_c critical stress, Pa

τ_{exit} stress at exit, Pa

ω angular frequency, rad/s

Chapter 1

THESIS OUTLINE

1.1 Background

Peroxide-induced controlled degradation of polypropylene (PP) is a technique that has been used industrially during the last four decades as a convenient post-polymerization approach to modify existing commodity polypropylenes to meet various processing requirements. With this treatment, PP resins of controlled rheology (CRPP) can be produced having lower molecular weight (MW) and narrower molecular weight distribution (MWD) through free radical induced scission reactions. The chemical reaction kinetics involved as well as the rheological properties of CRPPs have been systemically studied and presented in several publications. However, these studies are focused on the production of CRPP from Ziegler-Natta type polypropylenes (ZN-PP) which have broad MWDs. Experimentation and modelling studies on the application of this technique on metallocene based polypropylene (mPP) are non-existent in the literature .

As mPP possesses narrower MWD than ZN-PP, the evolution of MWD and rheological properties during controlled degradation should be different and it would be of interest to fully understand this process. In this work, CRPPs are produced from both types of commodity PPs (ZN-PP and mPP) under various peroxide concentrations and their molecular weight characteristics, rheological properties as well as extrusion performance are examined for comparison. In addition, the degradation reactions are modelled using previously developed kinetic models.

1.2 Objectives

The objectives of this work are to:

1) investigate the development of CRPPs from two commercial origins (ZN-PP and mPP) both through experiments and modelling studies.

2) prove that by employing virgin materials of both types, CRPP series with tailor-made properties can be produced (e.g. with same MW but different MWD, or with same melt flow rate (MFR) but different MW and/or MWD) .

3) compare the stability of processing behavior of these tailor-made CRPP materials during extrusion.

1.3 Thesis Outline

Chapter 1:

The background and the initial objectives of this work are overviewed. A brief outline of different chapters is introduced for the readers.

Chapter 2:

A literature review of the studies related to this project is provided with emphasis on the CRPP technology (in particular peroxide-induced CRPP) and melt-fracture characteristics of the extruded CRPP.

Chapter 3:

The peroxide-induced CRPP from a conventional ZN-PP is presented, during which the conditions for CRPP production as well as the rheological characterization methods are established.

Chapter 4:

A kinetic modelling computer program for the CRPP process is developed and the molecular weight evolution process of the CRPPs from ZN-PP and mPP is investigated through numerical simulations.

Chapter 5:

Raw materials are selected from both ZN-PP and mPP origin. Target properties for the CRPPs are set and CRPPs with tailor-made properties are produced and characterized.

Chapter 6:

An extrusion line for the processing study of the tailor-made CRPPs is designed and extrusion experiments are performed. The extrusion behaviors of various CRPPs are assessed in view of their associated rheological characteristics.

Chapter 7:

The results of the entire work are summarized for: a) CRPPs produced from ZN-PP and mPP and b) extrusion performance of CRPPs and their rheological properties. Finally, critique is posed to some shortages of this work and potential future work is proposed based on the results obtained so far.

Chapter 2

LITERATURE REVIEW

2.1 Controlled Rheology Polypropylene (CRPP)

2.1.1 Origin of CRPP technique

Rheological properties of polymer melts are very important as they affect many processing production processes such as extrusion. The rheological or flow properties of polymer melts are dictated by the molecular structure, molecular weight (MW) and molecular weight distribution (MWD) [1]. For many commercial end uses, the rheological characteristics of many C3+ polyolefins, such as Ziegler-Natta polypropylene (ZN-PP) [2-5], are not suitable in high shear rate conditions like extrusion and injection molding processes. This is due to their extremely high MW and/or broad MWD which results from the broad activity of catalytic sites of the catalyst during the polymerization processes. Virgin PP resins are usually produced this way for a very wide range of end use applications.

As the MW and MWD significantly determine the rheological properties and the performance during processing, these characteristics must be controlled. However, the control of MWD of PP in the conventional polymerization is difficult because it requires the addition of chain terminators and chain transfer agents. In addition, these operations decrease the output of the reactor and are not economical [6]. This motivated the development of controlling/improving of rheological properties of polypropylene resins by means of degradation of MW, modification of MWD and/or polymer chain structure in a relatively low cost post-reactor reactive extrusion

(REX) process. This is the so called “Controlled Rheology” or “Controlled Degradation” process. Hence, the polypropylene produced this way with specific rheological properties is called Controlled Rheology Polypropylene (CRPP). The main concepts/requirements for developing this REX process were:

1) some of the strain imposed on the polymer chains during processing would be frozen into the product in high speed processes, and thus the elasticity could be a major factor for PP’s processability.

2) PP’s high MW “tail” was responsible for the high elasticity level.

3) the tail could be reduced/modified by a random chain scission process conducted at high temperature during extrusion.

2.1.2 CRPP production through thermal oxidative degradation

In 1986, Kowalski et al in Exxon Chemical mentioned the term and concept of “Controlled Rheology” in a paper [8, 9], which was also the name of their research project in the past 20 years dating back to 1964-65. After the introduction of a commercial PP, it was found difficult to process it and studies had pointed to the relationships between the processing behavior and the rheological properties of PP in melt. In Kowalski’s study in 1963[10], the melt elasticity of PP was very high and stress decay rate was slow.

In 1971-1975, Staton et al [9, 10, 11] published some patents on chain scission by free radicals generated from oxygen in air at very high extruder barrel temperatures (700-800 °F). This process was used commercially for some years. Unlike the general temperature profile, they fixed the highest temperature zone at the feed end of the extruder. In this area, the air was still

present before the melt was sealed so that radicals could be generated to a maximum extent and easily controlled.

Also, they combined a mixing means for mixing an oxygen-containing gas with PP, a reactor for heating the thermoplastic polymer under shear and a measuring device for detecting the shear stress in the polymer (which relates to MW and MWD), and a feedback device for changing the conditions of the extruder in response to the parameter measured by the rheometer device (see Fig. 2.1). According to this invention, the MW of the PP could be controlled by this controlled scission reaction and resulted in unique rheological properties suitable for certain processing operations. Watson et al [12] also invented an economical and convenient way to control the rheology of C3+ polyolefins by injecting, under pressure, certain critical quantities of oxygen and inert gas, such as air, into the polymer melt during extrusion.

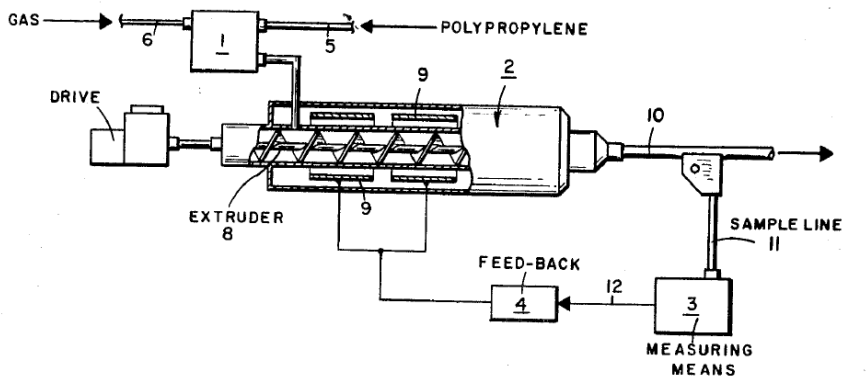

Fig. 2.1 Schematic diagram of a system for the controlled scission of a thermoplastic polymer [9].

The thermal degradation of PP [13] occurs via random scission followed by a radical transfer process. This process does not involve chain branching or cross linking. While in the presence of oxygen, the fundamental mechanism of the thermal-oxidative degradation of PP [14] is:

Initiation:

RH → R• + H

Propagation:

R• + O_2 → ROO•

ROO• + RH → R• + ROOH

ROOH→RO• + •OH

ROOH + RH → RO• +R• + HOH

RH + RO• → ROH + R•

2.1.3 Organic peroxide induced CRPP

Along with the development of REX, it had become known that various chemical reactions and modifications can take place during extrusion in the polymer bulk phase. Numerous techniques of modifying polymers in this process had been invented. These modifications can be accomplished in such a way that significant changes of the polymer composition and/or rheology properties can be effected. After the 1960s, a variety of the chemical reactions and modifications were studied during reactive extrusion and many of them were directed to the grafting of monomers to polymers in this tag-along process. This way, the polymer composition could be changed significantly along the rheology. In 1965, Nowak and Jones [15] invented a new method to graft acrylic or methacrylic acid to polyolefins with organic peroxides employed as initiators.

In 1975, Steinkamp et al [16] invented a process to improve PP rheological properties with a peroxide instead of oxygen as the free radical generator for the polymer melt during the controlled degradation of polypropylene in an extruder (see Fig. 2.2). They compared this with the thermal-oxygen method they invented previously [9, 10, 11]; this method permitted the use of much lower extruder temperatures and high throughputs therefore it was more economical. They found two essential controlling factors in this reactive extrusion operation for significant modifications of polymers. One of these factors was that the reagent or reagents, which are to interact with the polymer, must be thoroughly and intensively mixed with the polymer over a very short interval of time. Thus, a much higher order of magnitude of mixing was required. In order to accomplish this intensive mixing or dispersion, a high shear-thin film was used in the reaction zone. Another aspect was that one or more decompression zones (i.e., reduced pressure zones accompanied by injection orifices or conduits) should be provided at a point where the polymer is in a molten state. This provided efficient reactions when reactants were introduced in the reduced pressure zone under a pressure head. Due to the reduced pressure, the reactants were easily distributed over the total surface area of the polymer melt.

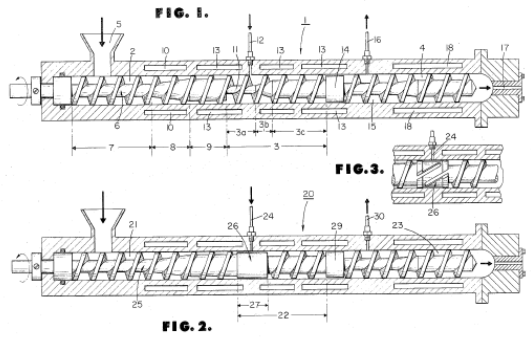

Fig. 2.2 Extrusion design by Stenkamp et al [16] to introduce peroxide during the process.

Later on, some reaction models and simulations of the peroxide initiated degradation of PP melt were proposed and developed. Tzoganakis et al [5, 19] presented a plausible reaction mechanism for the free radical degradation of PP as shown by the following scheme:

Initiation:

$$I \xrightarrow{Kd} 2R\cdot$$

Chain scission (β-scission):

$$P_n + R\cdot \xrightarrow{K_1} P_r\cdot + P_{n-r} + R$$

Transfer:

$$P_n + P_r\cdot \xrightarrow{K_2} P_r + P_s + P_{n-s}\cdot$$

Thermal degradation:

$$P_n \xrightarrow{K_3} P_r\cdot + P_{n-r}\cdot$$

Termination:

$$P_n\cdot + P_r\cdot \xrightarrow{K_4} P_n + P_r$$

During heating in this process, the peroxide decomposes and produces primary radicals which will attack the tertiary hydrogen atoms on the backbone of the polypropylene chains randomly. As a result of the steric hindrance effect of the methyl group [27, 28], the polymer radicals are not stable and the polymer chains will break into one shorter polymeric chain and one polymer radical with a double bond end and a radical end respectively. This reaction is called β-scission.

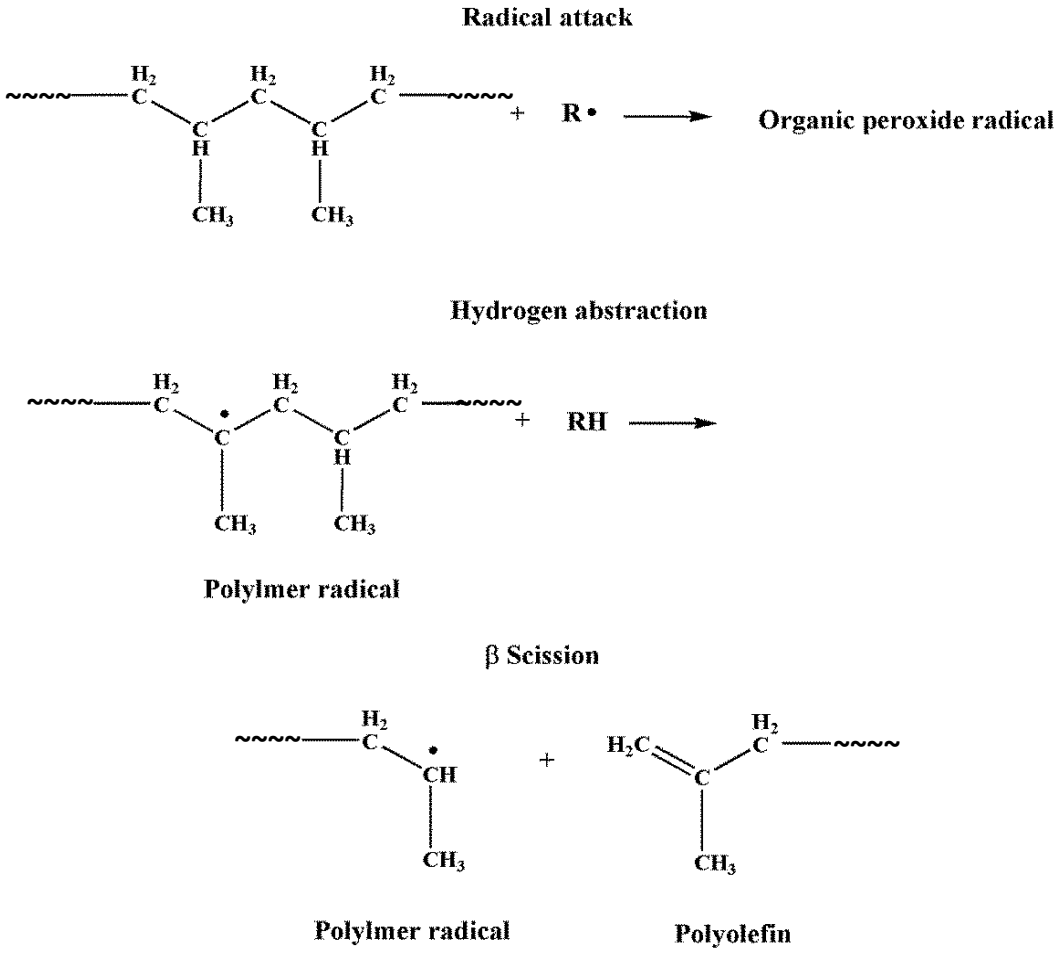

Fig.2.3 Reaction scheme of β-scission of polypropylene [26].

The peroxide used for this process must have a sufficiently high reactivity and low evaporation rate at the extrusion temperature. Furthermore, the peroxide preferably should to not produce odor and color changes in the products [27]. Examples of peroxides typically accepted in industry for this degradation reaction are given below in Table 2.1.

Although the mono- and di-functional peroxides are conventional free radical initiators commonly used for CRPP production, multi-functional peroxides have also been studied. Scorah

et al [33] evaluated a tetra-functional peroxide initiator, polyether tetrakis(t-butylperoxy carbonate), compared with a di-functional one, 2,5-bis(tert-butylperoxy)- 2,5-dimethylhexane, at the same functional group concentration level. The di-functional peroxide seems more effective at reducing molecular weight at higher temperature (230°C) and the tetra-functional one was more effective at the lower temperature (200°C) and the trends were reversed at the high peroxide concentration level. At high processing temperatures and low levels of peroxide concentration, the tetra-functional initiator seemed to lead to chain extension/coupling, but no evidence of architectural change was seen in the CRPP molecules such as branching and cross-linking. Results were explained by considering the competition between chain scission and chain extension brought about by mono-radicals and multi-radicals, respectively, formed from initiator decomposition.

Table 2.1 Industrial peroxides used for CRPP

Chemical Name	Abbreviation
2,5-Dimethyl-2,5-Di-t-butyperoxyhexane	DHBP
2,5-Dimethyl-3-hexin-2,5-di-t-butylperoxide	DYBP
Di-t-butyl peroxide	DTBP
Dicumyl peroxide	DCUP

2.1.4 CRPP induced by other chemicals

Although organic peroxides have dominated as free radical generators for CRPP production, there are other chemicals which can be used to induce degradation of PP. Psarreas et al [37, 38] developed a method to use nitroxide instead of traditional peroxides to produce CRPP. The nitroxide they used was 2, 2, 6, 6-tetramethylpiperidine 1 –oxyl (known as TEMPO, see Fig. 2.4) which was formed from 2, 2, 6, 6-tetramethylpiperidine. As in the case of peroxides, increasing the concentration of nitroxide also induced decreasing of MWs and narrower MWD of the CRPPs. FTIR spectroscopy showed that the nitroxyl radical generator affects PP in the same way the regular peroxide does. Rheological characterization of the architecture of the modified PP confirmed a linear structure.

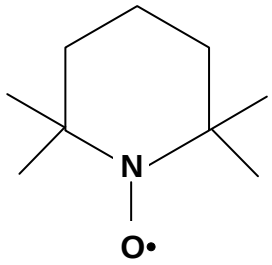

Fig. 2.4 Chemical structure of TEMPO formed from hydroxylamine.

2.1.5 High energy irradiation induced CRPP

Ionizing radiation (such as γ-rays and electron beams) and non-ionizing radiation (like microwaves and ultraviolet waves) have also commonly been used for the degradation of polymers. Black and Lyons [33] and Dole and Schnabel [34] studied the vacuum irradiation of PP. Irradiation of PP melts would increase the occurrence of branching and crosslinking reactions and lead to formation of double bonds.

The elongational viscosity of polymer melts plays an important role in many processing operations like film blowing, blow molding, foam expansion, fiber spinning and thermoforming [35]. Concerning the CRPP, the so-called high melt strength polypropylene (HMSPP) grades can be introduced mainly by radiation processes. These processes do not exhibit the characteristic odors accompanying the traditional peroxide-initiated degradation process [36].

1) By electron-beam irradiation

The electron-beam irradiation on polymers can generate modification effects in the macromolecular structure and material properties [39, 40]. The main molecular effects are chain scission, chain branching and cross-linking. Usually, all these reactions take place simultaneously and depend on different factors, such as the chemical structure and the morphology of the polymer as well as the irradiation conditions including after-treatment. In this way, the modification of linear polypropylene may result in long chain branching macromolecules. However, the molecular structure, particularly the topography of the long-chain branches (LCB), achieved by the electron beams is still widely unknown. The products irradiated with more than a specific electron beam dose showed a distinct strain hardening in elongational flow with changing the strain rate dependence although the MW had become significantly lower [39].

2) By γ-irradiation

Lucas et al [43] presented an invention in 1995 which provided a PP or PP/PE copolymer suitable for the thermoforming processes using gamma or electron beam irradiation by which the

thermoforming sag resistance property of the polymer was improved. They first mixed 500-3000 ppm of antioxidant with the first portion of PP or PP/PE copolymer, then irradiated the first portion with a total dosage from about 10 to 20 Mard of γ-ray in air. The first portion of the polymer was then mixed with a second non-irradiated portion of polymer to increase the thermoforming sag resistance during sheet extrusion.

In 2000, Lugao et al [44, 45] prepared the modified PP by γ rays (Co-60) and electron radiation in acetylene atmospheres followed by annealing. The double bond formation increased the production of branching and crosslinking reactions. Special care had to be applied to control crosslinking to avoid high gel formation and reduce the cost of acetylene. The γ irradiation of PP under acetylene has been shown to be a competitive technology due to its process flexibility and the low investment cost [45]. HMSPP was obtained at low dose, indicating that the control of the branching reaction was useful for the process of a polymer with special rheological properties.

3) By ultraviolet (UV) irradiation

Ultraviolet (UV) irradiation is another kind of high-energy irradiation that has been used as a modification, polymerization, grafting or crosslinking approach in polymer research for a long time. The stability and degradation of polymers exposed under UV also have been widely studied, hence it determined their environmental durability during end-use.

Carlsson et al [46] explained the photooxidative process of PP during this degradation. Qu et al [47] provided a mechanism for the photosensitizer, benzophenone (BP), photoreduction in the

photo-initiated crosslinking of polyethylene. For the photoreduction mechanism of BP see Fig. 2.5.

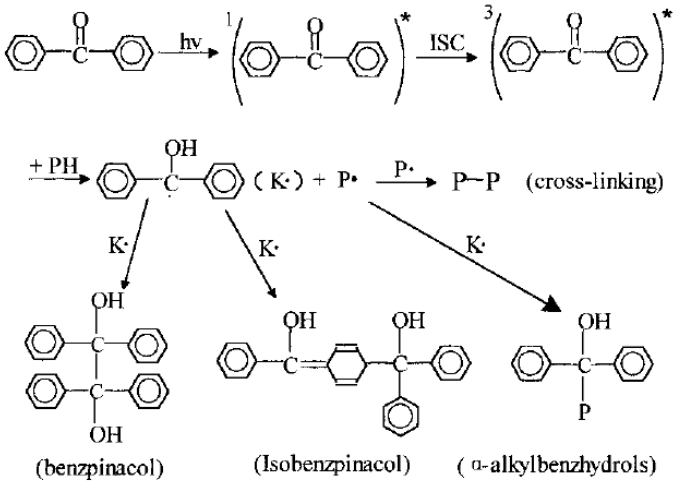

Fig. 2.5 Mechanism of benzophenone photoreduction[47].

The PP was sensitized by a primary photochemical process of hydrogen abstraction from the polymer substrate; even if singlet oxygen was produced in significant amounts, its overall contribution as an initiating process was small [48].

He and Tzoganakis [49] invented a UV-initiated REX process for the production of CRPP in the presence of the photo-initiator (BP). Through a short-open section of the barrel of the extruder, the UV light irradiated the PP melt which was already very well-mixed with the initiator. The screw design was as shown in Fig. 2.6.

The MWD could be significantly modified even at very low UV irradiation times and it was found that BP's concentration had a significant effect even at low levels. The reduction in

molecular weight and rheological properties were more significant at higher reaction temperatures in this process.

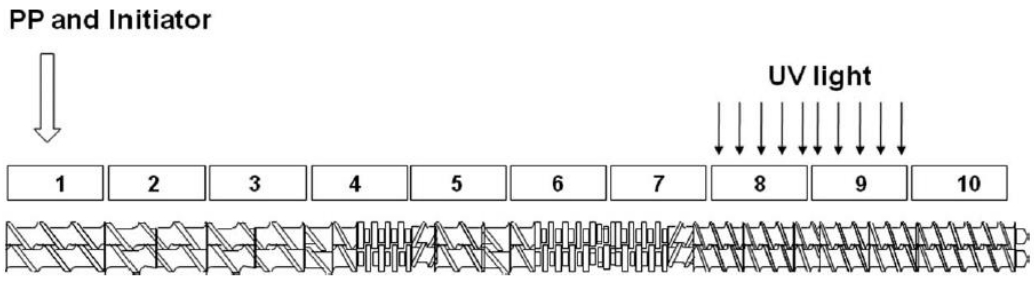

Fig. 2.6 Screw configuration and experimental set-up for the UV-initiated CRPP [49].

Amintowlieh et al [80-82] used UV radiation to modify the PP containing benzophenone (BP) in the solid state. Long chain branches (LCB) and crosslinked structures were formed in the irradiated solid PP sheets. Strain hardening of the modified sample was also observed from rheological measurements. It was found that high BP concentration and low lamp intensity was preferable to generate LCB within a thin thickness of the PP sheets sample (<1mm). By adding trimethylolpropane triacrylate into the recipe as a coagent, the required UV irradiation time was shortened. Scale-up experiments in a continuous fashion were conducted on PP strands extruded from a twin screw extruder by in-situ UV photomodification. The irradiation time required for formation of LCB was significantly lower than in batch reactions due to low thickness of the strands. Moreover, post-extrusion stretching of the strands limits chain mobility and restricts β-scission reactions.

2.2 Studies for Peroxide Induced CRPP

2.2.1 Extrusion factors

Regarding the CRPP technique, the organic peroxide-induced random scission of the polypropylene, owing to its convenient operation and low cost, has been intensively studied academically and is the most common approach employed nowadays in industry. This project will also resort to this method.

The main controlling factors for the peroxide promoted CRPP in a REX process are: the reaction temperature, the peroxide chosen, the concentration of peroxide, and the screw speed together with the residence time (RTD) of the resin in the extruder.

Tzoganakis et al [5, 19, 20] carried out organic peroxide promoted degradation of PP experiments in sealed glass ampoules and a single-screw extruder. The degradation extent of the linear PP can be indicated by melt flow rate (MFR) through its correlation with average molecular weight. The MFR of CRPP increased with peroxide concentration, reaction temperature and reaction time. The MFR increased linearly with peroxide concentration up to a certain level and then it started to level off at higher concentration [28, 32].

The presence of oxygen dramatically enhanced the degradation rate due to the formation of highly reactive peroxy radicals which were probably generated from the reaction of the primary peroxide radicals and oxygen. Although oxygen could improve the efficiency of this process, however, it resulted in unfavorable color of the products [5].

During reactive extrusion of PP with peroxide or other additives in the extruder, the residence time distribution (RTD) of the raw materials in the extruder is a crucial factor that can be used to analyze mixing and product uniformity. Suwanda et al [29] measured the residence time distributions of peroxide-initiated CRPP by a tracer technique and combined the test results with their batch kinetics model for the prediction of the MWD changes due to the reaction. Tzoganakis et al [30] used radioactive manganese dioxide (MnO_2) as the tracer and analyzed its neutron activation during this process in a single-screw extruder at different screw speed, temperature and peroxide concentration levels. 2 g of PP-MnO_2 mixture 1% in MnO_2 as the trace material was injected in a pulse function to the feed of the extruder. The extrudate was collected at specific time intervals and then irradiated in a nuclear reactor to determine the concentration of MnO_2 by its induced radioactivity. Changes of viscosity resulting from the degradation reaction largely affected the flow pattern and hence the RTD in the extruder. Higher level of peroxide concentration would broaden the RTD while an increase of extrusion temperature would narrow it. The screw speed affected significantly the mean residence time (due to its effect on flow rate) but not the breadth of the RTD.

In the peroxide induced CRPP, the peroxide is usually either premixed with the polymer or injected in the feed throat or along the extruder. However, Dickson et al [55] performed a pulsed peroxide addition during the reactive extrusion process and compared the results to the common continuous addition protocol. It was shown that pulse amplitude, pulse period, and pulse profile can be manipulated to control the average molecular weight and polydispersity.

In the process of β-scission two shorter polymer radicals are generated and are thought to terminate by disproportionation yielding a terminal double bond. A study [56] of the vinylidene group of the CRPP proved the degree of scission increases with peroxide concentration.

2.2.2 Molecular weight evolution and rheological properties

PP extruded without peroxide only degrades by thermal or mechanical degradation and does so without significantly changing the MWD [5]. When peroxide was added, due to the random nature of the β-scission scheme of CRPP, the original high MW tail content was reduced and narrower MWD resin was produced. The CRPP melt was more Newtonian [27, 28, 31] due to the narrower MWD. The viscosity curve became flatter and the power law index increased as the peroxide concentration increased.

The MWD of a polymer plays a critical role on its entire properties. Control of the MWD would require means of MWD monitoring that offer reliable, accurate, and rapid measurements. Rheological measurements provide an attractive candidate in this regard, provided the MWD information can be extracted from the rheological data [58]. It is well known that the rheological properties of polymer melts depend strongly on the underlying molecular structure, specifically, molecular weight, MWD, and long chain branching (LCB) [57].

For MWD determination of PP, gel permeation chromatography (GPC) was found to have reproducibility problems for the polydispersity index. GPC testing of PP was also time consuming and not suitable for quality control of plant operations. Zeichner and Patel [50] proposed to use the cross-over modulus, G_c, specifically for polypropylenes made by Ziegler–

Natta catalysis and degraded by chain scission. They defined a "polydispersity index", PI, which was expressed as $PI = 10^5/G_c$ with the units of $[G_c] = [Pa*s]$, and where G_c is the crossover modulus value when G'=G''.

This rheological PI value showed a good correlation with PDI of the MWD. However, this technique has its limitations for CRPPs at high MFR level. Specifically, one cannot obtain the crossover modulus with MFRs higher than 40 due to frequency limitations of commercial rheometers. Yoo [52] introduced the modulus separation (Modsep) method to quantitatively determine the polydispersity of MWD of PP homopolymers with ultra-high MFR values (at which the crossover modulus cannot be obtained) at a G_{ref} of 500 or 1000Pa.

Because of the strong dependence of rheological data on the underlying molecular structure, specifically, molecular weight, molecular weight distribution (MWD), and long chain branching (LCB) etc., there are other rheological measures of polydispersity such as ER, ET, RDR, PDR proposed by Shroff and Mavridis [61].

The extensional viscosities [28] of CRPPs were decreased distinctively even at low peroxide level and the extensional viscosities seemed to be more independent of the strain rate compared to the virgin PP. This rheological characteristic is very helpful for stretching processes of PP, such as fiber spinning, since it prevents necking during extension and allows higher speeds of the production line.

2.2.3 Modeling studies of peroxide induced CRPP

Based on the reaction kinetic scheme proposed by Tzoganakis et al (see Section 2.1.2), Suwanda et al [57] simplified the model by only considering the disproportionation termination and proposed kinetic functions which associated reaction parameters with discrete polymer chain length concentrations at different reaction times. The chain length concentration distribution can be calculated from the output MWD curve from size exclusion chromatography. Assuming certain parameters were constant within small reaction time intervals, they modeled [58] the CRPP process from the virgin Ziegler-Natta type polypropylene. The model prediction and experimental results were comparatively in good agreement.

The REX of CRPP and the polymer melt flow in either single or twin screw extruders was also modeled:

1) In Single Screw Extruders

During this REX process, the polymer melt in the extruder is undergoing laminar mixing and controlled degradation. Thus, the polymer rheology and the hence the flow are both affected by the reaction in the screw channel. Strutt [59] et al studied the influence of the channel geometry, extruder operating conditions, and peroxide level and addition pattern for the steady-state non-isothermal non-Newtonian reactive flow of molten polypropylene in a single-screw extruder (SSE). Numerical simulations were carried out using the kinetic reaction model promoted by Tzoganakis et al [19] described in section 5.1, along with the conservation equations of mass, momentum, and energy for this process. Then, the degree-of-fill profiles and the flow

efficiencies of peroxide initiated CRPP in SSE were investigated by finite element simulation techniques.

In this work [59] the effect of screw channel geometry, screw speed, pressure to drag flow ratio, inlet peroxide level, peroxide feeding distribution pattern and screw speed was studied. It was found that the simulated average degree-of-fill profiles agreed very well with the expected performance based on the screw design. The mixing ability of the flows was found to be very similar to that of two-dimensional flow. Neither screw speed nor inlet peroxide distribution would affect the flow efficiency. However, the pressure-to-drag flow ratio and the channel aspect ratio were found to have significant influence on the flow efficiencies as well as the average outlet peroxide conversion and outlet molecular weight.

2) In Twin Screw Extruders

Boyd et al [60] performed simulation of this reactive flow in a forward conveying element of a self-wiping co-rotating twin screw extruder (TSE) using the same approach. Similar results observed as in the modeling in the SSEs. The average flow efficiencies were found to remain at values close to those for two-dimensional flow, with fluctuations in the channel intermeshing regions.

2.3 Melt-fracture of CRPP

2.3.1 Melt-fracture phenomena

In an extrusion process, the surface appearance quality of the extrudate is one of the essential features of the products. Polymer melt fracture is expressed by the visual experience on extrudate

surface distortion of polymer melts during extrusion through dies at, frequently, high shear rate. In 1945, this distortion phenomenon was mentioned for the first time by Nason [65] when he described a high temperature and high pressure rheometer for plastics. The term "melt fracture", was coined by Tordella [66] in 1956 due to the audible tearing noise which usually accompanied the extrudate distortion and this term has been widely used. Nowadays, this phenomenon is still of great importance and has attracted a lot of scientific attention. This is due to the tremendous consumption growth of plastic materials that are being extruded into final products and due to the fact that melt fracture phenomena affecting product surface quality can severely limit production rates. Polymer melt extruded products in the form of strands, fibers, tubular blown films, pipes and tubes are prone to exhibit this defect under particular extrusion conditions.

The type and degree of the rough surface or/and distortion amplitude of the extrudate surface was investigated and classified in many literature studies via optical microscopy or even scanning electron microscopy for different materials. Table 2.2 lists some of the melt fracture description of these materials at certain extrusion conditions.

Based on numerous practical experiments, there exist many factors which influence the degree of extrusion distortion of thermoplastics, including:

1) Chemical structure of the polymer:

   Chemical nature of repeating unit, molecular weight and its distribution, branching, comonomer(s);

2) Extrusion die：

   E.g. the capillary die: entrance geometry, length to diameter ratio, material composition of the

orifice wall;

3) Extrusion conditions:

Extrusion temperature (including die temperature), flow rate (or shear stress, as in a variety of studies a critical shear stress was usually found for the onset of melt fracture);

4) Additives and fillers:

The chemical and interfacial nature of the additives and fillers.

Considering these factors a number of effective methods have been proposed to suppress melt fracture and to improve the extrusion ability. These include modification of the extrusion die by reducing the entrance angle, smoothly converging the entrance, coating the die wall with fluorine material wax as additive in the polymer melt, etc.

Table 2.2 Surface description of melt-fractured polymer extrudates.

Thermoplastic	Extrusion condition	Surface description
Ziegler-Natta type, linear low-density ethylene-octene copolymer, MFR=1g/10min [65]	L/D=~0, 2α=180° @150°C*57s^{-1}	Pitted, cracked
	L/D=~0, 2α=180° @190°C*99s^{-1}	Orange peel
	L/D=~0, 2α=180° @150°C*244s^{-1}	Wavelets
	L/D=11.5, 2α=180° @190°C*763s^{-1}	Stick-spurt
	L/D=11.5, 2α=180° @150°C*1370s^{-1}	Surface distorted
	L/D=11.5, 2α=180° @190°C*3200s^{-1}	Surface & volume distorted
Metallocene type, very-low-density ethylene-octene copolymer, MFR=1g/10min [65]	L/D=~0, 2α=180° @150°C*43s^{-1}	High-frequency low amplitude ridged
	L/D=~0, 2α=180° @150°C*76s^{-1}	Screw-treaded
	L/D=~0, 2α=180° @150°C*763s^{-1}	Sausage-like volume distorted
	L/D=~0, 2α=180° @150°C*5720s^{-1}	Chaotic volume-distorted
	L/D=11.5, 2α=180° @150°C*183s^{-1}	Distorted, irregular screw-treaded
	L/D=11.5, 2α=180° @150°C*320s^{-1}	Helical volume distorted
Metallocene type, HDPE, MFR=1g/10min [65]	L/D=~0, 2α=180° @150°C*14s^{-1}	Pitted, sharkskin

continued from Table 2.2

LLPE [67,68]	From low shear rate to high shear rate	Smooth
		Sharkskin
		Stick-spurt
		Smooth (superflow)
		Gross melt fracture
PS [69]	L/D=~0, @200°C, from low shear rate to high shear rate	Smooth
		Helical, small amplitude
		Helical, high amplitude
		Chaotic distortion
PP[70]	L/D=20,@200°C from low shear rate to high shear rate	Smooth
		Grossly distorted
		Helical screw thread
		Chaotic distortion

α is the half entrance angle.

2.3.2 Melt-fracture mechanisms

To solve the melt fracture problem, a significant effort was spent in understanding its origin. In the past half century, great efforts through empirical and theoretical approaches were made to understand melt fracture phenomena. In this process, extrusion curves (shear stress versus shear rate) obtained from experiments were usually employed to combine with the extrusion distortion amplitude or flow instability at different apparent shear rate (or stress) range [67]. For example, see Fig. 2.7.

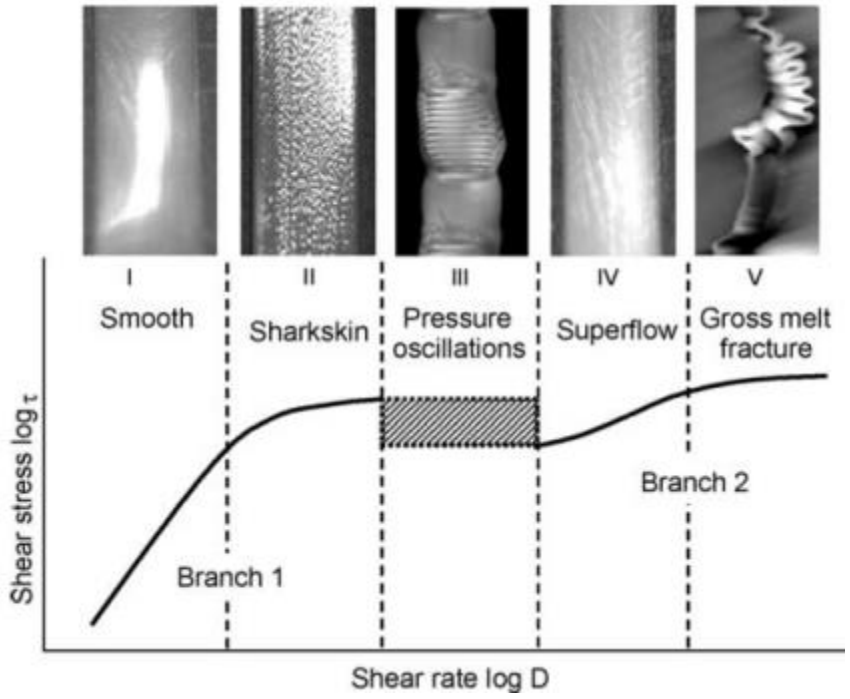

Fig. 2.7 Examples of different forms of extrusion distortion of HDPE with extrusion curve study [67].

Many mechanisms have consequently been proposed, however, there is not such a general one that can be commonly employed on the whole family of thermoplastics. But mainly these studies provide the basis for associating the polymeric system, in particular the rheological properties, to the dynamics of stress and kinematics of strain.

1) Fracture

Tordella [70] found that beyond a certain critical shear stress, the melt breakdown occurs during plastic extrusion and suggested the melt fracture was possibly a cohesive failure. Following this fracture hypothesis, Cogswell [71] proposed that the surface distortion was caused by rupture of the surface layer of the extrudate which was highly stretched once it came out from the die. Theoretically at the die wall, the velocity of the polymer melt equals zero. However, the layer near the wall of the emerging material would accelerate the velocity on the free boundary while

the core of the bulk decelerates. Thus, at the die exit, the surface layer is stretched and would cause rupture if the stretching rate exceeds the critical break stress. This was confirmed by Gogos [72] by extrusion swell studies and other simulation works which indicated that at the point of separation between the die and polymer melt the stretch ratio reaches infinity. Cogswell [22] also found more elastic polymers (more broad MWD or branched) allowed more acceleration of the surface layer stretching without surface distortion. The stored elastic energy of the polymer melt during the flow is responsible for the fracture requirement.

2) Cohesive failure

The discontinuity of the extrusion curves at the onset melt fracture point suggests that the disentanglements of the polymer chains may be responsible for melt fracture. Wang [73] found the stick-slip transition in capillary flow of linear polyethylene melts. At the critical shear stress, τ_c, present at the onset of the discontinuity of the flow curve, a structural transition along the die wall of the surface extrudate layer was observed. Flow induced disentanglements between the adsorbed polymer chains to the die wall and the polymer melt bulk were thought to result by interfacial layer transition. The disentangled surface layer thus exhibits a significantly lower shear viscosity, as slip, than the entangled bulk, as stick. Temperature was found to be essential to the critical shear stress. The distortion period decreased with stress which followed the time-temperature superposition principle.

Local transition of the surface layer was also observed by Barone et al [74] at the die exit as the layer oscillated between the state of entanglement and disentanglement. This could result in a

recoil-stretch transition of the surface polymer chains and the local stress would relax and increase periodically when $\tau_{exit} > \tau_{c.}$

3) Adhesive failure

Corresponding to the cohesive failure mechanism mentioned above, there is an adhesive mechanism supported by some literature studies based on the polymer melt-die wall combination that the onset of melt fracture may result from the detachment of polymer melt from the die wall.

The detachment only happens when the polymer chains gain high enough stress to overcome the adhesion energy from the die wall. Following this direction, Hatzikiriakos et al [75] related the stress at the onset of slip to the work of adhesion. A sessile drop profile analysis of the polymer fluid was used to test the surface tension as well as adhesion energy. For the polymer melt under flow, the stretched polymer will store energy and once it can overcome that friction between the polymer chains and die wall, the polymer chains will detach.

2.3.3 Melt-fracture study of CRPP

Intensive melt fracture experimental and theoretical studies have been based on polyethylene. However, with respect to polypropylene, the literature sources are limited. In 1964, Bartos detected the melt fracture of a range of polymers including [76] polypropylene. The critical shear stress of onset of melt fracture for PP was found to be 0.069~0.16 Mpa. According to results from Ui et al [77] on the extrusion study of many polymer melts, the obtained flow curve of PP

exhibits continuity which is not like the frequently reported breakdown of flow curve at the onset range of melt fracture of many other polymers such as high density polyethylene.

The melt fracture characteristics of CRPPs were studied by Baik and Tzoganakis [22] by means of capillary rheometry experiments. The various grades of CRPPs were produced by different peroxide concentrations first, and then the flow curves and extrudate characteristics of these resins were determined in a capillary rheometer. It was found that the severity of melt fracture decreased with increasing shear rate for a given material and temperature and in some cases, the extrudates exhibited completely smooth surfaces. With the visual observation for the collected CRPP extrudates, at the onset point, the smooth surface turned into rough surface while there was no surface melt fracture observed. As the shear rate increased, it became pitched screw thread, then smooth again and finally developed chaotic distortion. This evolution of surface distortion observation from CRPPs was in agreement with the results from PP by Ballenger et al [78]. For CRPPs produced with different peroxide dosage (thus different MWD), they also found the critical shear rate at onset of melt fracture increased from narrow distributed CRPPs. Interestingly, CRPPs with narrower MWD exhibited higher critical wall shear stress while the onset point was independent of the temperature.

Chapter 3

EXPERIMENTAL

In this chapter, an experimental study for the production of CRPP from a commercial Ziegler-Natta catalyst based polypropylene (PP) is described. The materials used as well as the procedures and characterization techniques are discussed. The same techniques are used in the experiments discussed later on in the thesis.

CRPPs were produced at elevated temperature (200°C) in a batch mixer, where the virgin PP pellets were melted and mixed with an organic peroxide at different concentrations to initiate random scission of the polymer chains. The peroxide was used either in pure liquid form or diluted with acetone or isopropyl alcohol. The purpose of using a solvent (acetone and isopropyl alcohol) was to check whether the solvent commonly used for CRPP has any influence on the process.

Rheological properties, such as complex viscosity, storage and loss moduli, and melt flow rate (MFR) of the CRPPs were characterized in an effort to follow changes in molecular weight of the starting PP and the evolution of these properties with the peroxide concentration was investigated.

3.1 CRPP Production

3.1.1 Materials

1) Polypropylene:

The polypropylene used in this chapter was kindly supplied by INGENIA Polymers Corp. This was a Lyondell Basell Profax PDC1274 that had been ground into powder form. Its density and MFR are listed in Table 3.1.

Table 3.1 Properties of Lyondell Basell Profax PDC1274 polypropylene.

Properties	Metric	Test Method
Density	0.902 g/cc	ASTM D792
Melt Flow Rate	12 g/10min	ASTM D1238, 230°C * 2.16 kg

2) Organic peroxide:

The peroxide used in these experiments was 2, 5-bis(tert-butylperoxy)-2, 5-dimethyl hexane (DHBP) and was purchased from SIGMA-ALDRICH with the trade name of Luperox® 101 (L101). Its chemical structure and properties are shown in Fig.3.1 and Table 3.2.

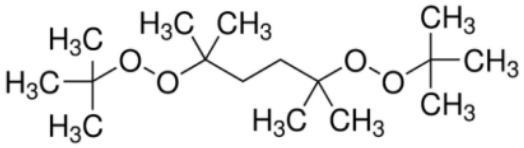

Fig. 3.1 Chemical structure of the 2, 5-bis(tert-butylperoxy)-2, 5-dimethyl hexane (DHBP).

Table 3.2 Properties of the Luperox® 101 (L101) peroxide.

Properties	Value
Chemical formula	$C_{16}H_{34}O_4$
Formula weight	290.44 g/mol
Boiling point	55 - 57 °C @7 mmHg
Density	0.877 g/cm^3 at 25 °C
Flash point	65 °C (closed cup)

3) Acetone:

The acetone used in this work was wash-grade from Chemical Stores at the University of Waterloo supplied by Sigma Aldrich.

4) Isopropyl alcohol or 2-propanol (IPA):

The HPLC grade isopropyl alcohol was purchased from SIGMA-ALDRICH.

The properties of the two solvents are shown as Table 3.3. All materials were used as received.

Table 3.3 Properties of acetone and isopropyl alcohol.

Properties	Acetone	Isopropyl alcohol
Boiling point	56 - 57 °C	82.5 °C
Density	0.791 g/cm^3 at 25 °C	0.786 g/ cm^3 at 25 °C
Flash point	-17 °C	11.7 °C

3.1.2 Equipment

A Haake Rheocord 90 batch mixer equipped with a RHEOMIX 3000 chamber was used in these experiments (see Fig.3.2 a) along with a set of roller-blade rotors (see Fig. 3.2 b).

a.

b.

Fig.3.2 The HAAKE batch mixer system: (a.) Rheocord 90 equipped with RHEOMIX 3000, (b.) roller-blade rotors employed for mixing.

All input and output data are recorded by the RC9000 software for processing analysis. A snapshot of the RC9000 Control and Data Acquisition panel is shown in Fig.3.3.

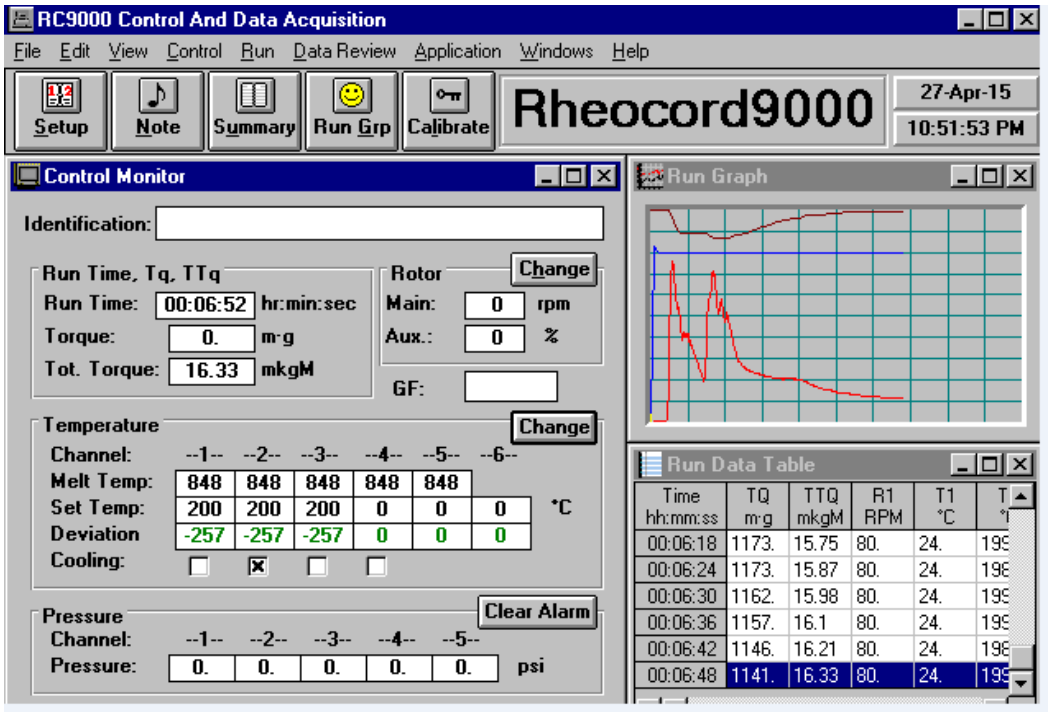

Fig. 3.3 A snapshot of the RC9000 Control and Data Acquisition interface.

Primary variables measured are torque and processing temperature. In these experiments, variations in torque reflect changes in material viscosity originating from molecular weight changes.

3.1.3 Experimental Procedure

The experimental factors used in these experiments are as follows.

1) Rotor speed

A rotor speed of 80 rpm was used to ensure that the polymer melt was well mixed with the liquid peroxide.

2) Mixing temperature

The reaction temperature for CRPP production is one of the most important factors to be considered. Batch mixer chamber temperature was selected by considering the melting point of the PP material (150-165 °C) and the decomposition kinetics of the peroxide as well as the possibility of thermo-oxidative degradation of PP in the open chamber.

3) Mixing time

The process for CRPP production in a batch mixer involves two steps. In the first step, PP is loaded into the mixer and melted under heat and shear from the rotors. In the second step, liquid peroxide or its solution was added dropwise into the polymer melt and chemical reaction starts.

The end of the first step was indicated by the stabilization of the torque over time. Once the peroxide was introduced into the mixing chamber, there need to be adequate time to ensure complete decomposition of it and reaction with the PP melt.

The effect of temperature and time on the decomposition kinetics of the Luperox 101 peroxide was calculated at first. The technical data we can use is the half-life time data of this peroxide and its relationship with temperature in the form of Arrhenius equation:

$$t_{1/2} = (\ln 2 / k_d)$$
$$k_d = A * \exp(E_a / RT) \quad (3.1)$$

where

$t_{1/2}$, is the half-life time of the peroxide,

k_d is the decomposition rate constant,

A, is the collision frequency factor,

E_a, is the activation energy,

R, is the universal gas constant, and

T, is the chemical reaction temperature.

For Luperox 101 half-life times are 2.9 and 0.2 seconds [37] at 230 and 290 °C, respectively. Then equation (3.1) was used to estimate A and E_a assuming 1st order kinetics and calculate the half-life time as a function of temperature:

$$t_{1/2} = 2.05449^{-16} * \exp(18710.6/T) \quad (3.2)$$

where T is in degrees Kelvin.

The residual or undecomposed peroxide at various temperatures and times is calculated and shown in Table 3.4. At 210°C and 3 minutes, the reaction can reach a conversion of about 99.99%.

Table 3.4 Residual peroxide at various decomposition temperatures and times.

		Reaction time			
Temp/°C	$t_{1/2}$/s	1min	2min	3min	5min
180	175.54	78.91%	62.26%	49.13%	30.59%
190	71.98	56.11%	31.49%	17.67%	5.56%
200	30.65	25.74%	6.63%	1.71%	0.11%
210	13.52	4.61%	0.21%	0.01%	0.00%
220	6.16	0.12%	0.00%	0.00%	0.00%
230	2.90	0.00%	0.00%	0.00%	0.00%

Considering these factors, CRPP production in this project was carried out at 80 rpm, 210°C for 3 minutes of reaction time (time after melting).

3.1.4 Peroxide Addition Protocol

Table 3.5 Recipe design of the CRPPs.

Sample Name	PP0	A0	A1	A2	A3	A4	B1	B4	B8	C4	C8
L101/ppm			500	1000	1500	2000	500	2000	2000	2000	2000
Acetone/ml							20	20		200	
IPA/ml									20		200
Remark	Pure	Processed	Add pure peroxide during mixing				Add the solution during mixing			Pre-mix the solution	

(Blanks in this table indicate zero values of peroxide or solvent.)

In many studies on liquid peroxide-induced CRPP process in an extruder, peroxide is added either in a pure form or in a solution form. The effect of peroxide addition protocol in the current experiments was explored through experiments shown in Table 3.5.

The mixing procedure and addition of peroxide is illustrated by the mixing graph shown in Fig. 3.4. After the temperature of the mixer became stable, the polymer was fed into the mixer step by step. The torque of the rotor increased sharply and then dropped as the polymer was melting. When the torque became stable, the polymer had been melted thoroughly (ca. 3 min) and it was ready to add the peroxide/solution into the open mouth of the mixer. After addition of the peroxide, the torque dropped as the viscosity reduced due to polymer chain scission. In another 3 minutes, the torque reached another plateau which indicated completion of the reaction.

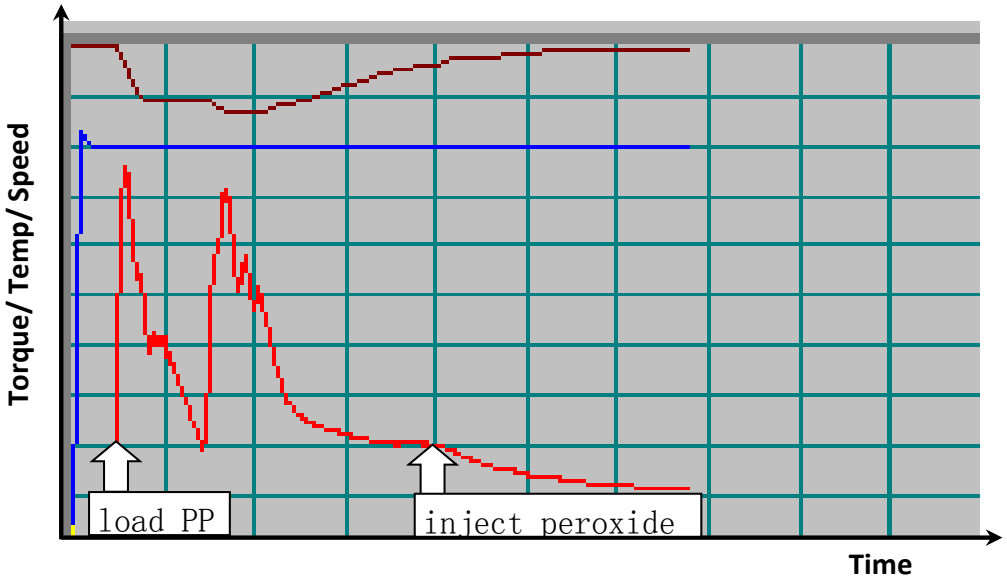

Fig.3.4 Mixing curve of CRPP in the RHEOMIX 3000 batch mixer.

3.1.5 Mixing Results

The effect of chain scission could be estimated from the torque plateau value after adding the peroxide in Fig. 3.5, Fig. 3.7 and Fig. 3.8. In comparison to the torque corresponding to sample A0 (processed pure polypropylene without peroxide), the final torque decreases for samples A1-A4 as the concentration of the peroxide concentration increases from 500 to 2000 ppm.

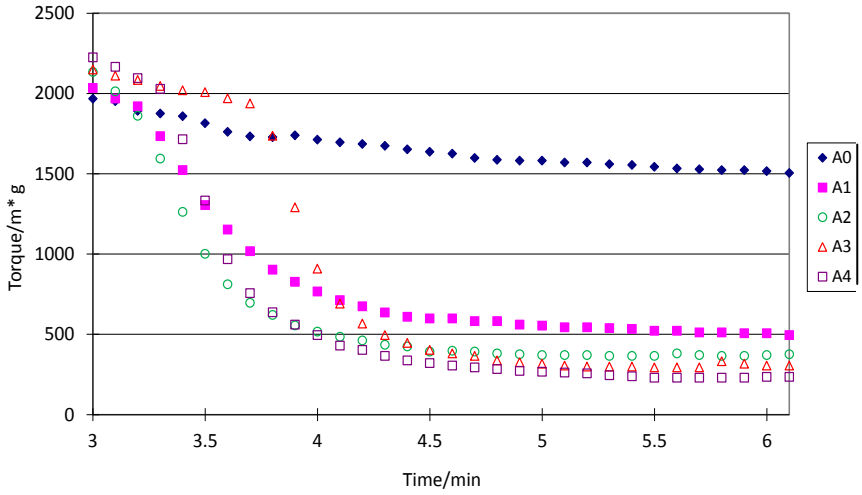

Fig.3.5 Mixing torque of samples A0, A1, A2, A3 and A4.

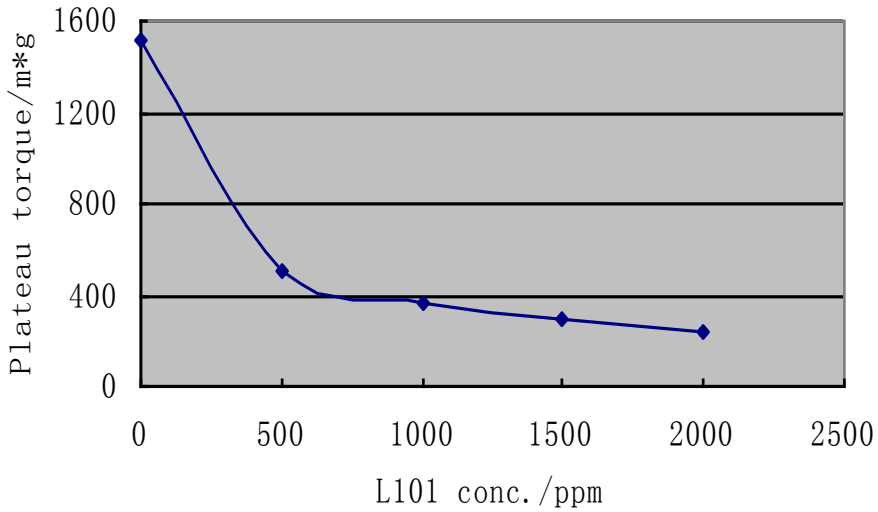

Fig. 3.6 Final torque plateau level as a function of peroxide concentration.

The final plateau torque declined as a function of peroxide concentrations as shown in Fig. 3.6. This is due to the reduced viscosity of the produced CRPPs.

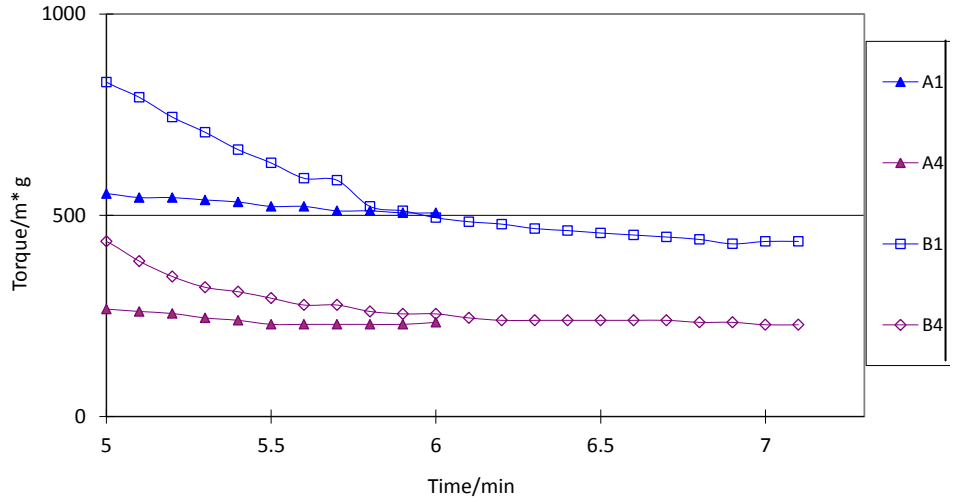

Fig. 3.7 Comparison of the mixing torque of samples A1, A4 with B1, B4.

In Fig. 3.7 the effect of peroxide addition protocol on the final torque is highlighted. Samples corresponding to equivalent peroxide concentrations (A1-B1 and A4-B4) exhibit the same torque. Therefore, the acetone solvent used in B1, B4 had no effect on the viscosity level. The similar torque levels achieved for A4 and B8 indicated that IPA as the solvent also had no effect. However, the higher viscosity/torque level of the C4 and C8, indicated that premixing of the solution with part of the polymer, had an effect. The premixing method seems to lead to less degradation perhaps due to some peroxide loss by evaporation during premixing. There may exist some chemicals in the raw polypropylenes, e.g. antioxidant, which can react with the peroxide during melting and before mixing and decrease its efficiency during CRPP production.

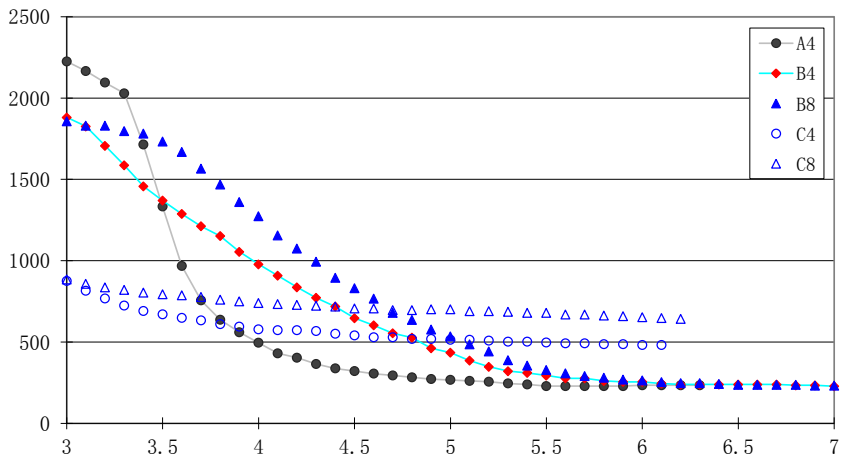

Fig. 3.8 Mixing torque of A4, B4, B8, C4, C8 samples.

3.2 Rheological Characterization

The rheological properties of the produced CRPPs can be characterized by various types of rheometers. In this research, a rotational rheometer with parallel-plates-rheometry (PPR) was applied in its oscillatory shear mode.

3.2.1 Sample Preparation

After mixing, the CRPP was scraped out from the batch mixer and cooled down and resin was in the form of a bulk chunk. The dried resin chunks were ground into pellets or grains with a lab Wiley Will grinder (see Fig. 3.9).

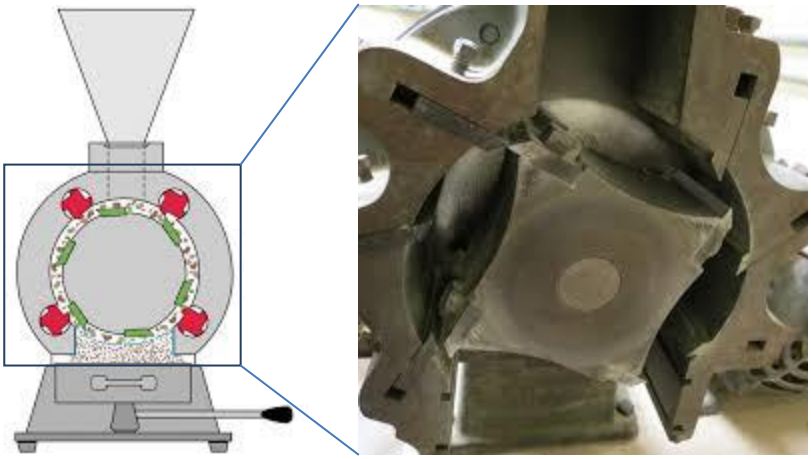

Fig. 3.9 The Wiley Mill grinder with rotational blades.

Fig. 3.10 The hot-press with a thermocontroller.

The ground sample was then melted and molded under a 13×13×2 mm square steel mold by the hot-press machine (PHI Press, see Fig. 3.10) at 180°C and 20000 pounds in 3min. The pressed

CRPP square sheets were quenched in a water bath to avoid thermal-oxidation degradation at room temperature. 25mm(diameter)×1mm flat disks were then cut out from the quenched CRPP sheets by a round sharp-edged cutting die (ODC Tooling and Molds Inc.).

3.2.2 Rheological Measurements

Fig. 3.11 The TA AR2000 rotational rheometer.

Rheological characterization was performed using a TA AR2000, a stress-controlled rotational rheometer (TA Instruments, New Castle, DE, see Fig. 3.11). 25mm diameter parallel-plates were employed for the measurements. As illustrated in Fig. 3.12, the upper plate floated by flowing air which can be driven by a rotation motor with low friction, whereas the lower plate functioned as

a stage for loading samples and to detect the normal force which was transmitted to the plate surface. During the test, pure nitrogen gas purged the test chamber to keep the samples in an inert atmosphere and to avoid their degradation at high temperature (180°C).

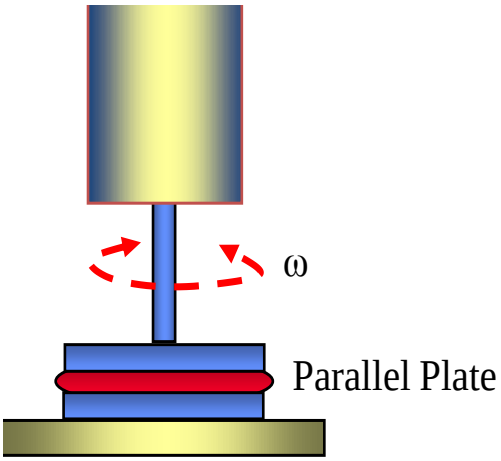

Fig. 3.12 Illustration of the oscillating parallel-plates geometry during the test.

The cut sample disks were introduced on the lower plate in the preheated test chamber at180°C. In 3 min, the samples were well melted and the upper plate was ready to lower down to the target gap around 1mm until it touched the polymer melts. If necessary, one can trim the rim of the sample and wait till the normal force relaxed close to zero before conducting the measurement.

All of the samples were firstly submitted for strain sweeps from 0.01 to 20% at 100Hz to make sure the applied strains during the following frequency sweeps were within the linear viscoelastic (LVE) region.

3.2.3 Rheological Results and Analysis

Fig. 3.13 shows a strain sweep example from PP0 sample at 200°C and 100 Hz to check its linearity between the strain of 0.01~20%. At a strain lower than 8%, the viscosity and modulus assumed a fixed value, in the LVE regime. A favorable strain below 8% could therefore be chosen for frequency sweep tests. Considering the free surface at the rim of sample, under high strain amplitude, the polymer melt might flow out of the plates easily. Therefore, a more moderate strain of 5% could be imposed for the frequency sweeps from 0.01 to 100 Hz (or s^{-1}). In the same way, frequency sweeps were carried out for other samples to obtain their rheological properties such as complex viscosity (η*), storage and loss moduli (G' and G") etc. for comparison.

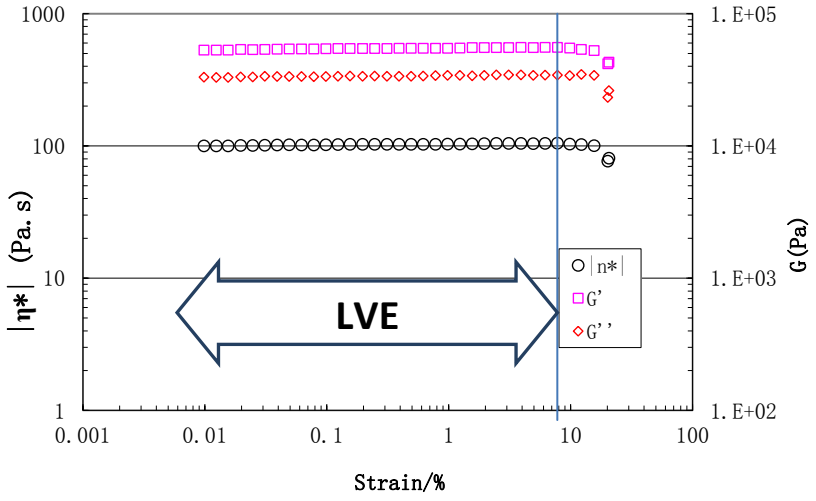

Fig. 3.13 Strain sweep of PP0 from 0.01~20% at 200°C and 100Hz.

Compared to the virgin material PP0, the complex viscosity level of the peroxide-modified resins strongly decreased, as seen from Fig. 3.14, and the declining magnitude increased with the

loading dosage of peroxide from 500~2000ppm (A1~A4). A slight viscosity drop from the virgin resin to the processed material (A0) indicated that the thermal oxidation during mixing could be neglected.

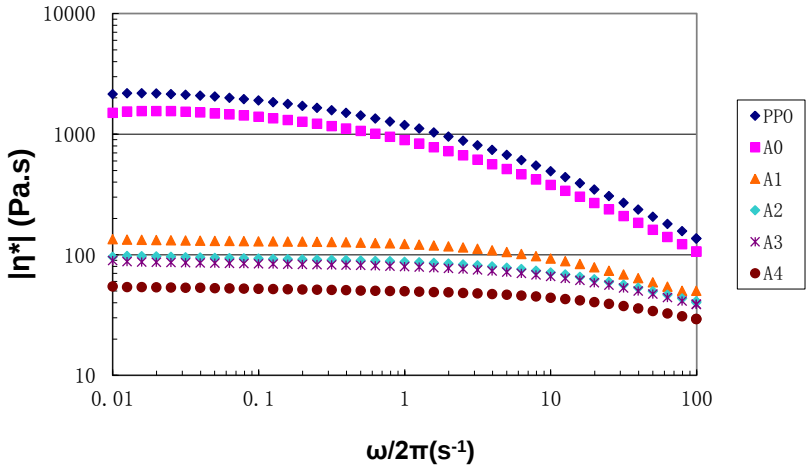

Fig. 3.14 Frequency sweep from 0.01~100Hz of PP0 at 200°C and 5%strain.

For polymers with linear structure, it is known that the zero-shear viscosity is associated with the weight average molecular weight, M_w, in a power law relationship whose the order is around 3.4~3.6 [1]. The zero-shear viscosity can be taken from the low frequency region, if the frequency is low enough to reach the Newtonian flow region (constant viscosity) near the terminal zone (shear rate close to zero)：

$$\lim_{\omega \to 0}(G''/\omega) = \lim_{\omega \to 0}\eta' = \eta_0 \qquad (3.3)$$

According to η_0 as function of peroxide concentrations, as presented in Fig. 3.15, we deduced that the molecular weight of the virgin polypropylene had been degraded into lower and lower levels. In addition, based on the data Fig. 3.14, CRPPs' Newtonian region became broader and

their shear-thinning at high shear frequency became weaker along with increasing peroxide amount. This implied a narrower MWD distribution [1].

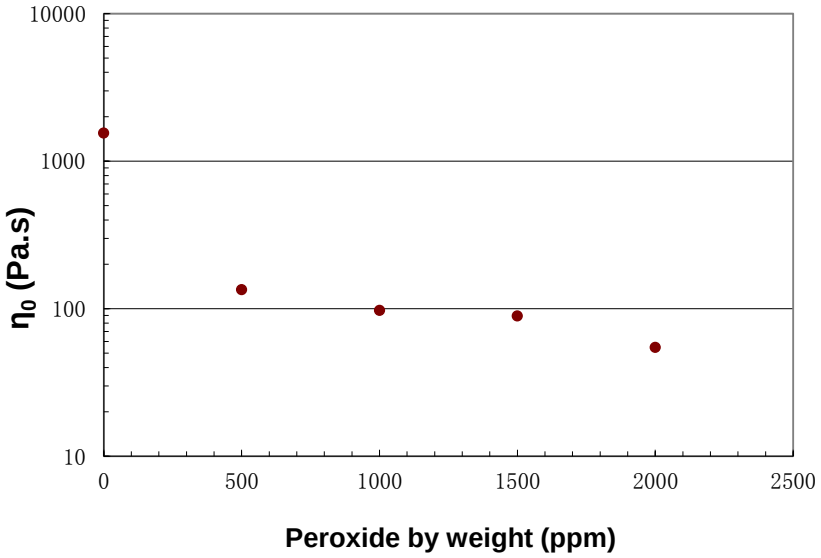

Fig. 3.15 Decrease of zero-shear viscosity with increasing peroxide concentration.

Concerning the MW and MWD, size extrusion chromatography (SEC, or gel permeation chromatography, GPC) are the most broadly used for most polymers. With regard to semicrystalline plastics such as isotactic polypropylene (i-PP) in this work, one challenging procedure in SEC is that the polymer should be dissolved in a suitable organic solvent with high polarity (such as 1,2,4-trichlorobenzene, TCB) and at high temperatures (140~150°C) to make sure that polymer chains are well dissolved and separated. However, rheological properties from the frequency sweep, if obtained from an adequate span of frequency and treated properly, can provide the MWD information indirectly [61, 62], namely, rheological PI. For linear polypropylenes we can use this convenient way. Quantification methods of the polydispersity from rheological data were applied and summarized by Shroff and coworkers [61]. These

included rheological polydispersity (PI), modulus separation (ModSep), ER(rheological polydispersity index of high molecular weight chains) and ET etc.

The rheological polydispersity indices of virgin PP (PP0) resin as well as its CRPPs were calculated based on the frequency sweep data and are compared in Table 3.6. From the ModSep and ER, we found that the CRPPs held narrower MWD than the virgin material, and higher peroxide loading dosage resulted in CRPP within narrower MWD. In addition, we also noticed that the rheological polydispersity of processed resin, A0, was broader. Thus, thermal oxidation degradation, unlike the peroxide free radical-induced degradation of polypropylene, would lead to a broad distribution which is not favored by industry.

Table 3.6 Rheological polydispersity of PP0 and its CRPPs.

	For G_{ref} =1000Pa			For G_{ref} =500Pa			
Sample	ω(G'ref)	ω(G''ref)	**ModSep**	ω(G'ref)	ω(G''ref)	**ModSep**	**ER**
PP0	0.3285	0.0903	3.64	0.1799	0.0411	4.38	1.37
A0	0.4278	0.1191	3.59	0.2353	0.0549	4.29	1.42
A1	6.1640	1.3147	4.69	3.6623	0.6359	5.76	0.56
A2	8.6707	1.8890	4.59	5.0186	0.9095	5.52	0.71
A3	10.0308	2.0962	4.79	5.8530	1.0074	5.81	0.70
A4	16.1443	3.3743	4.78	9.5772	1.6338	5.86	0.58

The effect of the two solvents, acetone and isopropyl alcohol (IPA), on the degradation efficiency of peroxide was checked by comparing the viscosity level of CRPPs produced at the

same peroxide concentration with and without these two solvents. According to Fig. 3.16, A1 and B1 samples resulted from 500ppm Luperox 101 with and without acetone respectively, and showed a similar viscosity. The same observation was obtained from the A4 and B4 samples produced at 2000 ppm of the peroxide. Therefore, as long as the peroxide or its solution was directly added during mixing, regardless of low or high peroxide concentration level (500 and 2000 ppm), the presence of acetone had no obvious effect to the consequent CRPP. Regarding the IPA solvent, the viscosity of B8 achieved the same level as B4 and A4 at the same peroxide dosage of 2000ppm. This indicated that IPA also had no distinctive effect on the process.

Owing to the above results, we can confidently use either acetone or IPA as solvent for peroxide during the CRPP production if needed, e.g. once the required amount of peroxide is out of the lowest scaling range of the pipette, we can dilute the peroxide in solution to expand the metering volume to cope with it.

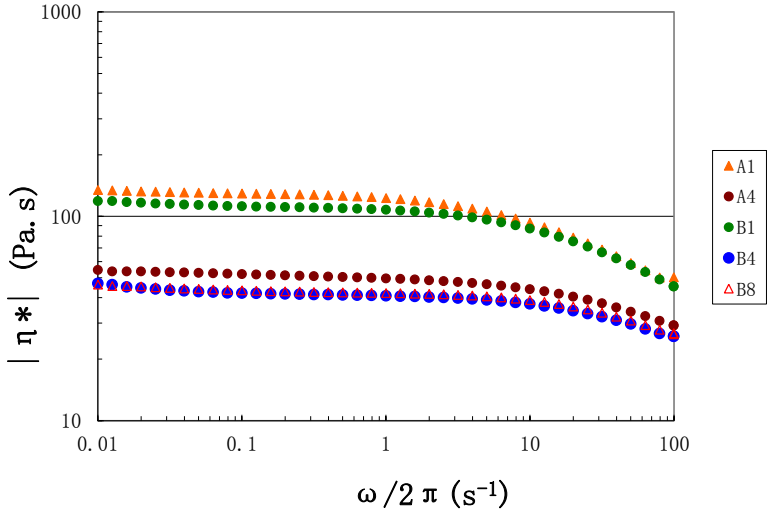

Fig.3.16 Effect of acetone/IPA solvents on the peroxide-induced CRPP when the peroxide/peroxide solution was directly added during mixing.

Two addition methods of the peroxide into the polymer matrix were examined, direct addition and pre-mixing, were also compared. During the production of A4, B4 and B8, the metered 2000ppm peroxide or its solution by the auto-pipette was dropped into the polypropylene melt, directly, into the mixer. Their degradation level had no big change as indicated by Fig. 3.17. With respect to C4 and C8, the 2000 ppm Luperox101 with 200 mL solvent (acetone and IPA, respectively) was pre-mixed with 200 g polypropylene in a beaker at first and then dried on aluminum foil inside a fume hood over 16h. Later, the peroxide-coated polymer pellets were introduced into the preheated mixer and mixed over the same period of time as above, 6 min. However, C4 and C8 presented higher viscosity levels. Thus the pre-mix method would reduce, to an unpredictable magnitude, the efficiency of peroxide for this degradation process.

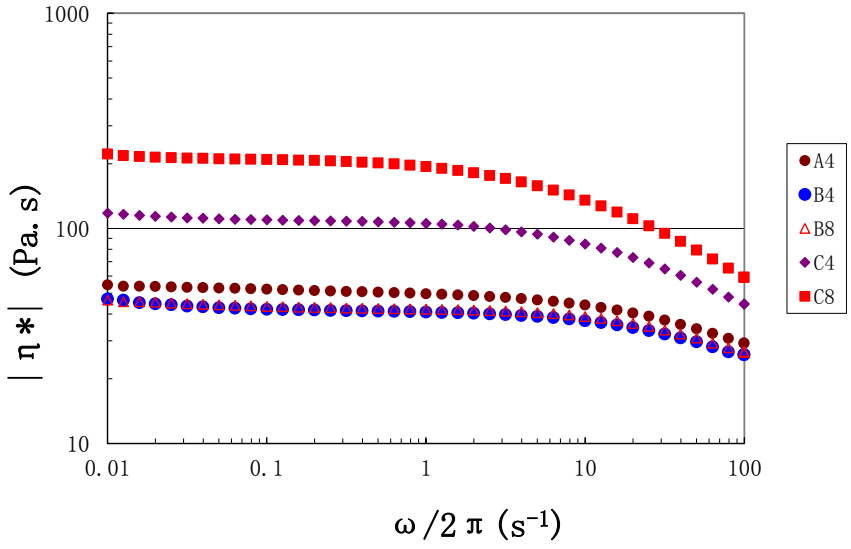

Fig. 3.17 CRPPs compounded with the two addition methods of peroxide into the polypropylene matrix.

3.3 Chapter Summary

In this chapter, preliminary experiments were carried out according to the procedures described. An organic peroxide (Luperox 101) was used to induce degradation of a Ziegler-Natta type polypropylene, with and without acetone or isopropyl alcohol as solution, samples were produced and studied at various peroxide concentrations by two addition ways for the peroxide: direct addition or pre-mixing. Results from these preliminary experiments indicated that:

- Higher concentration of the peroxide resulted in lower viscosity CRPPs.
- The MW of the origin material, detected from the zero-shear viscosity, was dramatically degraded along the increase of peroxide loading.
- Their MWD, determined from rheological polydispersity values, were narrowed with the addition of peroxide.
- In the direct addition method of peroxide, the solvents, neither acetone nor isopropyl alcohol, had obvious effect on the degradation process. The peroxide can therefore be diluted into these solvents to improve the volume scaling operability and accuracy.
- The pre-mixing of the peroxide with polymer, comparing with the direct addition approach, could reduce the efficiency of peroxide for degradation, arbitrarily. Thus, the direct addition method is preferred.

Chapter 4

KINETIC MODELLING STUDY

In this chapter, the process of peroxide initiated controlled degradation of both Ziegler-Natta and metallocene catalyst based polypropylenes (ZN-PP and mPP) was modelled using previously developed kinetic models. For that purpose, a MATLAB code was developed and the effect of kinetic parameters in the model on molecular weights and MWDs was investigated.

Model predictions were compared to experimental data for CRPPs produced from mPP. At low peroxide concentrations, the model predictions deviated from experimental data. The reason for this discrepancy is attributed to potential branching reactions due to the presence of terminal vinylidene groups in the virgin mPP. At high peroxide concentrations, however, the modelling predictions agreed well with experimental data. This was due to the dominant role of chain scission versus potential branching reactions.

In addition, the production of CRPPs from a pair of PPs from both types (ZN-PP and mPP), having similar initial average molecular weight, was modelled using the same code. It was found that, comparatively, the Mw of the ZN-PP CRPP series declined more drastically than that of the mPP series during degradation. Moreover, the decrease of their Mn followed the same trend. Thus, the PDI of the ZN-PP based CRPPs decreased faster than that of the mPP at the same peroxide loading level. As expected, the PDI of both CRPP series approached asymptotically a limiting value of 2, the so-called “most probable distribution”, which agreed with a literature study of the random scission process on linear polymers.

4.1 Kinetic Modelling of Peroxide-Induced Degradation of Polypropylene

As mentioned in section 2.1.3, the most studied and plausible kinetic model is the one proposed by Tzoganakis et al [5, 19] involving initiation, chain scission and termination reactions. The full model they proposed is repeated below for clarity.

Initiation:

$$I \xrightarrow{Kd} 2R\cdot$$

Chain scission (β-scission):

$$P_n + R\cdot \xrightarrow{K_1} P_r\cdot + P_{n-r} + R$$

Transfer:

$$P_n + P_r\cdot \xrightarrow{K_2} P_r + P_s + P_{n-s}\cdot$$

Thermal degradation:

$$P_n \xrightarrow{K_3} P_r\cdot + P_{n-r}\cdot$$

Termination:

$$P_n\cdot + P_r\cdot \xrightarrow{K_4} P_n + P_r$$

The inter-macroradical transfer and thermal degradation reaction were found not to be very significant and they were omitted from the simplified kinetic model that was developed.

With proper quantification for the output data from size exclusion chromatography (SEC) by Suwanda et al [29, 57], the function between the polymer chain size concentrations versus the β -scission kinetic parameters was established. They also modelled the peroxide-induced degradation process of polypropylene [58]. The quantification they studied was also for the commercial polypropylene tested in high temperature SEC (at 145°C) with anti-oxidant. As illustrated in Fig.4.1, the final output of the SEC commonly is the normalized differential molecular weight distribution of the polymer where the ordinate of the curve is termed normalized weight fraction, $W_N(logM)$ *(or dw/d(logM))*, with its slice of a logarithm of molecular weight, *logM*, and the area under the curve is equal to 1.

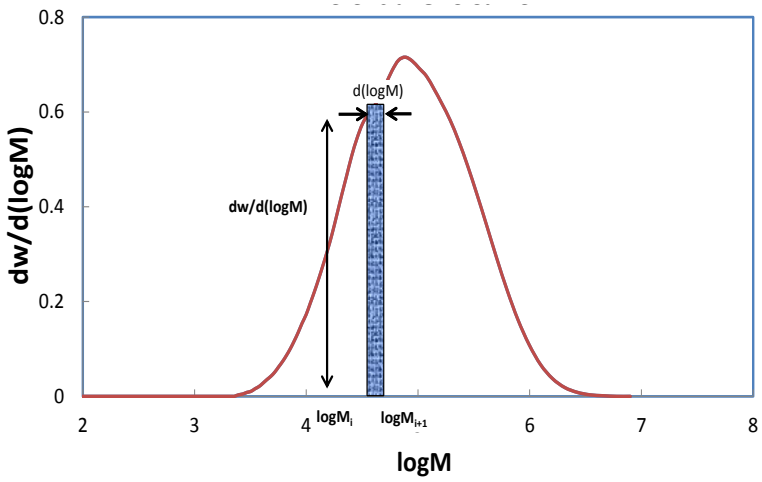

Fig.4.1 Differential molecular weight distribution output from SEC.

Suwanda et al [29] transformed the weight fraction of the output into a number fraction expression:

$$[P_r] = \frac{\rho_P}{\ln 10 * m_0 * r^2} W_N(\log M) \tag{4.1}$$

Where:

r, was the chain length of the polymer chains with a degree of polymerization of r,

$[P_r]$, was the number fraction of the polymer chains between the chain length of "r" and "r+1",

ρ_P, was the density of the polymer,

m_0, was the molar mass of the monomer.

Therefore, the differential weight fraction of the SEC curve was transformed into a differential "chain length distribution". This expression for the chain length number was employed for the modelling [58]. Based on the reaction mechanism proposed by Tzoganakis et al, the relationship of initial and new concentration of the polymer chains with a length of "n", $[P_n]$, after a reaction time *dt* was calculated as:

$$[P_n] = \frac{-\lambda_3}{\lambda_2} + \frac{(\lambda_2[P_n^0] + \lambda_3)}{\lambda_2} * \exp(\lambda_1 \lambda_2 dt) \tag{4.2}$$

with

$$\lambda_1 = \frac{2 f k_d [I] m_0}{\rho_P}$$

$$\lambda_2 = 1 - n$$

$$\lambda_3 = (1+k) * \sum_{n+1}^{\infty} [P_n] + (1-k) * m_0 / 2\rho_p \sum_{r=1}^{n-1} \left(\sum_{i=r+1}^{\infty} [P_i] \right) \left(\sum_{j=n-r-1}^{\infty} [P_j] \right)$$

λ_1, λ_2, λ_3 are parameters in the reaction equation and could be considered as constants if dt was short enough,

dt time increment in seconds,

m_0 =42 g/mol, molecular weight of monomer unit,

ρ_P =750 Kg/m^3, density of polypropylene at 210℃,

$[P_n^0]$ concentration of polymer with a chain length of "n" at time t,

n polymer chain length,

k $= \frac{k_{td}}{k_{tc} + k_{td}}$, k_{td} and k_{tc} were the termination reaction constants by disproportionation and combination respectively. If only disproportionation was considered, then k=1.

For the decomposition of the initiator,

$$[I] = [I]_0 \exp(-k_d dt),$$

[I] the initiator concentration at time t,

$[I]_0$ concentration of the initiator at time t=0,

$k_d = A\exp(-E_a / RT)$, (4.3)

the decomposition rate constant of the initiator. For Luperox101 (DHBP, 2,5-bis(tert-butylperoxy)-2,5-dimethylhexane) used in this chapter, $k_d = 1.98 * 10^{12} * \exp(-14950/T)$, where T as the reaction temperature is in Kelvin.

f initiator efficiency. According to the literature [19], f=0.6.

4.2 Numerical Simulation Study of CRPP Production

4.2.1 Coding in MATLAB

A numerical simulation study of the degradation process for CRPP production in this work was realized by MATLAB based on the polymer chain length function presented in equation (4.2). The procedure was as follows:

1) The differential molecular weight distribution data of the starting resin from SEC (or Gel Permeation Chromatography, GPC) were stored in the Microsoft Excel document with a name of "'MWD modeling by Matlab.xlsx". The data from the horizontal axis and vertical axis were stored in the first 2 columns of sheet2, respectively.

2) Parameter values for "k_d, f, I_0, total time, time intervals, m_0, dt" were input into corresponding grids in sheet3 of a .xlsx file.

3) Load the .xlsx file into the MATLAB and ran the script. The results were exported into the file "matlab output". The exported data were in the form of dw/d(logM) vs. logM, and the corresponding MWD curves, as well as the average molecular weights, were calculated.

The logic underlying this MATLAB script was:

1) For this reaction process at a specified temperature, T, and a certain decomposition rate of the peroxide initiator controlled by k_d, a total reaction time, t, was assigned to the model to reach the final reaction conversion, ξ.

2) The calculation was then divided into time intervals, dt= total time t/ time steps number.

3) At time t=0, the original chain length distribution of the polymer $[P_0]$ was transformed using function (4.1). For the next time, t=0+dt, the $[P_n^0]$ turned into $[P_n]$ based on function (4.2). $[P_n]$ was taken then as the initial value for the calculation of the second time step. The calculation carried on for the i-th time step, t=0+i×dt, till to the final loop step. This loop calculation was resorted to a 'for loop' in the MATLAB script.

4.2.2 Sensitivity analysis of model predictions

The sensitivity of model predictions to certain parameter values involved in equation (4.2) was first tested. More specifically, the effect of: (i) time steps, (ii) overall reaction time and (iii) number of discrete MW points in the MWD on the predicted MWD was evaluated.

For the purpose of these calculations, the starting resin MWD was that of PPA sample (Exxon Mobil PP2252E1) and the degradation simulations were carried out at a peroxide concentration of 400ppm Luperox101.

1) Effect of time steps

The effect of time steps on model predictions was evaluated at a peroxide conversion of 99.60% which corresponds to a reaction time of 600 seconds. Results are shown in Table 4.1 and a graphical representation is shown in Fig. 4.2.

Table 4.1 MW modelling results for CRPP from PPA at 180°C, L101=400ppm and f=0.6.

Conversion, ξ	Total reaction time, **t** (s)	Number of time steps	Time interval, **dt** (t)	M_n (g/mol)	M_w (g/mol)	MATLAB computation time (min)
0%				74,268	316,573	
99.60%	600	10	60.00	58,985	199,948	1
99.60%	600	100	6.00	56,006	183,580	1.5
99.60%	600	1000	0.60	55,704	181,990	10
99.60%	600	5000	0.12	55,676	181,849	30
99.60%	600	10000	0.06	55,673	181,832	180 or freeze

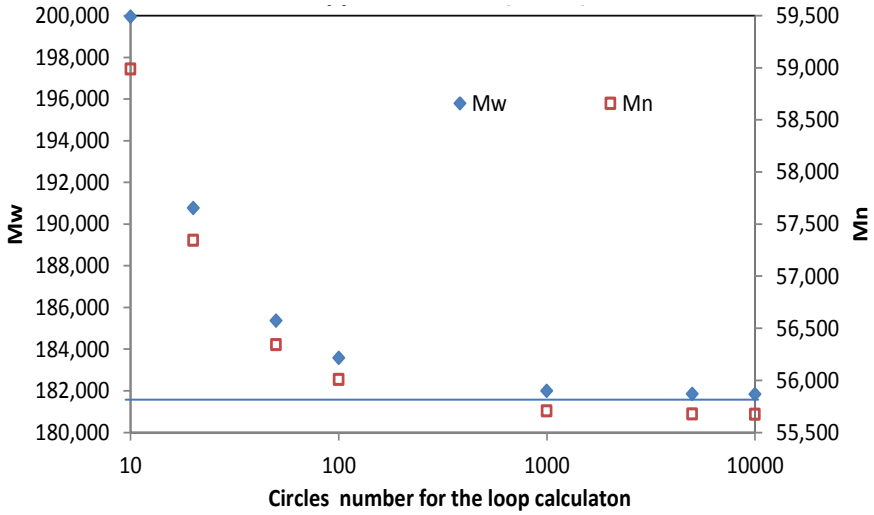

Fig. 4.2 M_w and M_n evolution of model predictions as a function of time steps (180°C, L101=400ppm, f=0.6 and a reaction conversion of 99.6%).

It can be seen that when the number of time steps is equal to or greater than 1000, the model predictions of M_w and M_n are constant suggesting that the minimum number of time steps to be used should be 1000.

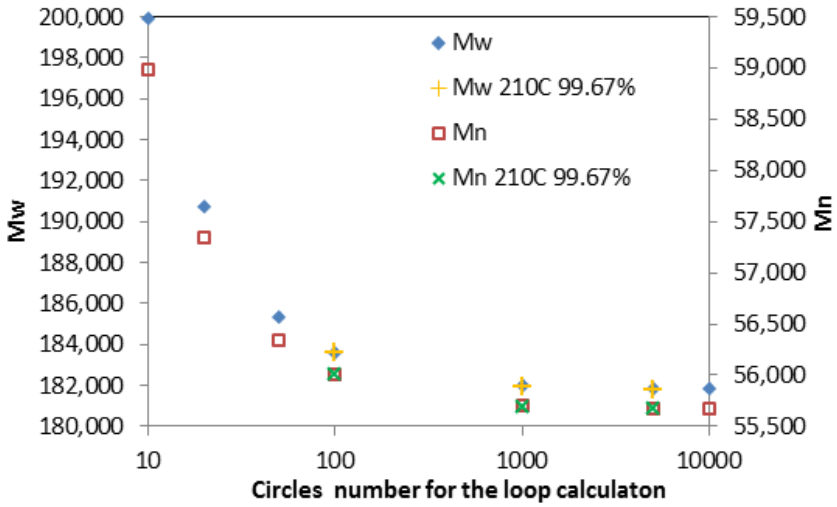

Fig. 4.3 M_w and M_n evolution of model predictions at different temperatures (180/210℃, L101=400ppm, f=0.6 and a reaction conversion of 99.60/99.67%).

The effect of time steps number on model predictions was tested at temperatures of 180℃ and 210℃ as well and the results are shown in Fig. 4.3. It can be seen again that the limiting number of time steps is 1000. Based on this result, 1000 time steps have been used in the rest of the simulations in this thesis.

2) Effect of total reaction simulation time

The effect of the total reaction time used in the simulations on the final MWD and MWs was tested as well. Results for M_w and M_n are shown in Fig. 4.4 using 1000 time steps, 210℃ and a peroxide concentration of 400 ppm. It can be seen that a reaction simulation time of approximately 100 seconds is adequate to capture the final MWs.

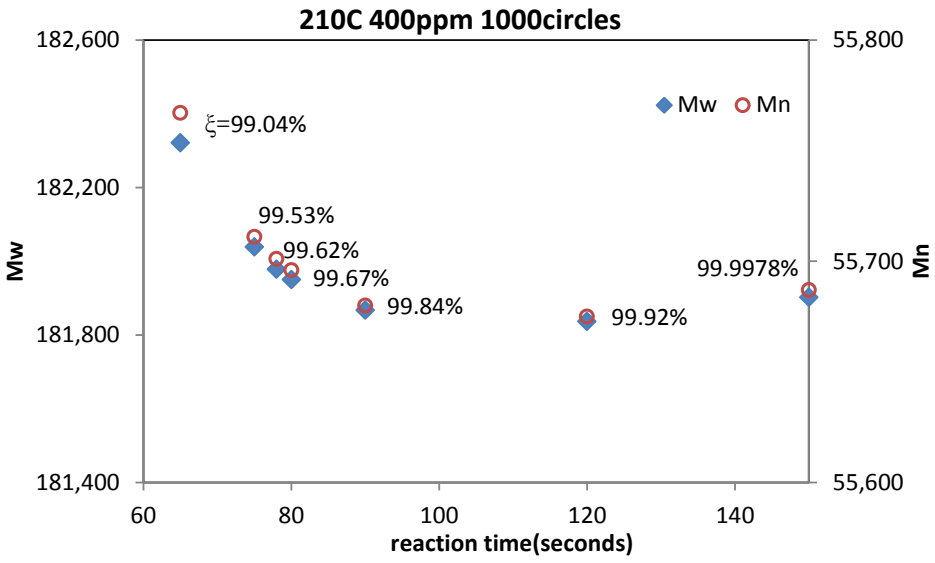

Fig. 4.4 Effect of the total reaction simulation time on MW predictions.

3) Effect of number of discrete MW points in MWD

The original MWD of PPA obtained from GPC measurements contained 1090 discrete MW data points. Simulations were carried out using that MWD as well as a condensed one containing 130 data points. Simulation results highlighting the effect of MWD sample size on model predictions are shown in Fig. 4.5. Based on this, it was decided to use a large MWD sample size to ensure more accuracy in the predictions and to preserve the constancy of λ_3 in the model equation (4.2).

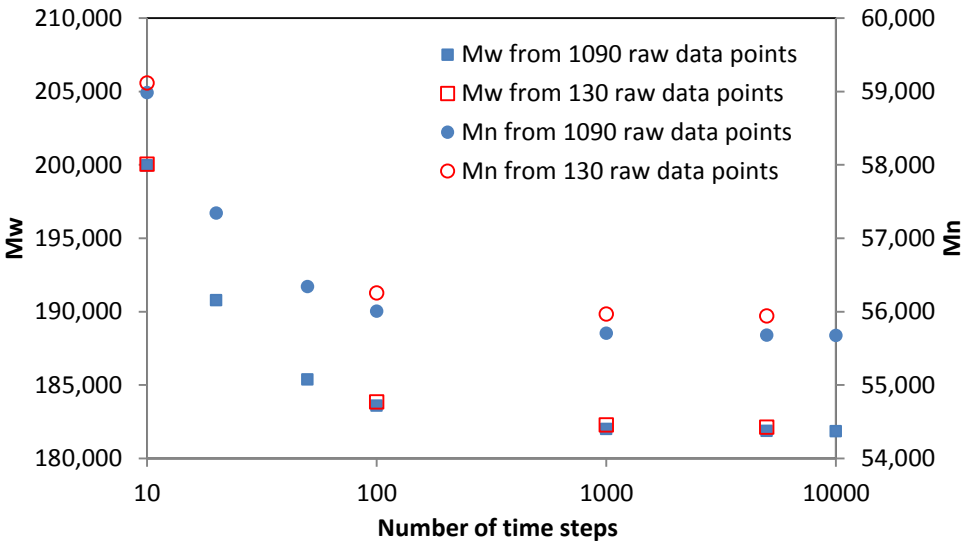

Fig. 4.5 Effect of MWD raw data size on the predicted M_w and M_n.

4.2.3 Comparison of model predictions and experimental data for CRPP from mPP resin

All literature studies have focused on the simulation of CRPP from Ziegler-Natta based polypropylene (ZN-PP) resins. Here, a comparison is made between model predictions and experimental data for a metallocene PP (mPP) resin.

The experimental data were obtained from a previous unpublished study from Professor Tzoganakis' lab. A metallocene type polypropylene (sample mPP249) with a polydispersity index (PDI) of 3.10 was used as the virgin resin to generate a series of CRPPs by peroxide induced degradation at various initiator concentration levels ranging from 100 to 1500ppm. Molecular weight distribution curves were tested by GPC for both virgin PP and CRPPs and are shown in Fig. 4.6.

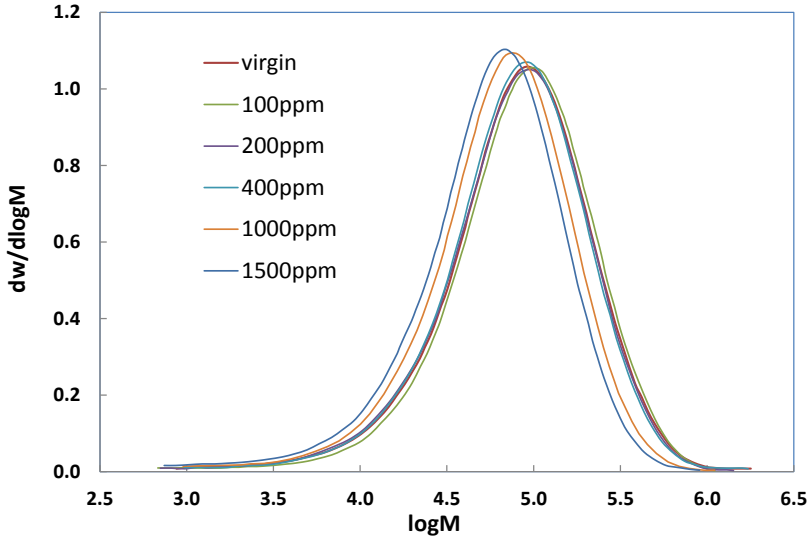

Fig. 4.6 Evolution of MWD curves of mPP249 from experimental study.

The predicted evolution of MWD as a function of peroxide concentration is shown in Fig. 4.7 and a comparison between predicted and experimental MWDs and average MWs and PDI is shown in Fig. 4.8 and Fig. 4.9.

In comparison with previous studies on ZN-PP, it can be seen that the MWD does not change significantly due to the fact that the original MWD is close to the "most probable" one. Also, it

was found that at low peroxide concentration (<400 ppm), there is a slight increase in MW. This may be attributed to creation of long-chain branches generated by grafting of the terminal unsaturated ends in the metallocene PP on the macroradicals generated by scission reactions. A large fraction of terminal C=C in mPP can result from beta-hydride elimination during chain transfer in the polymerization process which is not common with Ziegler-Natta type catalyst. The conformation of the C=C bonds in virgin mPP will be discussed in Chapter 5.

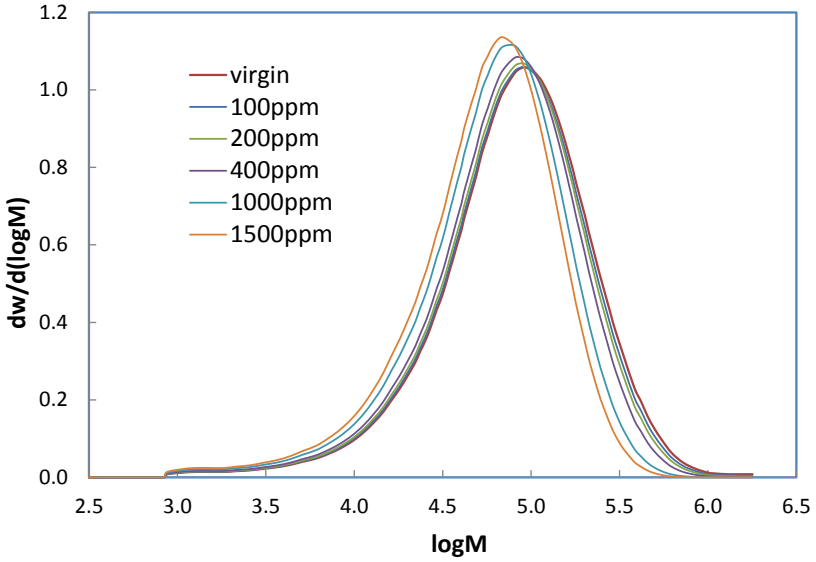

Fig. 4.7 Model predictions of MWD evolution as a function of peroxide concentration for mPP249.

However, once the concentration of the peroxide reached higher levels (>400 ppm for this resin), a reduction in MW as a function of peroxide concentration was observed similar to the one in ZN-PP based CRPP.

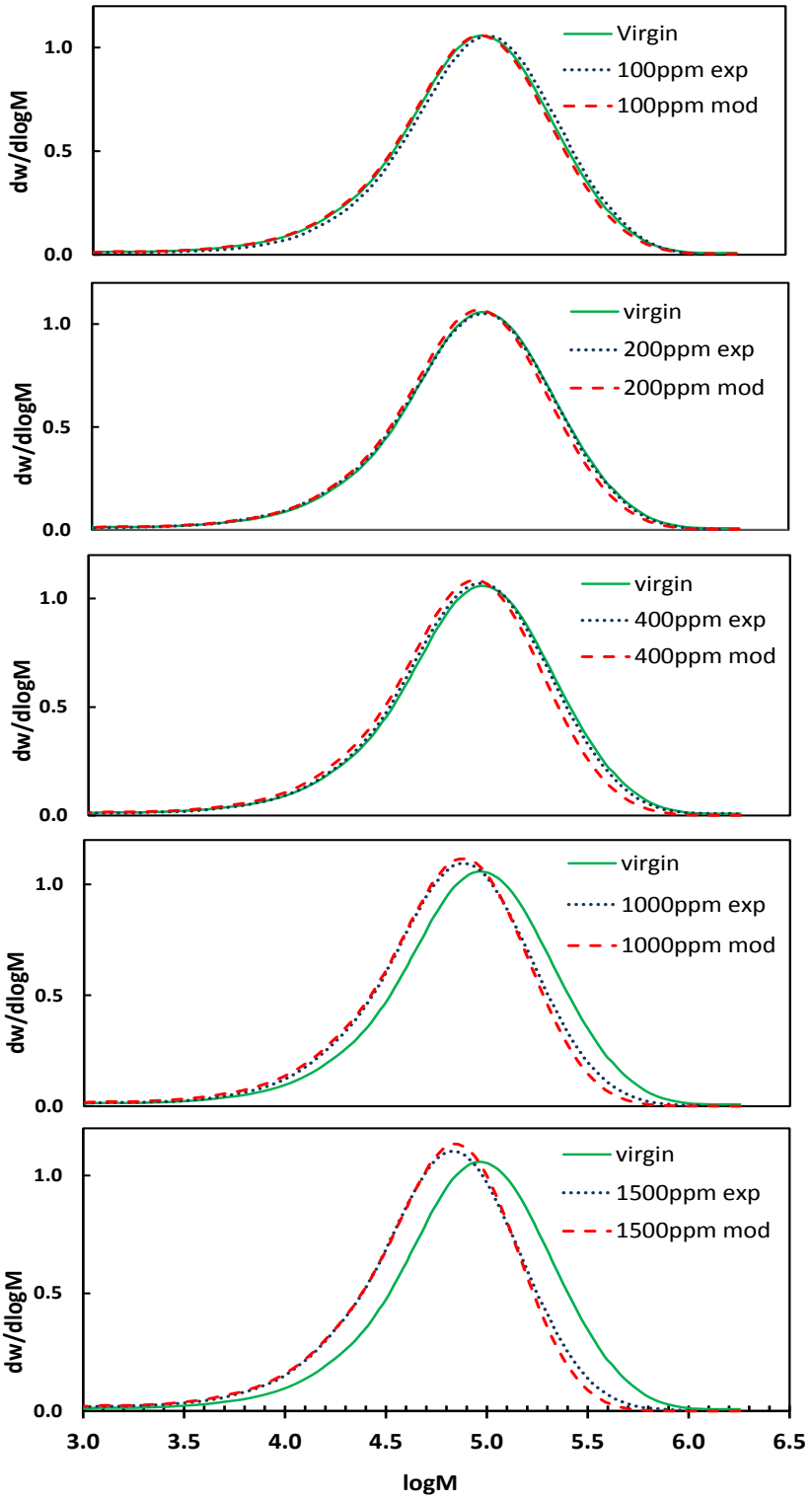

Fig. 4.8 Comparison of experimental and predicted MWD curves at various levels of peroxide concentration.

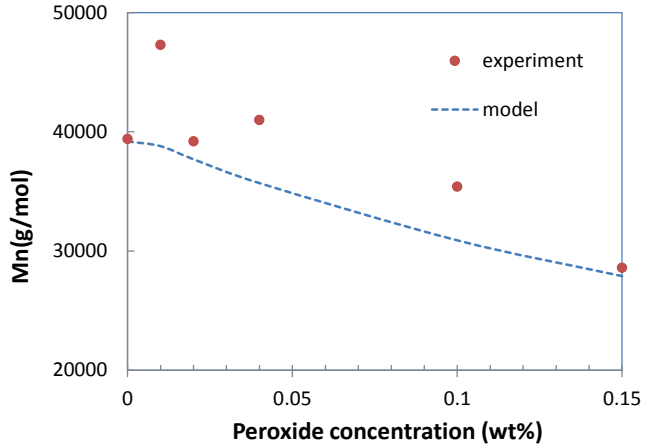

a.

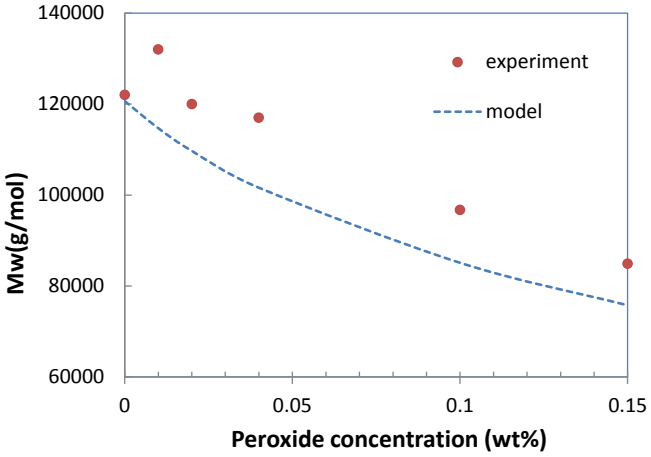

b.

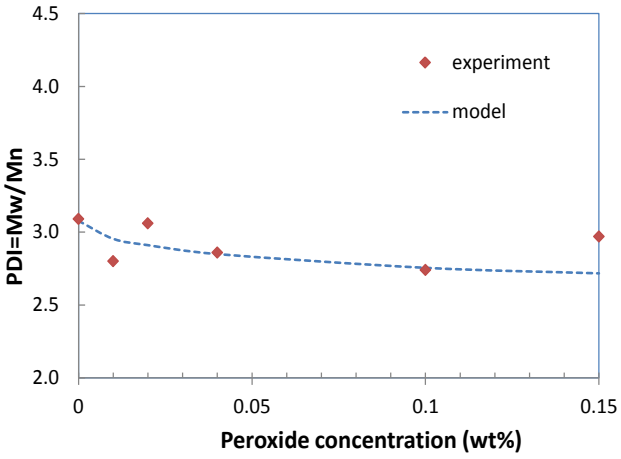

c.

Fig. 4.9 Comparison of experimental and predicted average MW and PDI as a function of peroxide concentration.

4.2.4 Modelling study of ZN-PP and mPP based CRPP

In this section, a modelling study is presented for degradation of mPP and ZN-PP having similar weight average molecular weights. The starting MWD curves and the average MW data are shown in Fig. 4.10 and Table 4.2.

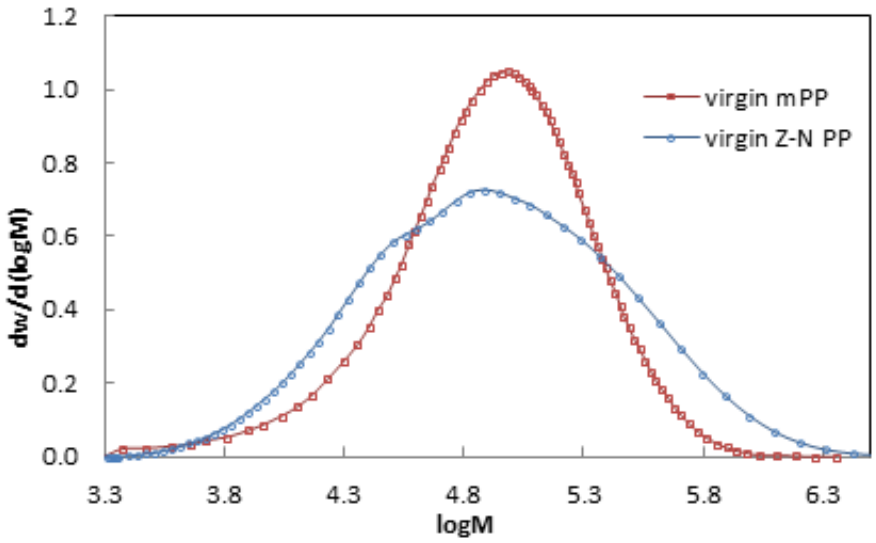

Fig. 4.10 GPC curves of two types of original polypropylene resins with similar average MW levels.

Table 4.2 Average MWs of the virgin mPP and ZN-PP resins.

Orginal PPs	M_n, g/mol	M_w, g/mol	PDI
ZN-PP	4.22E+04	1.75E+05	4.15
mPP	4.56E+04	1.18E+05	2.58

Only disproportionation termination was taken into account this time with the model parameters set as in Section 4.2.2. The concentration of peroxide was 100, 200, 400, 1000, 1500 ppm by

weight fraction of neat polymer. Model predictions for the evolution of MWDs are shown in Fig. 4.11 for both types of resin. It can be seen that for the ZN-PP resin, the MWD becomes narrower as peroxide concentration increases (in agreement with past studies) while the shape of the MWD of the mPP resin remains almost unchanged. In addition, the ZN-PP MWDs move to the left (lower MWs) faster than those of the mPP ones. This indicates a faster reduction of MW for ZN-PP resins. These trends in changing average MW and shape can also be clearly seen in Figures 4.12 and 4.13.

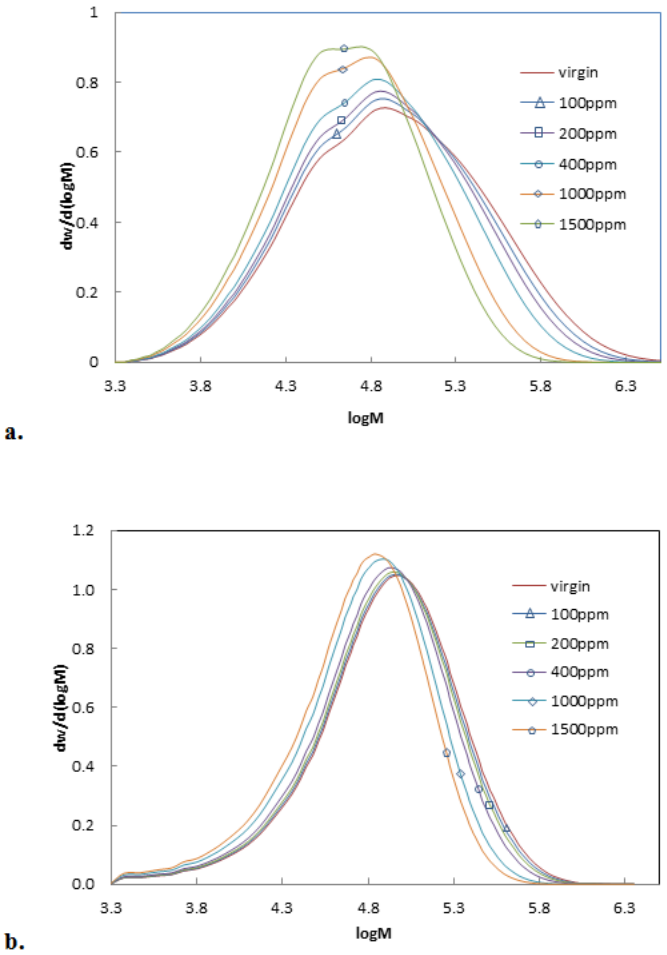

Fig. 4.11 Predicted MWDs of CRPPs from (a) Z-N PP and (b) mPP.

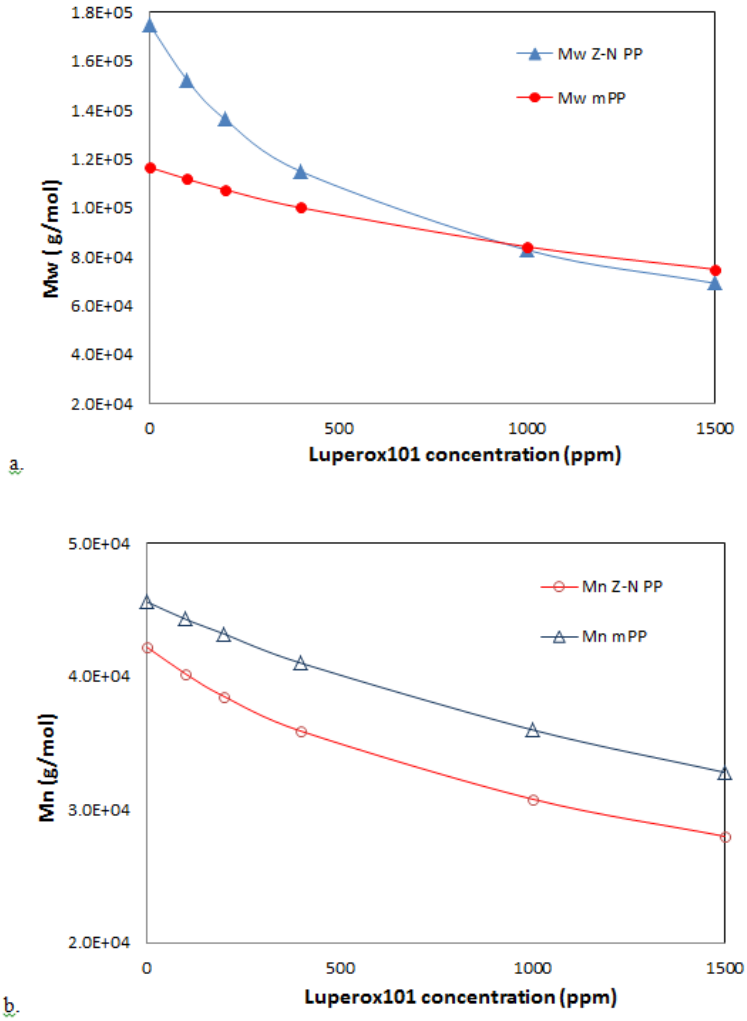

Fig. 4.12 Effect of peroxide concentration on (a) M_w and (b) M_n for mPP and ZN-PP based CRPPs.

A clear difference in PDI evolution can be observed in Fig. 4.13. However, at high peroxide levels both types of resins lead to similar PDI values.

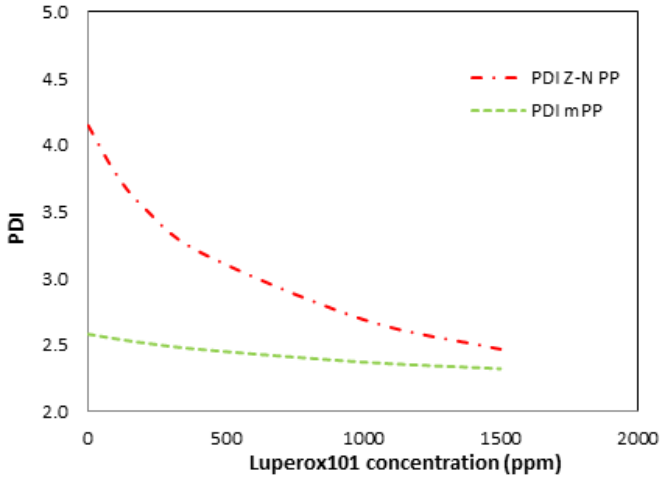

Fig. 4.13 Evolution of the PDI of CRPPs produced from ZN-PP and mPP.

The peroxide initiated degradation of polypropylene is a random scission process. Kotliar [59] studied the resulting molecular weight change of linear polymers undergoing random chain scission. The calculation process resorted to Schulz-Zimm molecular weight distribution function. With increasing scissions per initial number-average of molecule, as shown in Fig.4.14, the weight to number average molecular weight ratio, which is PDI, decreased down asymptotically to PDI=2, the so-called "most probable distribution".

Boyd et al [60] also evaluated the effect of MWD of a theoretical depolymerization initiated by random scission. It also approached the most probable distribution as the degradation process progressed.

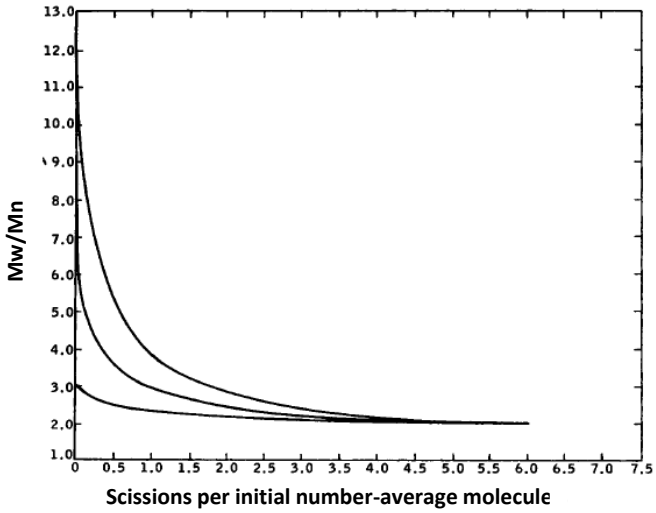

Fig. 4.14 The development of weight to number average molecular weight ratio of a linear polymer under random scission studied by Kotliar [59].

Our results are consistent with those of Kotliar [59] and Boyd et al [60] indicating that the PDI of both ZN-PP and mPP decreased to a limiting value of 2 by increasing concentration of peroxide and for ZN-PP, whose MWD was broader, the reduction in M_w was more drastic compared to that of mPP, whose PDI was already close to 2.

The results of this brief simulation study suggest that the molecular weight characteristics of CRPPs can be controlled not only by peroxide concentration but also by the selection of virgin resin type (mPP vs ZN-PP). This is exploited and presented in the following chapters.

Chapter 5

TAILOR-MADE CRPPS FROM ZN-PP AND m-PP RESINS

5.1 Introduction

Based on the modelling results of Chapter 4, the MWD evolution process in the production of CRPPs is quite different depending on the nature of the virgin resin. In the case of ZN-PP resins, addition of peroxide leads to reduction of both MW and PDI. However, in the case of mPP resins, addition of peroxide leads to reduction of MW leaving the PDI (already very close to the most probable distribution value of 2) relatively unchanged. This difference in degradation behavior can be exploited to produce CRPPs with specific rheological characteristics. It is well known, that weight-average MW controls the zero-shear viscosity of linear PP while PDI dictates its shear thinning behavior. Thus, by employing ZN-PP polypropylenes one can produce CRPP resins having different zero-shear viscosities and different levels of shear thinning while employing mPP one can produce CRPP resins of varying zero-shear viscosity having similar shear-thinning characteristics.

Based on this, four virgin polypropylenes, including ZN-PPs and mPPs with varying molecular weights, were chosen for the degradation study described in this chapter. The objective of this study was to produce CRPPs with tailor-made rheological properties and to illustrate the effect of the starting resin on these properties. All of these resins were commercially available and their trade name and melt flow rate (MFR) are listed in Table 5.1.

Table 5.1 Selected virgin polypropylenes.

PP resins	Supplier & grade	Catalyst type	MFR, g/10min @ 230°C * 2.16 kg
PPA	Exxon Mobil PP 2252E1	ZN-PP	3.5
PPB	Exxon Mobil Achieve 1654	mPP	16.0
PPC	Basell Pro-fax PH350 (ground by INGENIA Polymers)	ZN-PP	11.2
PPD	Exxon Mobil Achieve 1605	mPP	32.0

In the plastics industry, the flow rate of molten plastic at elevated temperature under a certain load is usually measured to characterize its viscosity and approximately (indirectly) its molecular weight. For polyethylene, it is called the melt flow index (MFI) and for polypropylene, it is called melt flow rate (MFR). MFI or MFR are used widely although they represent one point on the viscosity flow curve, usually at low shear rates. Measurement of MFI or MFR can be achieved easily with high repeatability, making this test very valuable. As seen in Table 5.1, the MFR of the chosen polypropylenes range from 3.5-32.0 g/10min, and two of them are Ziegler-Natta type while the other two are metallocene based. In these materials, PPD having the highest MFR value, i.e. the lowest viscosity level, is injection molding grade or used for fiber spinning. PPD is also a metallocene type and has a relatively narrow molecular weight distribution. In these experiments, resins PPA, PPB, and PPC were degraded to the molecular weight or MFR of PPD and rheological behaviors of the resulting CRPPs were compared to those of PPD material.

5.2 Characterization of the Virgin Resins

The molecular weight and the rheological properties of the starting resins where first obtained in order to select appropriate conditions for the production of tailor-made CRPPs.

5.2.1 Molecular weight determination by HT-GPC

The molecular weight distributions (MWD) of the starting resins were obtained (see Fig. 5.1) through gel permeation chromatography (GPC). Average MWs, PDI and intrinsic viscosity [η] were obtained from the GPC test.

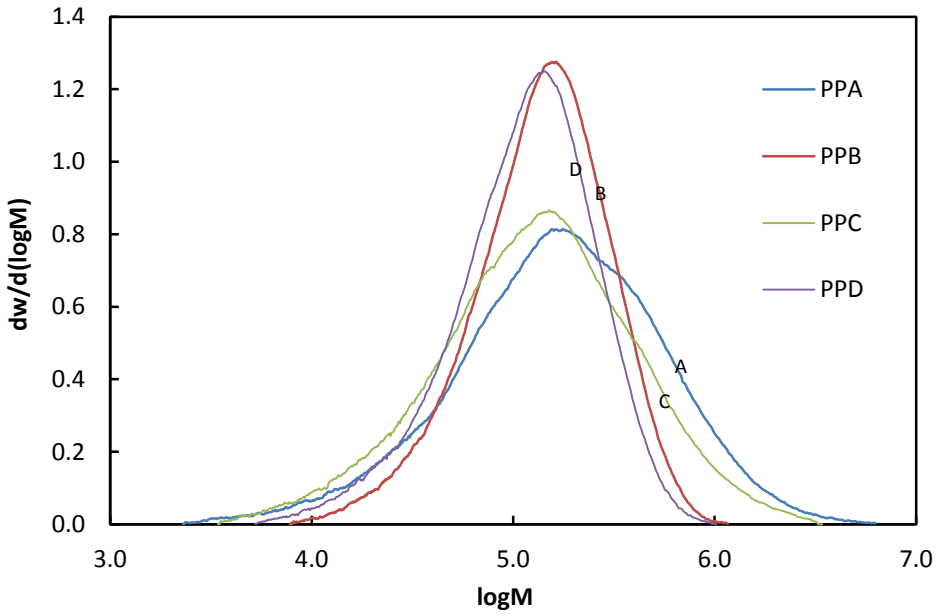

Fig. 5.1 MWD of the virgin polypropylene resins from HT-GPC.

In this work, a high temperature GPC (HT-GPC) unit (Polymer CHAR (Spain)), with refractive index, FT-IR and viscometer detectors, was employed to determine molecular weight. 1, 2, 4-trichlorobenzene (TCB) was used as the GPC eluent at 140 °C. 13-15 mg of polypropylene

sample was dissolved in 9 ml of TCB, with 50 mg/l Irganox 1010 to avoid degradation, at 160 °C for 90 minutes. The solutions were inspected visually first for complete dissolution prior to injection.

The MWD curves of the virgin resins are shown in Fig. 5.1 and average MWs and PDI values are listed in Table 5.2.

Table 5.2 Average MW and PDI values of virgin resins.

Sample	M_n, g/mol	M_w, g/mol	M_z, g/mol	PDI
PPA	74,300	316,600	924,900	4.26
PPB	98,200	177,800	273,900	1.81
PPC	65,300	234,800	643,900	3.60
PPD	76,900	149,200	234,600	1.94

5.2.2 Rheological characterization by oscillatory shear rheometry

Frequency sweep tests from 0.01 to100Hz of the virgin materials in their LVE region were performed using a TA Instruments AR2000 rheometer with 25mm diameter parallel-plates at 180°C. All samples were firstly hot-pressed at 180°C into 1 mm thick disks and cooled down by quenching in a water bath before the test. The procedure of the test was described in Section 3.2 of Chapter 3. The results are presented in Fig. 5.2.

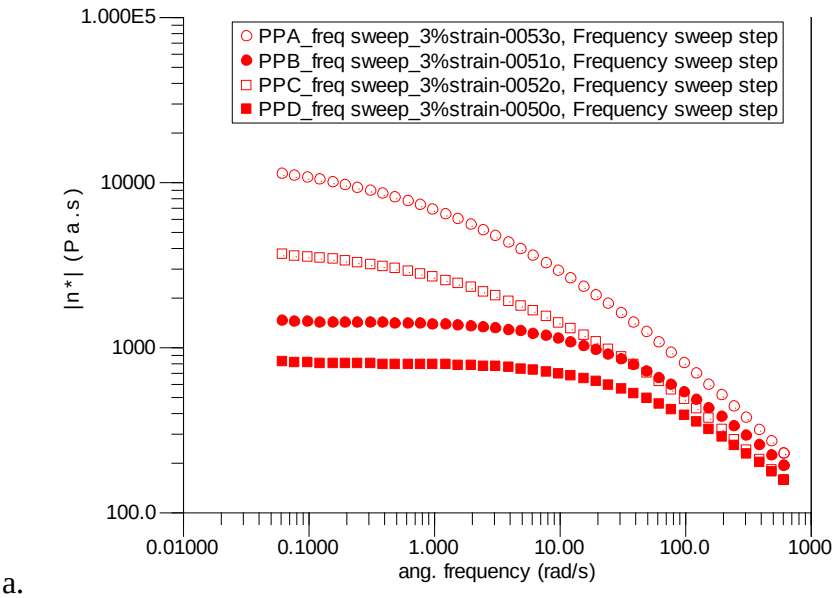

a.

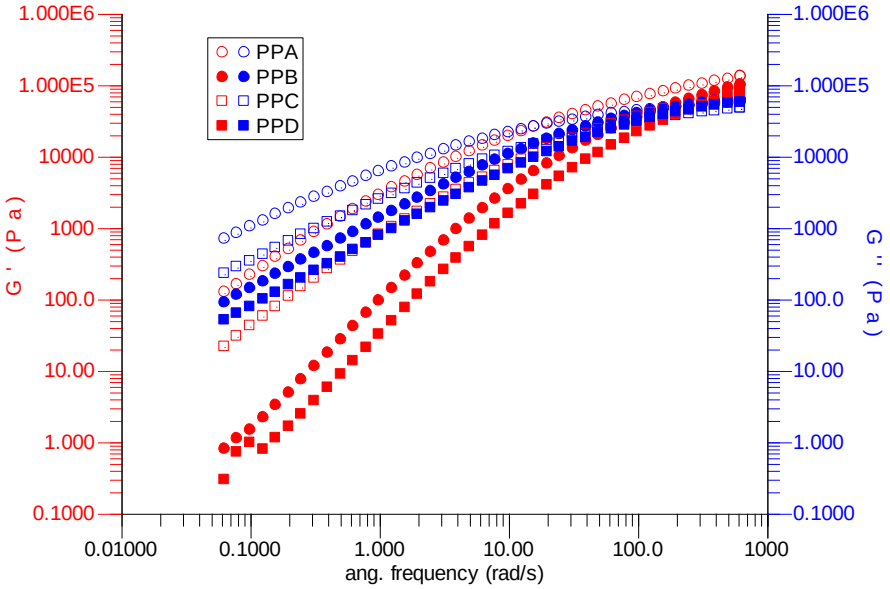

b.

Fig. 5.2 Complex viscosity (a) storage and loss moduli (b) of virgin materials from frequency sweep test.

The zero-shear viscosity as determined from the complex viscosity in the terminal zone (very low frequencies), follows the same trend as the corresponding weight average molecular weight as: PPA>PPC>PPB>PPD. The width of the Newtonian plateau region of the mPPs was larger

than that of the ZN-PPs and at high shear frequencies the ZN-PPs exhibited stronger shear-thinning than mPPs as expected due to the broader ZN-PPs' MWD. The larger separation between G' and G" for mPPs compared to ZN-PP also implied this result. Using the G' and G" values, the calculated Modsep index values are listed in Table 5.3 along with PDI values. A good correlation exists between ModSep at 500Pa and PDI (see Fig. 5.3) and it can be used to estimate and compare the polydispersity of the CRPPs.

Table 5.3 Polydispersity of virgin PPs from rheology and GPC.

Sample	ModSep@500Pa	ModSep@1000Pa	PDI
PPA	3.07	3.74	4.26
PPB	7.29	5.63	1.81
PPC	4.45	3.72	3.60
PPD	7.30	5.65	1.94

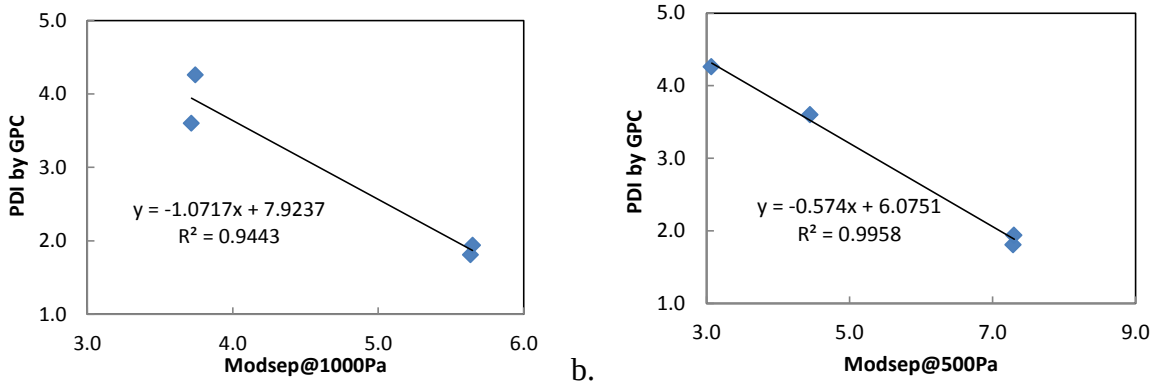

Fig. 5.3 Polydispersity measurement from rheology and GPC.

The correlation between zero-shear viscosity (η_0) and weight-average MW is shown in Fig. 5.4 and the regression equation is shown in Equation 5.1:

$$\eta_0 = 7E\text{-}16 * M_w^{3.4874} \quad (5.1)$$

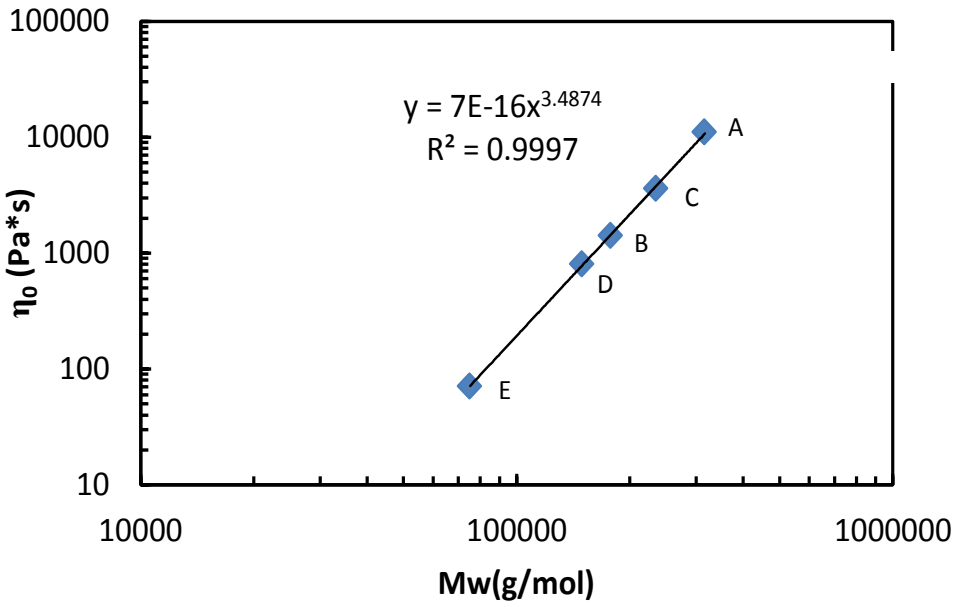

Fig. 5.4 Correlation between zero-shear viscosity (at 180°C) and weight-average molecular weight.

(*Sample E was another linear ZN-PP not for this project with a M_w of 75,200 g/mol)

The dependence of η_0 on M_w was in very good agreement to literature results [1] for polymers with linear structure. This correlation will be used in the following experiments to determine the M_w by measuring η_0 instead of employing time-consuming GPC measurements.

5.3 Production of Target CRPPs

In this study, CRPPs were produced from the starting virgin resins PPA, PPB and PPC. The objective was to produce CRPPs having similar properties to those of PPD. Weight-average MW and MFR are used as key properties.

In order to come up with the conditions for producing such CRPPs, first the effect of peroxide concentration on the degradation path for PPA, PPB and PPC is studied. By producing CRPP

series from different original resins with increasing peroxide dosage, the dependence of MW and MFR on peroxide concentration will be obtained and it will be later used for preparing PPs of tailor-made properties.

5.3.1 Tailor-made CRPPs having similar molecular weight (MW)

Using the three virgin resins (PPA, PPB, PPC) experiments were carried out to produce a series of modified CRPPs. The range of peroxide concentrations used was based on previous screening tests and on kinetic model simulations. Peroxide concentrations of 400, 500, 700, 1000 ppm for PPA, 50, 100, 200, 300 ppm for PPB and 100, 250, 350, 500 ppm for PPC were employed in the batch mixer process described in Chapter 3.

Oscillatory shear (frequency sweep) tests of all products were carried out at 180°C to obtain the zero-shear viscosity, $\eta_{0.}$ Following that, equation (5.1) was used to estimate the M_w of these materials. The evolution of η_0 and M_w with peroxide concentration of the three CRPP series is shown in Fig. 5.5. Based on this information, the amount of peroxide required to degrade PPA, PPB and PPC to the MW of PPD, was estimated (indicated by dashed lines in Fig. 5.5). These peroxide concentrations are 880, 100 and 390 ppm for PPA, PPB and PPC, respectively.

Using these peroxide concentrations, the target CRPPs, named A880, B100 and C390, were produced in the same way in the batch mixer. The target materials were then subjected to oscillatory shear measurements to check the zero-shear viscosity level. The viscosity curves of A880, B100 and C390 are plotted along with that of PPD in Fig. 5.6 and it can be seen that all have similar zero-shear viscosities implying similarity in M_w.

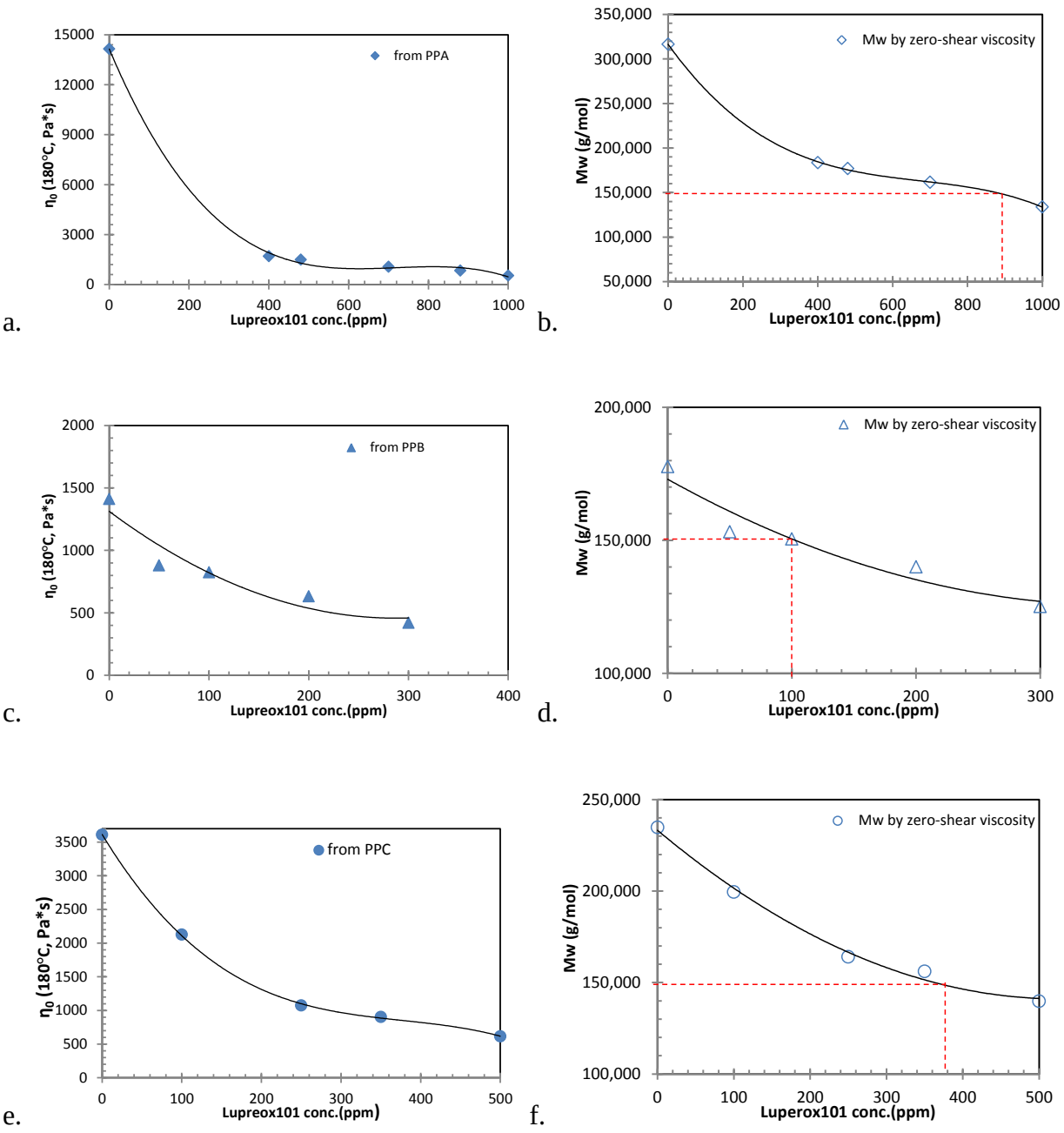

Fig. 5.5 Evolution of η_0 and M_w with peroxide concentration of CRPPs from PPA, PPB and PPC.

(Solid symbols refer to η_0 and open symbols refer to Mw; Diamond, triangle and circle symbols stand for CRPPs from PPA, PPB and PPC, respectively. The dashed lines were drawn to guide the eye for the target CRPPs with respect to the peroxide requirement.)

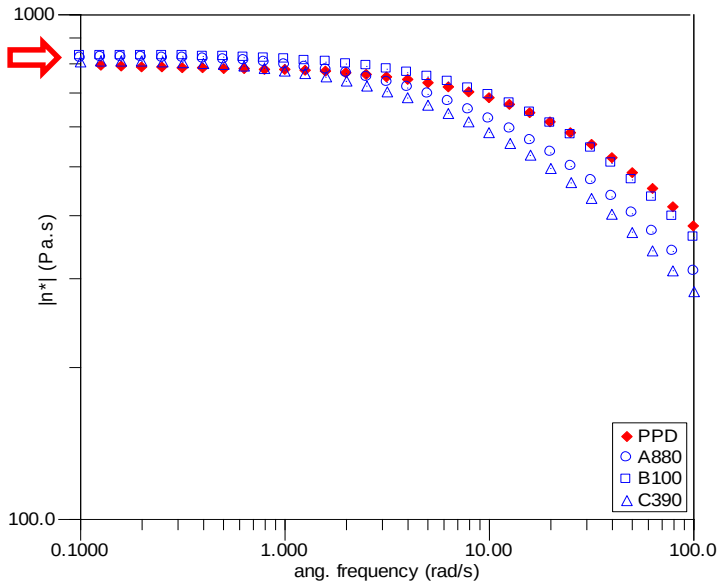

Fig. 5.6 CRPPs with similar zero-shear viscosity as PPD.

In other words, CRPPs with similar M_w were produced successfully and their processing behavior will be discussed in the next chapter.

5.3.2 Tailor-made CRPPs having similar Melt Flow Rate (MFR)

As mentioned previously, the MFR test is used widely in the plastics industry due to its simplicity and repeatability. The MFR values of the CRPPs produced in Section 5.2.2 were measured by a MFR tester (KAYENESS, Fig. 5.7) following the ASTM D1238 standard at 230 °C and a loading weight of 2.16 kg.

a.

b.

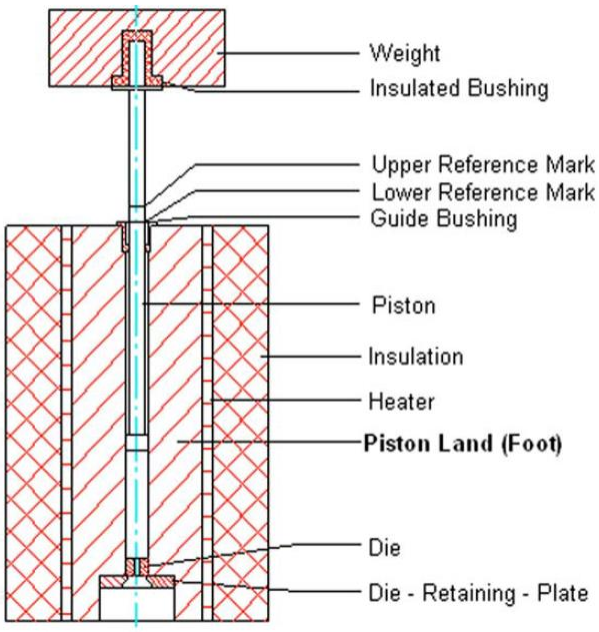

Fig. 5.7 MFR tester and drawing of the inner extrusion plastometer (a&b).

a.

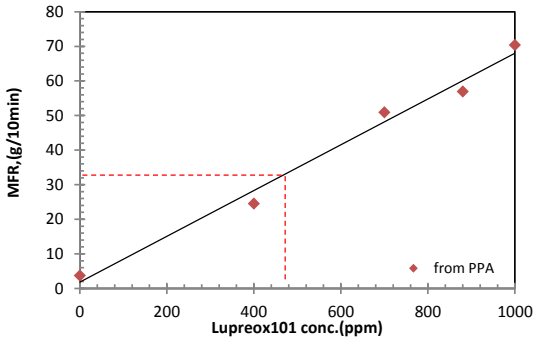

b.

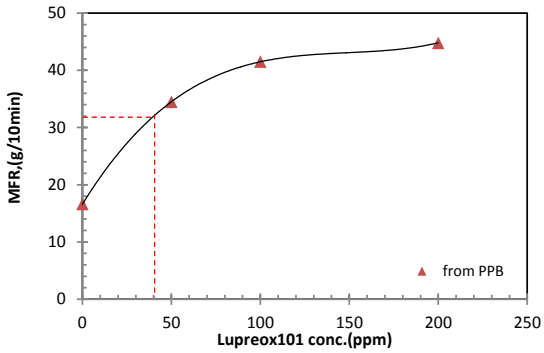

c.

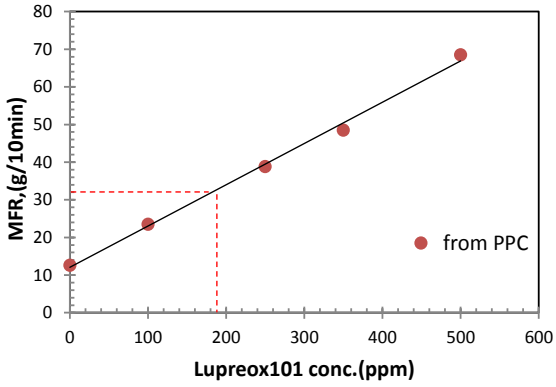

Fig. 5.8 Evolution of MFR along with the peroxide concentration of CRPPs from PPA, PPB and PPC.

The evolution of MFR with peroxide concentration for the three series of CRPP is shown in Fig. 5.8. The dashed lines illustrate the peroxide dosage required to produce CRPPs with the same MFR of PPD (MFR of PPD =32 g/10 min). These are estimated to be 480, 40 and 190 ppm for PPA, PPB and PPC, respectively. Using these concentrations, three target CRPPs, named A480, B40 and C190 were subsequently produced and their MFR levels are compared in Fig. 5.9. These CRPPs having similar MFR were also studied in terms of their processing behavior as discussed in the next chapter.

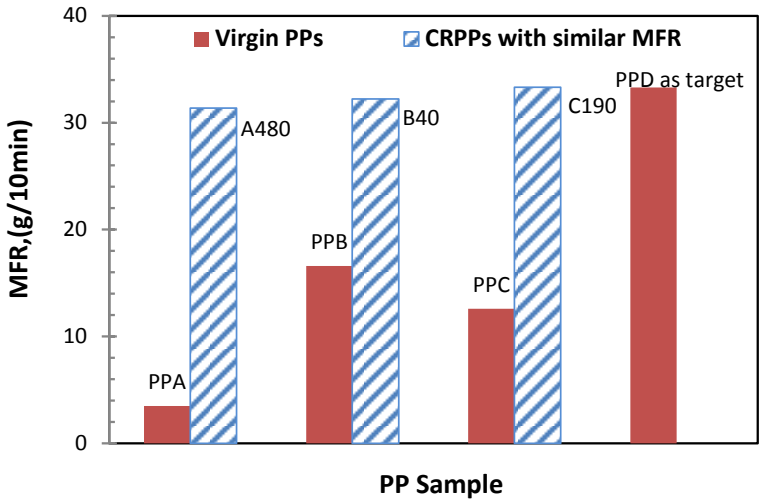

Fig.5.9 Comparison of the produced CRPPs with the similar MFR value as reference resin.

5.3.3 Comparison of modelling and experimental results

The kinetic model discussed in Chapter 4 was used to predict the M_w of the target CRPPs produced experimentally in this chapter. The effect of peroxide concentration on the predicted M_ws is shown in Fig. 5.10 (dashed lines) along with the experimental values (symbols in Fig. 5.10) estimated from the zero-shear vs. M_w correlation.

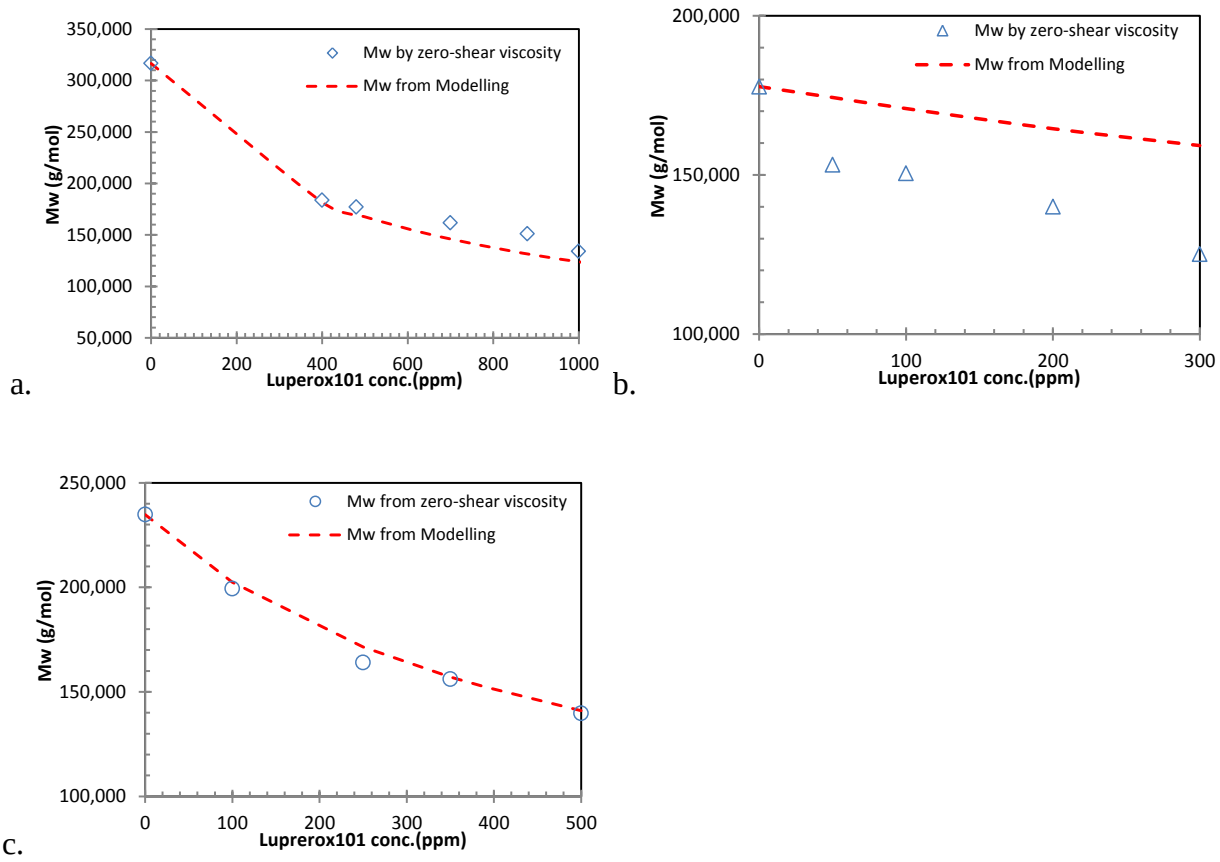

Fig. 5.10 Comparison of modelling and experimental results for CRPPs produced from PPA, PPB and PPC (a, b and c, respectively).

By inspection, it can be seen that the agreement is very reasonable for the CRPPs produced from ZN-PP resins (PPA and PPC).

However, for the CRPPs from PPB, a metallocene type polypropylene, the predicted Mw values were higher than the experimental ones. This discrepancy may be attributed to the presence of terminal double bonds in the mPP, PPB. Such terminal double bonds may participate in the degradation reactions and potentially lead to formation of branched chains. From such a

branched material, the M_w estimated from η_0 would be lower. To investigate the presence of double bonds, FT-IR analysis of the starting mPP and ZN-PP was performed. The virgin resins were hot-pressed into very thin layers (~0.15 mm) at 180 °C and quenched in a cool water bath. The spectra were acquired by a FT-IR spectrometer (FTLA 2000, ABB Inc., Canada) at wavenumber range from 4000 to 400 cm^{-1} and 1cm^{-1} resolution with 16 scans per sample. Terminal C=C bonds were detected from the IR spectrum peak at 888 cm^{-1}, the C-H out-of-plane bending of vinylidene [56]. The relative absorbance of the three samples was calculated and plotted together in Fig. 5.11 using the C-C-C bending peak at 459 cm^{-1} as the internal reference. It can be clearly seen that PPB and PPD (mPPs) indeed contain such terminal C=C bonds.

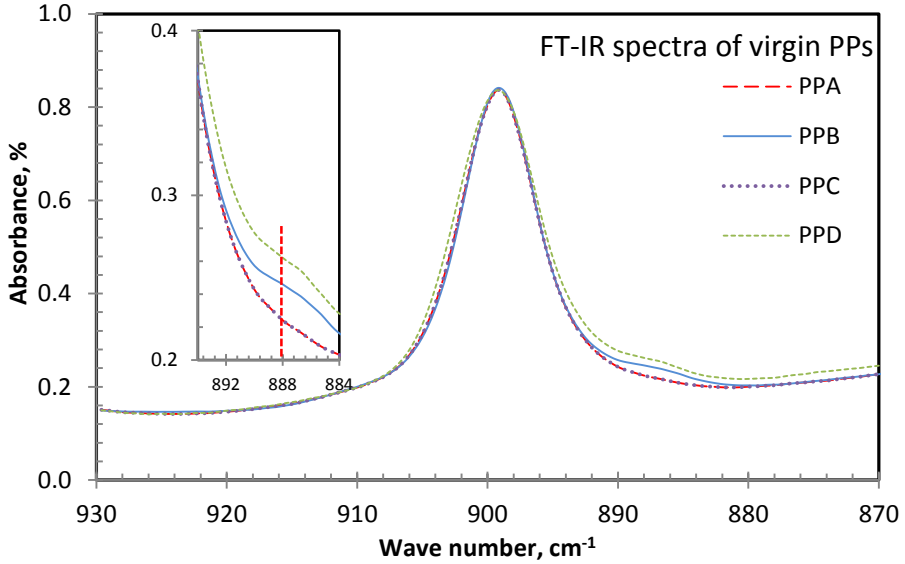

Fig. 5.11 Infrared absorbance of virgin PPs.

For most metallocene-based catalyst systems, β-hydride elimination is considered to be a predominant mechanism for chain termination [63-64] that usually leads to formation of

vinylidene chain ends. The presence of the terminal double bonds in PPB might contribute to a different reaction path, thus leading to the discrepancy between modeling and experimental results presented above.

5.4 Chapter summary

In this chapter, four grades of commercial polypropylenes, containing Ziegler-Natta and metallocene type, were chosen as the starting or reference material for CRPP production. Based on M_w and MFR, two series of tailor-made CRPPs were produced. Both of these CRPPs were subjected to extrusion for process behavior study which will be discussed in the following chapter.

During the production of CRPPs, the zero-shear viscosity was successfully employed for monitoring the molecular weight evolution due to its pronounced power-law relationship with the M_w. With respect to making those CRPPs with similar MFR, the materials were characterized by direct MFR testing.

Experimental results from this chapter were also taken to compare with the modelled results with a common peroxide efficiency. CRPP properties generated from ZN-PP type agreed quite well with this model. However, regarding the mPP, the degradation reaction took place with higher degree than the model described and this might be attributed to the contribution of the terminal C=C bonds in this type of virgin materials.

Chapter 6

RHEOLOGICAL CHARACTERIZATION OF CRPPS AND THEIR EXTRUSION BEHAVIOR

In this chapter, the extrusion behavior of CRPPs is studied. CRPPs with similar molecular weight (MW) or melt flow rate (MFR) produced in Chapter 5, together with the virgin PPD reference resin, are extruded continuously through a die and their melt fracture characteristics are compared.

6.1 Extrusion Set-up

6.1.1 Single screw extruder

CRPPs were produced in a batch mixer as described earlier but in multiple batches to collect adequate material for the continuous extrusion experiments. These materials were subsequently ground into uniform pellets for extrusion on a small scale using a single screw extruder. During single-screw extrusion, the mass flow rate of the polymer is controlled by the rotational speed of the screw, and the resistance of the die attached to the extruder.

A mini lab scale single screw extruder HAAKE Rheomex 252p was employed for this job. It can be attached onto the Rheocord 90 system with ports for temperature control and pressure measurement. The specifications of this extruder are given in Table 6.1.

Table 6.1 Specification of Rheomex 252p.

Barrel	
Diameter, D	19.05 mm(3/4”)
Length, L	25*D
Heating/cooling Zones	3 zones
Feed section, maximum flight depth	3.75 mm
Standard sensor ports	3
Optional sensor ports	up to 6, in total
Functionality	
Maximum torque	160 Nm
Maximum operation temp	450 °C
Maximum operation pressure	700 bar
Heat capacity	1000 W
Dimensions	
Weight	net 110 kg
Length/Width/Height	720/420/1200 mm

This Rheomex 252p has a L/D ratio of 25/1 and three independent heating zones. It is specially designed for testing the plastification and flow behavior of thermoplastics under process conditions. To connect the extruder barrel with the extrusion die, a connection zone (adapter) with a flow channel and heating band was joined with the end of the extruder by a flange. With another threaded tube and a flange, the prolonged barrel could then be connected with the

specialized dies. The set-up of the extrusion line is shown by Fig. 6.1. At the open orifice of the die, a water bath was set for cooling and collection of the extrudates.

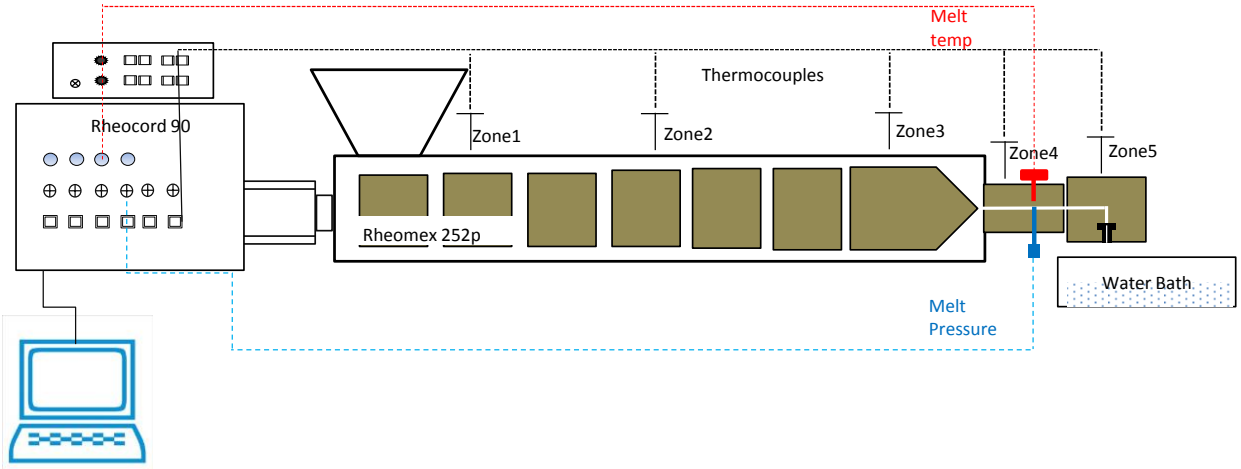

Fig. 6.1 Set-up of the single screw extrusion line with 5 heating zones.

The first 3 heating zones are for the HAAKE extruder itself. Zone 4 is for the connection zone and zone 5 is for the extrusion die, respectively, with the heating system having one heating band and one controlling thermocouple.

In zone 4, two open holes were drilled. One can be connected with a thermocouple to detect the temperature of the polymer melt and the other can be used for pressure measurements by connecting a pressure transducer. The pressure transducer was calibrated by a manual pressure oil pump before starting. All temperature and pressure signals were recorded by the Rheocord90 control panel.

6.1.2 Extrusion die

Zone 5 was designed for the die part. For this extrusion study, the extruded CRPP fibers were going to be collected for surface appearance investigation. Once the fibers came out from the die, they should be well cooled and collected without too much stretching and damaging the surface. For that purpose, a vertical extrusion die was preferred since the extrudate could fall down by gravity into a water bath filled with ice water so that the extrudate would be quickly quenched so the surface is solidified.

In this die design we employed existing capillary dies from our KAYENESS capillary rheometer. For that purpose, a die holder was designed in which capillary dies of different L/D could be accommodated. The assembly design drawing as well as the picture view is shown in Fig. 6.2. All dimensions are shown in millimeters. The upper part was the bulk section on which a heating band with the same width was fastened from the outside. The horizontal flowing channel was connected to zone 4 with the same diameter of 6.12 mm. In the bulk center, the flowing channel was transformed into the vertical direction with a diameter as the entrance of the standard die of 9.5 mm. The standard die could be fastened on the vertical channel by the lower section, a flange, with six bolts distributed outside the rim. The step height of the dies was a bit higher than the depth of the upper section step hole. As the standard dies were made from tungsten carbide with very high hardness, while the assembly was relatively soft carbon steel, once the die was held by the bolts and the flange, the die would hit into the bulk carbon steel to generate a sealing for the polymer melts.

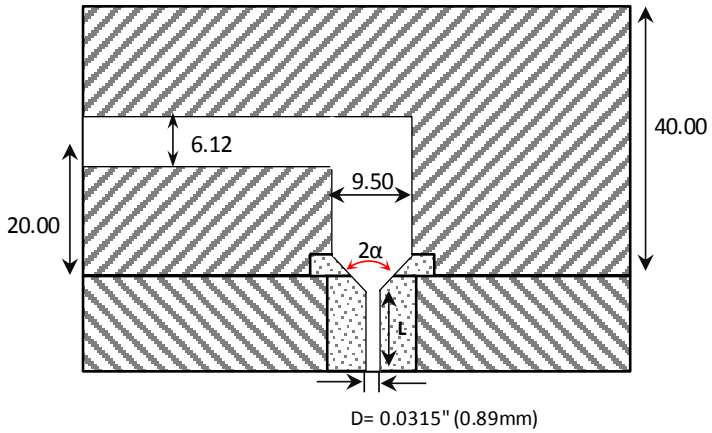

a.

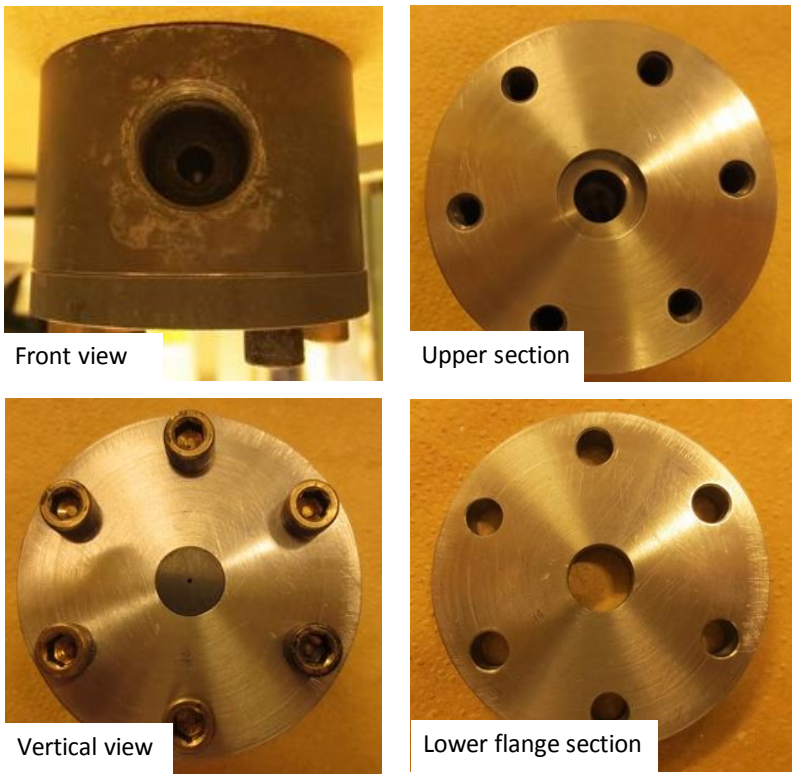

b.

Fig. 6.2 Cross section drawing (a) and picture views (b) of the vertical die assembly.

During this study, we used a die with an entrance angle of 90°, a diameter of 0.0315" and a L/D ratio of 9.

6.1.3 Extrusion profile

The heating temperature profile for the polypropylenes used here is shown in Table 6.2.

Table 6.2 Extrusion temperature profile for the processing study of CRPPs.

Zone	Zone1	Zone2	Zone3	Zone4	Zone5
Functionality	feeding	melting	pumping	adapter	die
Temperature, °C	80	180	190	190	140~240
Extrusion speed			1~100 rpm		

The ground CRPP pellets were fed into the hopper manually and by adjusting the rotation speed from 1 to 100 rpm, the extrusion speed was tuned. In the meantime, the processing data, such as the total torque and the pressure drop along the die were detected from zone 4 and recorded by the RC9000 Control and Data Acquisition software. The temperature of zone 5 was varied to study its effect on the extrudates and their processing.

6.2 Extrusion Behavior of the Virgin Polypropylene

The metallocene type virgin PPD resin, as the reference material, was firstly subjected to extrusion at various processing conditions.

The extruder was heated up and held to steady state for 10 minutes. Then adequate amounts of PPD pellets were introduced into the feed hopper. At a fixed temperature profile and rotation

speed (the extrusion speed), mass flow rate (MFR) in kg/h, was measured by weighing the mass of the extrudate collected within a certain span of time, for example, 15 seconds. Three measurements were taken and the average value is used for all analyses. The pressure was continuously recorded and only the pressure at the stable period was used as the pressure for that corresponding extrusion speed (see Fig. 6.3). The extrudate surface roughness was observed during the pressure stable period and quenched samples were collected from the water bath for later study.

The apparent shear rate at the wall of the capillary die was calculated by the equation:

$$\dot{\gamma}(R) = \frac{4Q}{\pi R^3} \tag{6.1}$$

where Q was the volumetric flow rate which could be calculated from the recorded MFR as Q=MFR/ρ (for these polypropylene melt at around 190°C temperature, ρ=0.75g/cm^3), and R was the diameter of the capillary.

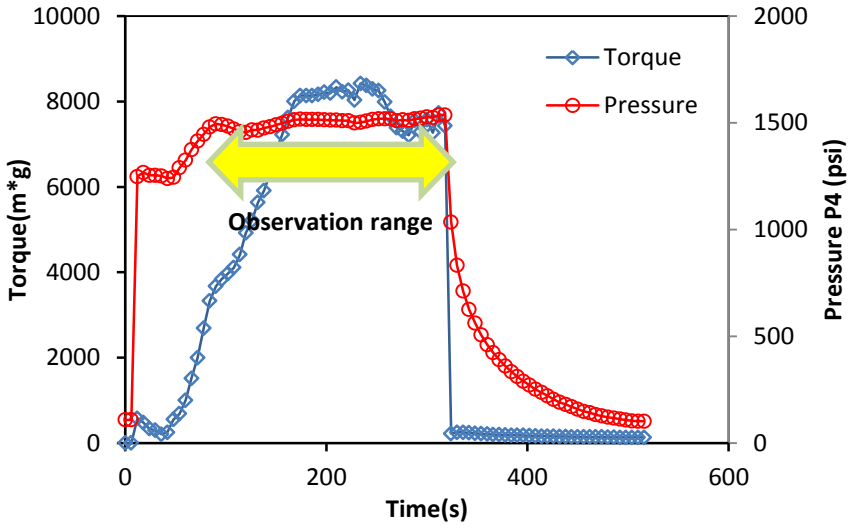

Fig. 6.3 Extrusion pressure and torque data of PPD at specific extrusion speed.

The pressure of the polymer melt flowing from the extruder and through the adapter (Zone 4) was recorded from a port as shown in Fig. 6.4. Assuming the viscosity along the flowing channel, η, is roughly constant, one can use the Hagen-Poiseuille equation as:

$$Q = \frac{\pi R_1^{\,4}}{8\eta\ L_1}(P_0 - P_1) = \frac{\pi R_2^{\,4}}{8\eta\ L_2}(P_1 - P_2) = \frac{\pi R^4}{8\eta L} P_2 \tag{6.2}$$

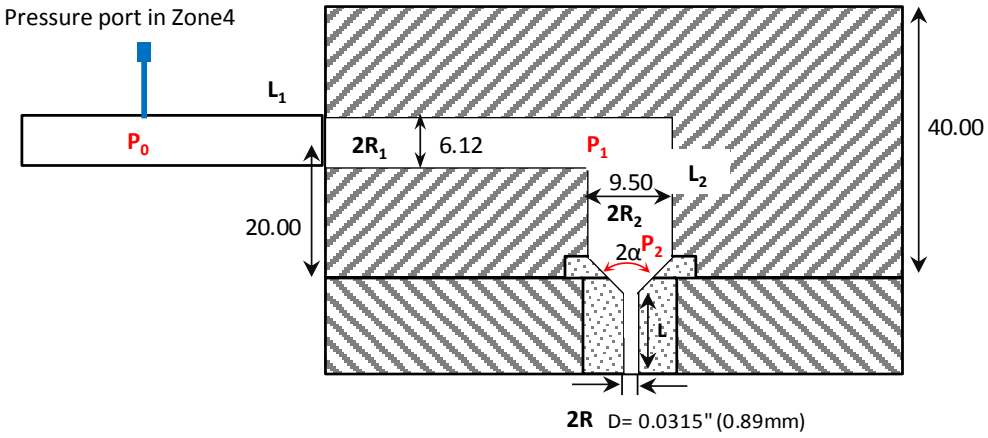

Fig. 6.4 Pressure distribution along the flow channel.

where L_1, L_2, L =85, 20, 8 mm and R_1, R_2, R = 3.06, 4.75, 0.89 mm, respectively. Then this yields:

$$\Delta P = P_2 \approx 92.5\% P_0 \tag{6.3}$$

Thus, we can roughly take the measured pressure from Zone 4 as the pressure drop of the polymer melt flow through the capillary die, ΔP.

6.2.1 Extrusion curves and melt-fracture

The extrusion of the PPD virgin resin was studied first at a die temperature of 140°C. The extrusion speed MFR is plotted against the rotational speed of the screw in Fig. 6.5. We can see that the MFR increases linearly with the rotation speed for this single screw extruder. Thus, the required MFR can be achieved by selecting the appropriate rotational speed (N).

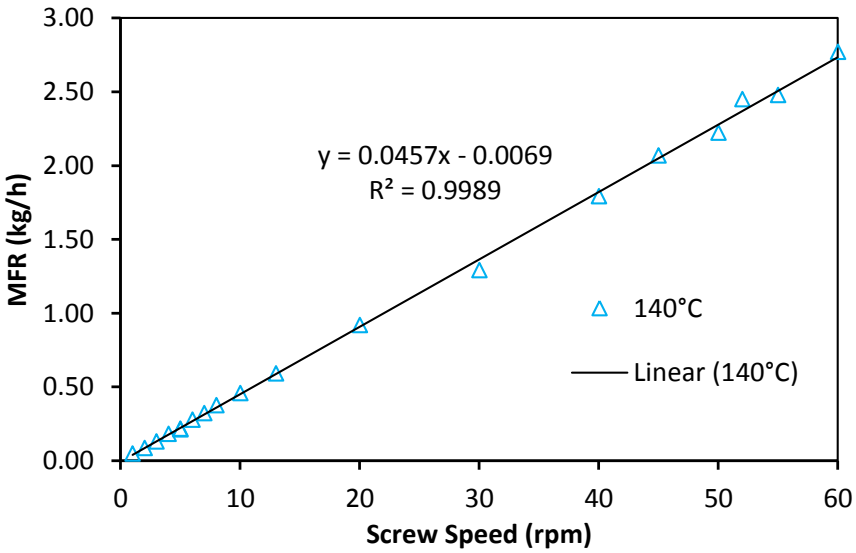

Fig. 6.5 Extrusion speed as a function of screw rotation speed for PPD at die temperature of 140°C.

The pressure drop between the entrance of the die and its open face, ΔP, is plotted against the apparent shear rate in Fig. 6.6. At low shear rate (<1000 s^{-1}in the curve), the pressure increased linearly with shear rate. A similar linear trend was observed at high shear rates.

For the steady flow of an incompressible fluid in a tube of radius R, driven by a pressure gradient (dP/dz) along the channel, a force balance on the cylindrical element of fluid gives:

$$\sigma(r) = \frac{r}{2}(-\frac{dP}{dz}) \tag{6.4}$$

At the wall, r=R, also both stress and (dP/dz) are negative, we get:

$$\sigma_w = -\sigma(R) = \frac{R}{2}(-\frac{dP}{dz}) = \frac{R}{2}(-\frac{dP}{dz}) \tag{6.5}$$

For a non-Newtonian fluid at the wall, the apparent viscosity is:

$$\eta_{app} \equiv \frac{\sigma_w}{\dot{\gamma}_{app}} = \frac{\sigma_w}{\dot{\gamma}_w(\frac{4n}{3n+1})} \tag{6.6}$$

where n is the shear thinning index in the power law model.

As a shear-thinning material, PPD was less viscous at higher shear rate, and therefore the shear stress at the wall was less which led to a lower pressure drop according to equations (6.6) and (6.5).

The quenched extrudate samples were collected during the steady pressure period for each run and their photos are displayed in Fig. 6.7. The shape of the extrudate changed from smooth to rough and the distortion of the extrudate became more and more obvious with increasing amplitude at higher shear rates. It was found that at a die temperature of 140 °C, the rough surface was observed at rotational speed of 8 rpm while the calculated apparent shear rate was

1996 s^{-1}. This critical condition can be seen as the onset point of the melt fracture occurrence and it lies on the transition zone (non linear part of curve) of the extrusion curve in Fig. 6.6.

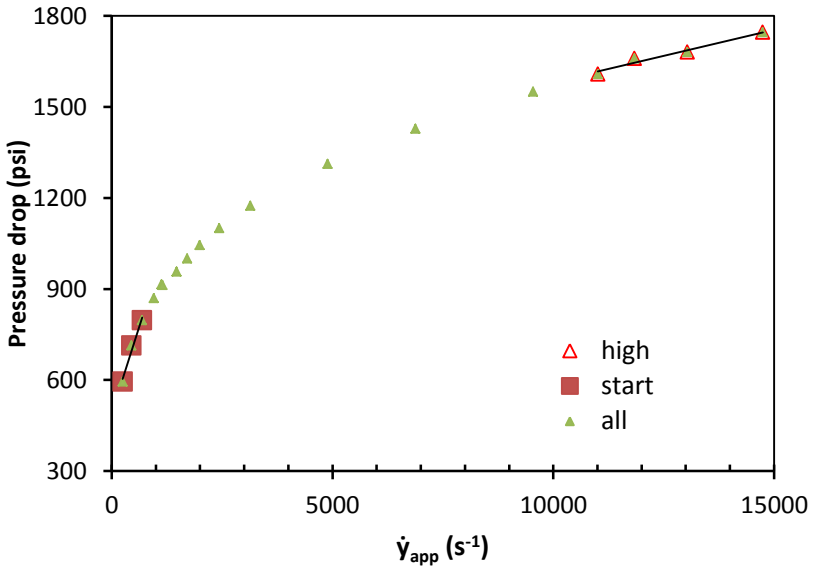

Fig. 6.6 Die pressure drop as a function of apparent shear rate for PPD during extrusion at die temperature of 140°C.

In addition, at the onset shear rate, the pressure curve of PPD was still continuous which was different from numerous reported cases of the pressure jump at onset of melt fracture of HDPE etc. materials [65].

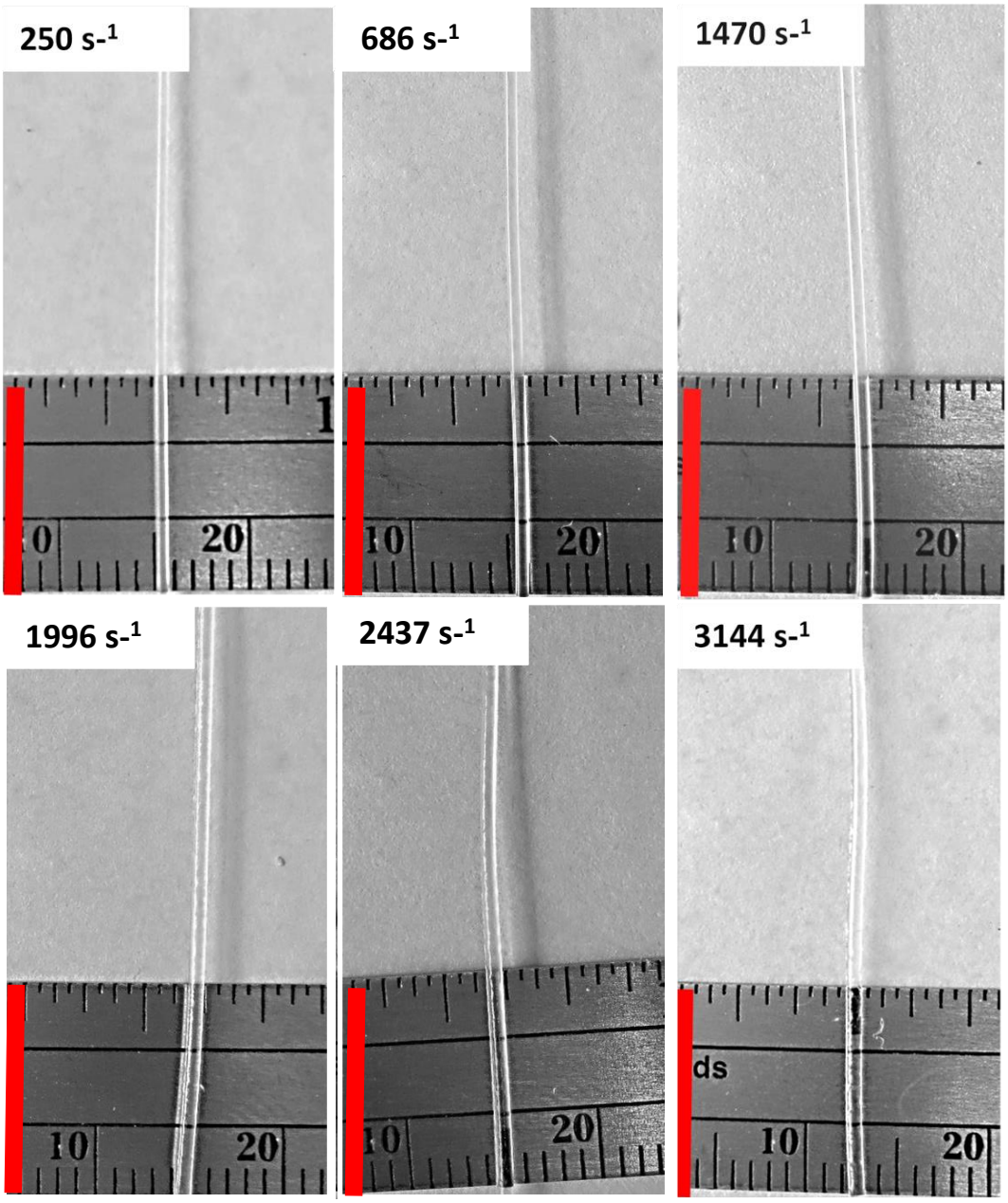

(Fig. 6.7, continued next page)

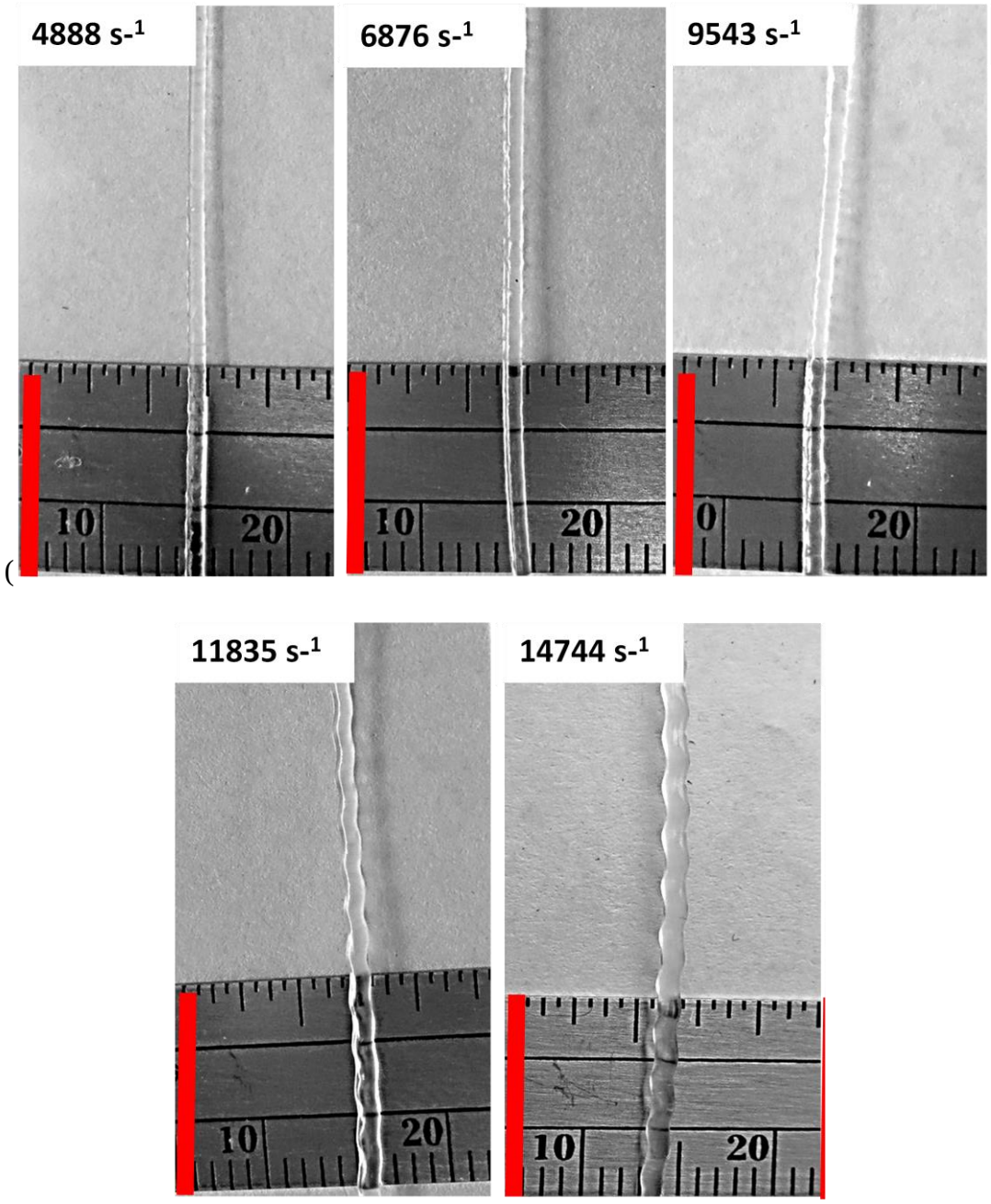

Fig. 6.7 Collection of PPD extrudates from 1 rpm to 60 rpm of screw rotational speed at T(die)=140°C

(the labelled number is the calculated apparent shear rate)

6.2.2 Extrusion at different die temperatures

The extrusion curves of PPD as well as the onset apparent shear rate was studied in a similar way at various die temperatures ranging from 140°C to 200°C. The results are presented in Fig. 6.8. The extrusion rate of PPD at these die temperatures varied linearly with screw rotational speed as expected. The pressure drop curves at higher die temperatures were shifted to lower level at the same shear rate since the viscosity of the polymer melt was reduced. The onset shear rate for melt fracture increased at high temperature, however, the pressure drop values for this critical point were almost the same (~1000 psi).

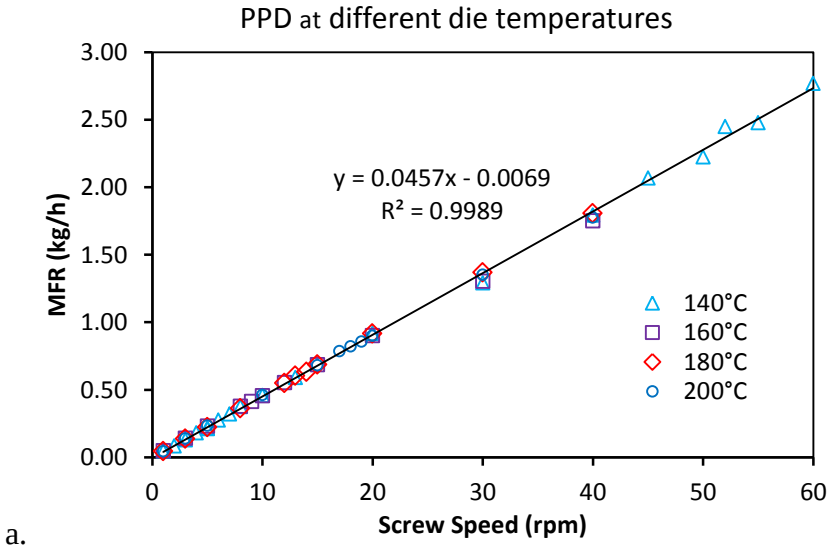

a.

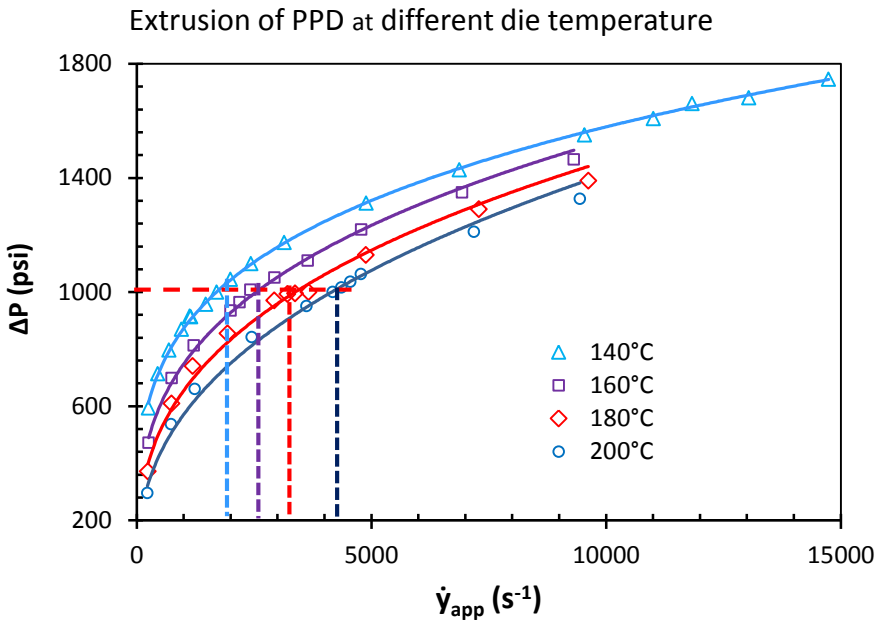

b.

Fig. 6.8 Extrusion curves of PPD at different die temperatures.

(the dashed line in (b) indicates the onset points of melt fracture)

6.3 Extrusion of CRPPs with Similar MW

6.3.1 Comparison of rheological properties

The produced CRPPs with similar zero-shear viscosity, PPD, A880, B100 and C390 as presented in Chapter 5, were compared here for their rheological properties in detail. First, the frequency sweep data from oscillatory shear measurements were fitted by Carreau-Yasuda model which describes the pseudoplastic flow with zero-shear viscosity at Newtonian region, shear-thinning with a power-law slope and no yield stress. It is expressed as:

$$\frac{\eta-\eta_\infty}{\eta_0-\eta_\infty}=[1+(\lambda\dot{\gamma})^a]^{(n-1)/a} \tag{6.7}$$

where the viscosity at infinite shear rate can be assumed as zero for our polypropylene melts; λ is an average relaxation time , where 1/λ is the critical shear rate at which the Newtonian plateau ends and viscosity begins to decrease with increasing shear rate. The power-law slope is (n-1) and the parameter α represents the width of the transition region between the Newtonian and power-law behavior.

The raw data and the model fitting of these CRPPS are illustrated in Fig. 6.9. The parameters yielded from the fitting as well as the rheological PI are summarized in Table 6.3. From the PDI and ModSep correlation in Fig. 5.5 from Chapter 5, PDI=-0.574×ModSep@500Pa+6.0751, we can estimate their PDI with sequence as: PDI (from narrow to broad: PPD, B100, A880, C390) = (1.88, 2.17, 2.84, 3.03). The shear thinning behavior followed the same sequence with increasing power law index, n. Regarding B100 which was derived from the metallocene PPB with similar narrow PDI as PPD, the MWD became broader. This probably resulted from the chemical reaction of terminal C=C bonds in the virgin resin leading to formation of LCB.

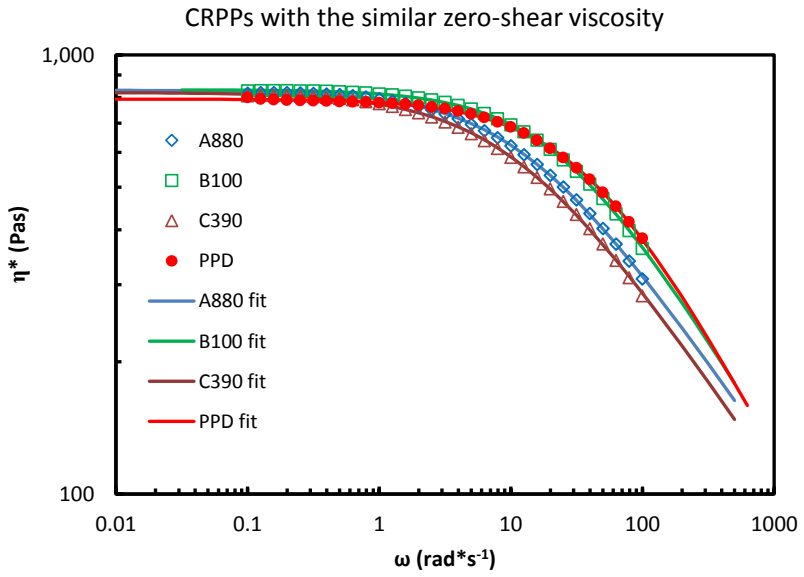

Fig. 6.9 Raw data and Carreau-Yasuda fitting of complex viscosity of CRPPs (tested at 180°C) with similar MW.

Table 6.3 Rheological characteristic parameters for CRPPs with similar MW.

Sample	η_0, Pa*s	a	λ, s	n	ModSep@1000Pa	ModSep@500Pa
A880	831.3	0.9083	0.08089	0.5649	4.55	5.64
B100	833.5	0.9810	0.04314	0.5069	5.30	6.81
C390	821.6	0.8664	0.09291	0.5583	4.32	5.30
PPD	793.7	0.9433	0.02567	0.4361	5.64	7.31

The relaxation time spectra (see Fig. 6.10) of these CRPPs were also calculated using NLREG (nonlinear regularization) program developed by Freiburg Materials Research Center [79]. Based on the Tikhonov regularization, from the G'(ω) and G"(ω) raw data determined by frequency

sweep, the relaxation time spectrum can be generated within the time range of the reciprocal of swept frequency.

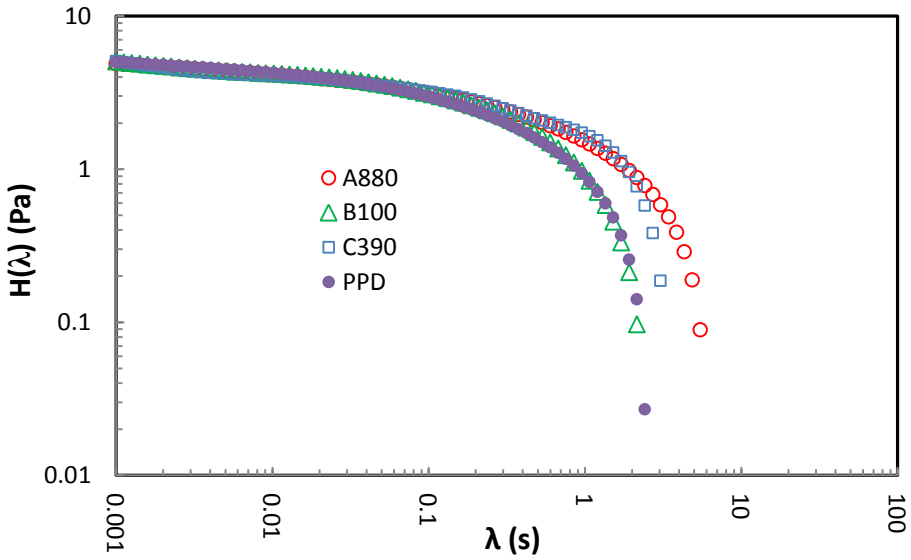

Fig. 6.10 Relaxation time spectra of CRPPs with similar MW.

6.3.2 Comparison of the extrusion behavior

All of the three new produced CRPPs were also introduced into the single extruder in the same way as the reference material, PPD, for extrusion study at a die temperature of 160°C. The extrusion curves of the CRPPs, together with the onset shear rate for melt fracture, were compared with the reference PPD. Following the PDI sequence from narrow to broad, the pressure drop rate of increase was reduced as their shear thinning strength enhanced from low to high, and the onset shear rate for melt fracture increased (see Table 6.4). However, the onset pressure drop for melt fracture of these materials were not the same and they increased with shear thinning behavior.

If we assume the approximation in equation 6.3 is valid for all these materials at the extrusion range in Fig. 6.11, from equation 6.5 we can get the onset shear stress at the die wall for the melt fractures as listed in Table 6.4. We can see higher onset shear stress was required for the materials of broader MWD while the M_w values were similar.

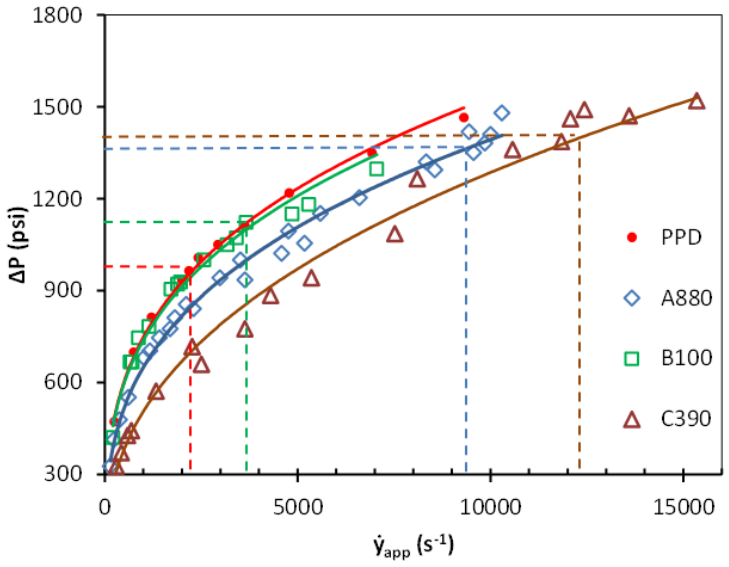

Fig. 6.11 Extrusion curves of CRPPs with similar MW at die temperature of 160°C.

Table 6.4 Onset conditions for melt fracture during extrusion of CRPPs with similar MW.

Sample	$\dot{y}_{app}(s^{-1})$	P_0(psi) [a]	ΔP(psi) [a]	σ_w(MPa) [b]
PPD	2194	964	892	0.17
A880	9447	1418	1312	0.25
B100	3667	1123	1039	0.20
C390	12076	1460	1351	0.26

(a. P_0 is the directly detected pressure from the transducer in Zone 4, and ΔP was calculated according to equation (6.3). b. shear stress at die wall was calculated from equation (6.5).)

6.4 Extrusion of CRPPs with Similar MFR

6.4.1 Comparison of rheological properties

The produced CRPPs with similar MFR, A480, B40 and C190 as demonstrated in Chapter 5 were also characterized by the rotational rheometer. Since the MFR test represents the flow ability of the polymer melts at the same applied pressure, here we compare their viscosity as a function of shear stress obtained from the frequency sweep data (Fig. 6.12).

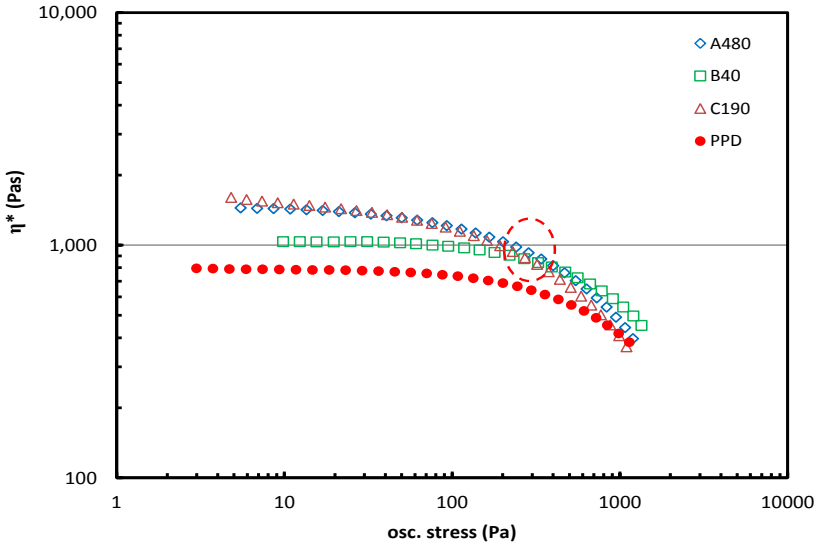

Fig. 6.12 Complex viscosity as a function of oscillatory shear stress during frequency sweep test of the CRPPs with similar MFR.

With respect to A480, B40 and C190, their viscosity is similar at a shear stress around 300 Pa as shown by the circle in Fig. 6.12. This result was in agreement with the MFR results. Although these samples had the same MFR of 32 as PPD (Fig. 5.11), these three peroxide-modified

materials exhibited higher viscosity than PPD at that stress of 300 Pa. This might be due to the fact that the antioxidant of their virgin materials had been consumed during CRPP production while the virgin PPD still maintained a certain amount of antioxidant as a commercial resin. During the 7 min preheating period of the MFR test, however, an open system without nitrogen gas protection as the rotational rheometer did, these resins would be degraded. Thus, their tested MFR were the same, although the peroxide-modified CRPPs' viscosity level was higher at the same shear stress level. Therefore, for this study, it would be better to add extra antioxidant into the peroxide-treated polypropylenes during the MFR test as well as the extrusion study.

6.4.2 Comparison of the extrusion behavior

These three CRPPs were also subjected to extrusion at a die temperature of 160°C. Their extrusion curves were compared as shown in Fig. 6.13.

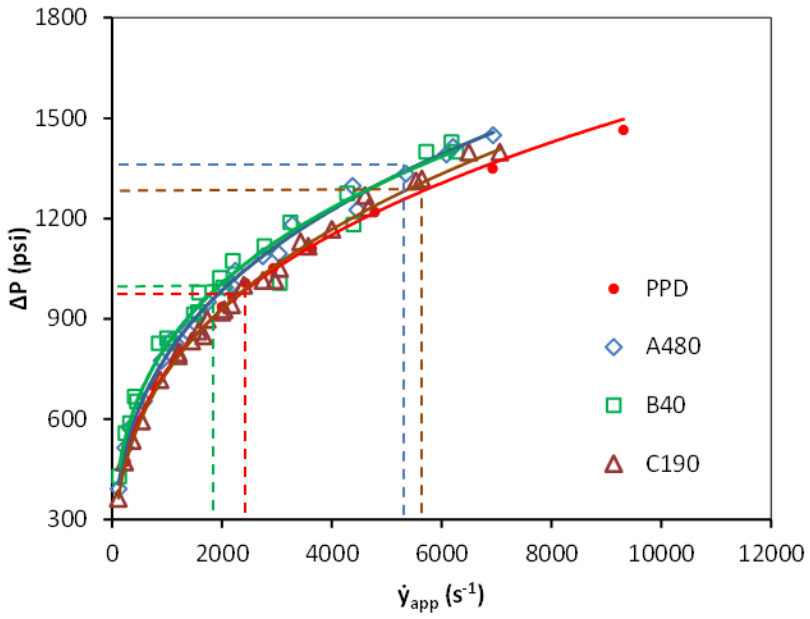

Fig.6.13 Extrusion curves of CRPPs with similar MFR at a die temperature of 160°C.

Table.6.5 Onset conditions for melt fracture during extrusion of CRPPs with similar MFR.

Sample	$\dot{\gamma}_{app}(s^{-1})$	P_0(psi) [a]	ΔP(psi) [a]	σ_w(MPa) [b]	η_0(Pa*s)[c]	ModSep@500Pa[c]
PPD	2194	964	892	-0.17	794	7.31
A480	5350	1333	4949	-0.95	1486	5.42
B40	1968	1022	1821	-0.35	1046	6.62
C190	5642	1318	5219	-1.00	1638	4.64

(a&b, see the remarks below Table.6.4. c, the zero-shear viscosity η_0 and the ModSep@500Pa listed here for the sake of comparison of their molecular weight and MWD. The η_0 were obtained from Carreau-Yasuda model fitting on the data from frequency sweep tests.)

It can be seen that all these materials exhibit similar pressure curves. The onset conditions for melt fracture of these CRPPs are shown in Table 6.5.

Comparing the onset conditions for melt fracture of B40 and B100, which both have similar PDI (see ModSep@500Pa), we can find that higher molecular weight (B40) resulted in lower onset shear rates. However, the onset shear stress was increased due to higher viscosity. In addition, from section 6.4.1 we learned that broad MWD (at fixed M_w level) increases the onset shear rate as well as the onset shear stress. The effect of molecular weight on the onset condition of melt fracture of the CRPPs can be summarized as Table.6.6.

Table.6.6 Effect of molecular weight characteristics on the onset conditions of CRPPs.

Factor	$\dot{\gamma}_{app}$ (onset)	σ_w (onset)	Factor of CRPPs in order
PDI↑	↑	↑	C190>A480>B40>PPD
M_w↑	↓	↑	C190>A480>B40>PPD

The onset shear stress results in Table 6.5, following an order as σ_w(C190)> σ_w(A480)> σ_w(B40) > σ_w(PPD), verify the conclusion in Table 6.6 as both M_w and MWD increase the onset shear stress. As Mw and PDI have opposite effects on the onset shear rate, C190 and A480 (produced from ZN-PP and having higher M_w and broader MWD), exhibited melt fracture at shear rates lower than PPD but higher than B40.

Chapter 7

CONCLUSIONS AND RECOMMENDATIONS FOR FUTURE WORK

7.1 CRPPs Produced from ZN-PP and mPP

Controlled rheology polypropylene (CRPP) technology was originally developed for modifying conventional Ziegler-Natta type polypropylene (ZN-PP) which usually has high molecular weight (MW) and high viscosity. Peroxide-induced random scission of the polypropylene chains is the most common method used for this process, and resins with lower molecular weight and corresponding narrower molecular weight distribution (MWD) are produced. In this work, metallocene type polypropylene (mPP), having narrow MWD, was treated with this technique in a modeling and experimental study.

Modeling results suggested that both mPP and ZN-PP will approach the "most probable distribution" with a polydispersity index (PDI) of 2 along the random degradation process by increasing the peroxide concentration. CRPPs produced from mPP exhibited MWDs with approximately constant PDI with average molecular weights decreasing with increasing peroxide concentration. Based on this observation, it is feasible to produce CRPPs by employing commodity mPP and ZN-PP resins.

In the experimental part of this work, materials from both origins were employed and tailor-made CRPPs were successfully produced having similar weight average molecular weights (but different MWD) or similar melt flow rate (MFR). With respect to the production of the first CRPP series, rheological data derived from oscillatory frequency sweep tests were properly

treated to monitor the molecular weight level as well as quantify the MWD without the need for time consuming high temperature GPC measurements. For the second group of CRPPs, the melt flow rate (MFR) test was adopted as this is one of the most popular specifications in the plastics industry owing to its convenience and important guiding significance to processing.

In conclusion, by peroxide-induced CRPP technique, certain PPs with tailor-made properties such as molecular weight and its distribution as well as rheological characters can be made from the two types of polypropylenes, ZN-PP or mPP, involving different molecular distribution evolution within the random scission process.

7.2 Extrusion Performance of CRPPs and their Rheological Properties

The two groups of CRPPs were subjected to single screw extrusion through a capillary die to study the flow curves and analyze the extrudate surface characteristics. Their flow behaviors were investigated by considering the rheological characterization in order to associate it with their extrusion results for interpretation.

Regarding the CRPPs with similar MW, broader MWD induces stronger shear-thinning which is thought to be responsible for the lower extrusion pressure at the same apparent shear rate. The increased breadth of MWD also leads to higher onset shear rate point for melt fracture, which coincides with previous observations from Baik and Tzoganakis [22] (however, their study was not based on CRPPs with the same MW unlike this work). Also, slightly higher onset shear stress at the die wall was observed for the CRPPs with broader MWD.

Concerning the CRPPs with similar MFR (but not the same MW and MWD), they exhibited similar pressure curves which can be attributed to the similar viscosities at a certain high shear stress range. Although CRPPs produced from ZN-PP have higher MW, their broader MWDs endow them with stronger shear-thinning at higher shear rate, thus they can present similar MFR with the CRPPs produced from mPP. As both MW and PDI promote the onset point of shear stress for melt fracture, critical shear stress values of the CRPPs made from ZN-PP were significantly higher than those of the CRPPs made from mPP. The contrast effect of MW and PDI on the onset shear rate make the melt fracture of CRPPs made from ZN-PP occur at slightly lower shear rates than of the reference mPP.

7.3 Recommendations for Future Work

On the basis of the extrusion study of the tailor-made CRPPs in this work, one of the main potential future efforts should focus on a more detailed study of melt fracture characteristics using dies of various L/D to estimate the Bagley corrections and consider the effect of pressure on viscosity.

In addition, the success of the production of tailor-made CRPPs from different origins provides a way to make polypropylenes with same MW but different MWDs, or even complex molecular weight composition patterns. Such a special series of materials can be applied to other flow phenomena studies, e.g. flow induced crystallization or flow-induced fractionation, by comparing their rheological characteristics. The established modeling program can be used to predict the required dosage of peroxide for CRPP production. Moreover, CRPPs having bimodal

distributions may be produced by employing mixtures of mPP and ZN-PP. This could be studied easily through numerical simulations but should be verified experimentally.

REFERENCES

1. Dealy, J. M., Wissbrun, K. F., *Melt Rheology and its role in Plastics Processing*, Van Nostrand-Reinhold, New York, (1989).

2. Bloor, J. Jr., *Ziegler-Natta catalysts and polymerization*, Academic Press, New York (1979).

3. Odian, G., *Principles of Polymerization*, John Wiley and Sons, New York (1981).

4. G.Natta, "Kinetic Studies of α-Olefin Polymerization," J.Polym.Sci, 34, 21-48 (1959).

5. Tzoganakis, C., Vlachopoulos, J., Hamielec, A. E., "Production of controlled-rheology polypropylene resins by peroxide promoted degradation during extrusion," Polym. Eng. Sci. 28(3), 170-180 (1988).

6. Psarreas, A., *Nitroxide-Mediated Controlled Degradation of Polypropylene*, Master Thesis (2006).

7. Kowalski, R. C., "Controlled Rheology PP Resins," *In History of Polyolefins*, Springer Netherlands, p.307-318 (1986).

8. Xanthos, M., *Reactive Extrusion: Principles and Practice*, Hanser Publishers, Oxford Univ. Press, New York (1992).

9. Kowalski, R.C., *Molten Polymer Elasticity*, Ph.D. Thesis, Polytechnic Institute of Brooklyn(1963).

10. Harrison, J. W., Keller, J. P., Kowalski, R. C., Staton, J. C., "Controlled degradation of polypropylene in extruder-reactor" U.S. Patent No. 3,608,001. Washington, DC(1971).

11. Bartz, K. W., Steinkamp, R. A., Watson, A. T., Wilder, H. L., "Process for controlling rheology of polyolifens" U.S. Patent No. 3,898,209. Washington, DC (1975).

12. Peterson, J. D., Vyazovkin, S., Wight, C. A., "Kinetics of the thermal and thermo-oxidative degradation of polystyrene, polyethylene and poly (propylene)," Macromol. Chem. Phys., 202(6), 775-784 (2001).

13. Nakatani, H., Suzuki, S., Tanaka, T., Terano, M., "New kinetic aspects on the mechanism of thermal oxidative degradation of polypropylenes with various tacticities," Polymer, 46(26), 12366-12371(2005).

14. Nowak, R.M., Jones., J.D., "Graft copolymers of polyolefins and acrylic and methacrylic acid and method of making the same," U.S. Patent No. 3,177,269. (1965).

15. Grail, T.J., Steinkamp, R.A., "Polymers with improved properties and process therefor," U.S. Patent No. 3,862,265. (1975).

16. David, C., Baeyens-Volant, D. "Statistical theories of main chain scission and crosslinking of polymers-application to the photolysis and radiolysis of polystyrene studied by gel permeation chromatography," Euro. Polym. J., 14(1), 29-38(1978).

17. Hudec, P., Obdržálek, L., "The change of molecular weights at peroxide initiated degradation of polypropylene," Angew. Makrom. Che., 89(1), 41-45(1980).

18. Tzoganakis, C., Vlachopoulos, J., Hamielec, A. E., "An Experimental and Numerical Investigation of Peroxide Initiated Degradation of Polypropylene in a Single Screw Extruder," Polym.Proc.Soc., 2nd Annual Meeting, Montreal, Canada, April (1986).

19. Tzoganakis, C., *Peroxide Degradation of Polypropylene During Reactive Extrusion*, PhD. Thesis, McMaster University(1988).

20. Barakos, G., Mitsoulis, E., Tzoganakis, C., Kajiwara, T., "Rheological characterization of controlled-rheology polypropylenes using integral constitutive equations," J. Appl. Polym.Sci., 59(3), 543-556(1996).

21. Baik, J. J., Tzoganakis, C., "A study of extrudate distortion in controlled-rheology polypropylenes," Polym. Eng. Sci., 38(2), 274-281(1998).

22. Pearson, D. S., Helfand, E., " Viscoelastic properties of star-shaped polymers," Macromolecules, 17(4), 888-895 (1984).

23. McLeish, T. C. B., Larson, R. G., "Molecular constitutive equations for a class of branched polymers: The pom-pom polymer," J. Rheol. 42, 81-110(1998).

24. Auhl, D., Stange, J., Münstedt, H., Krause, B., Voigt, D., Lederer, A., Lunkwitz, K., "Long-chain branched polypropylenes by electron beam irradiation and their rheological properties," Macromolecules, 37(25), 9465-9472(2004).

25. Krause, B., Stephan, M., Volkland, S., Voigt, D., Häußler, L., Dorschner, H., "Long-chain branching of polypropylene by electron-beam irradiation in the molten state," J. Appl. Polym.Sci., 99(1), 260-265(2006).

26. Tzoganakis, C., Vlachopoulos, J., Hamielec, A. E., "Controlled degradation of polypropylene," Chem. Eng. Pro., 84(11), 47-49(1988).

27. Tzoganakis, C., Tang, Y., Vlachopoulos, J., & Hamielec, A. E., "Controlled degradation of polypropylene: a comprehensive experimental and theoretical investigation," Polym. Plas. Tech. Eng., 28(3), 319-350(1989).

28. Suwanda, D., Lew, R., Balke, S. T., Paper presented at the 36th Canadian Chem. Eng. Conf., Sarnia, Ontario, Canada (1986).

29. Tzoganakis, C., Tang, Y., Vlachopoulos, J., Hamielec, A. E., "Measurements of residence time distribution for the peroxide degradation of polypropylene in a single-screw plasticating extruder," J. Appl. Polym.Sci., 37(3), 681-693(1989).

30. Tzoganakis, C., Vlachopoulos, J., Hamielec, A. E., Shinozaki, D. M., "Effect of molecular weight distribution on the rheological and mechanical properties of polypropylene," Polym. Eng. Sci., 29(6), 390-396(1989).

31. Tzoganakis, C., Tang, Y., Vlachopoulos, J., & Hamielec, A. E., "Controlled degradation of polypropylene: a comprehensive experimental and theoretical investigation," Polym.-Plas. Tech. Eng., 28(3), 319-350(1989).

32. Scorah, M. J., Zhu, S., Psarreas, A., McManus, N. T., Dhib, R., Tzoganakis, C., Penlidis, A. "Peroxide-controlled degradation of polypropylene using a tetra-functional initiator," Polym. Eng. Sci., 49(9), 1760-1766(2009).

33. Black, R. M., Lyons, B. J., "Effect of high-energy radiation on polypropylene," Nature, 1346-1347 (1957).

34. Schnabel, W., Dole, M., "Radiation chemistry of isotactic and atactic polypropylene I: Gas evolution and gel studies," J.Phy.Chem., 67(2), 295-299(1963).

35. Lugao, A. B., Otaguro, H., Parra, D. F., Yoshiga, A., Lima, L. F. C. P., Artel, B. W. H., Liberman, S., "Review on the production process and uses of controlled rheology polypropylene—Gamma radiation versus electron beam processing," Radiat. Phys. Chem., 76(11), 1688-1690(2007).

36. He, G., Tzoganakis, C., "A UV-initiated reactive extrusion process for production of controlled-rheology polypropylene," Polym. Eng. Sci., 51(1), 151-157(2011).

37. Psarreas, A., Tzoganakis, C., McManus, N., Penlidis, A., "Nitroxide-mediated controlled degradation of polypropylene," Polym. Eng. Sci., 47, 2118-2123(2007).

38. Psarreas, A., *Nitroxide-mediated controlled degradation of polypropylene.* Master thesis, University of Waterloo (2006).

39. Auhl, D., Stange, J., Münstedt, H., Krause, B., Voigt, D., Lederer, A., Lunkwitz, K., "Long-chain branched polypropylenes by electron beam irradiation and their rheological properties," Macromolecules, 37(25), 9465-9472(2004).

40. Krause, B., Voigt, D., Häuβler, L., Auhl, D., Münstedt, H., "Characterization of electron beam irradiated polypropylene: Influence of irradiation temperature on molecular and rheological properties," J. Appl. Polym.Sci., 100(4), 2770-2780(2006).

41. Pearson, D. S., Helfand, E., "Viscoelastic properties of star-shaped polymers," Macromolecules, 17(4), 888-895(1984).

42. McLeish, T. C. B., Larson, R. G., "Molecular constitutive equations for a class of branched polymers: The pom-pom polymer," J. Rheol., 42(1), 81-110(1998).

43. Lucas, B. M., Krishnamurthy, V., Bonser, J. R., "Propylene compositions with improved resistance to thermoforming sag." U.S. Patent No. 5,439,949. Washington, D.C.(1995).

44. Lugão, A. B., Hutzler, B., Ojeda, T., Tokumoto, S., Siemens, R., Makuuchi, K., Villavicencio, A. L. C. , "Reaction mechanism and rheological properties of polypropylene irradiated under various atmospheres," Radiat. Phys. Chem., 57(3), 389-392(2000).

45. Lugão, A. B., Artel, B. W. H., Yoshiga, A., Lima, L. F. C. P., Parra, D. F., Bueno, J. R., Otaguro, H., "Production of high melt strength polypropylene by gamma irradiation," Radiat. Phys. Chem., 76(11), 1691-1695(2007).

46. Carlsson, D. J., Wiles, D. M., "The photooxidative degradation of polypropylene, part I. photooxidation and photoinitiation processes," J. Macromol. Sci. R. M. C. 14(1), 65-106(1976).

47. Qu, B., Xu, Y., Ding, L., Rånby, B., "A new mechanism of benzophenone photoreduction in photoinitiated crosslinking of polyethylene and its model compounds," J. Polym. Sci. Pol. Chem., 38(6), 999-1005(2000).

48. Harper, D. J., McKellar, J. F., "Mechanism of the benzophenone-sensitized photodegradation of polypropylene," J. Appl. Polym.Sci., 17(11), 3503-3508(1973).

49. Sardashti, P., Tzoganakis, C., Polak, M. A., Penlidis, A., "Radiation Induced Long Chain Branching in High-Density Polyethylene through a Reactive Extrusion Process," Macromol. Reac. Eng., 8(2), 100-111(2014).

50. Zeichner, G. R., Patel, P. D., "A comprehensive evaluation of polypropylene melt rheology," In Proceedings 2nd world congress of Chem. Eng., Montreal, Canada, p.333 (1981).

51. Bafna, S. S., "Is the cross-over modulus a reliable measure of polymeric polydispersity?" J. Appl. Polym.Sci., 63(1), 111-113(1997).

52. Yoo, H. J., "MWD determination of ultra-high MFR polypropylene by melt rheology," Adv. Poly. Sci., 13(3), 201-205(1994).

53. Liu, S. L., Amundson, N. R., "Calculation of molecular weight distributions in polymerization," Chem. Eng. Sci., 17(10), 797-802(1962).

54. ulburt, H. M., Katz, S., "Some problems in particle technology: A statistical mechanical formulation," Chem. Eng. Sci., 19(8), 555-574(1964).

55. Dickson, S. B., Tzoganakis, C., Budman, H., "Reactive extrusion of polypropylene with pulsed peroxide addition: process and control aspects," Ind. Eng. Chem. Res., 36(4), 1067-1075(1997).

56. Thompson, M. R., Tzoganakis, C., Rempel, G. L., "Alder Ene functionalization of polypropylene through reactive extrusion," J. Appl. Polym.Sci., *71*(3), 503-516(1999).

57. Suwanda, D., Lew, R., Balke, S. T., "Reactive extrusion of polypropylene I: Controlled degradation," J. Appl. Polym.Sci., *35*(4), 1019-1032(1988).

58. Suwanda, D., Lew, R., Balke, S. T., "Reactive extrusion of polypropylene II: Degradation kinetic modeling," J. Appl. Polym.Sci., *35*(4),1033-1048(1988).

59. Kotliar, A. M., "Evaluation of molecular weight averages resulting from random crosslinking and chain scission processes for wide schulz-zimm distributions," J. Polym. Sci.: General Papers, 1(10), 3175-3182(1963).

60. Boyd, R. H., Lin, T. P., "Theoretical depolymerization kinetics III: the effect of molecular-weight distribution in degrading polymers undergoing random-scission initiation," J. Chem. Phys., 45(3), 778-781(1966).

61. Shroff, R., Mavridis, H., "New measures of polydispersity from rheological data on polymer melts," J. Appl. Polym.Sci., 57,1605-1626 (1995).

62. Yoo, H. J., "MWD determination of ultra-high MFR polypropylene by melt rheology. Adv. Poly. Sci., 13(3), 201-205(1994).

63. Maier, C., Calafut, T., *Polypropylene: The Definitive User's Guide and Databook*, Plastics Design Library, New York (1998).

64. Brintzinger, H. H., Fischer, D., Mulhaupt, R., Rieger, B., Waymouth, R. M., "Metallocene Catalysts for Stereoregular Polymerization," Angew. Chem. Int. Ed, 34, 1143(1995).

65. Koopmans, R., Den Doelder, J., Molenaar, J., *Polymer Melt Fracture*. CRC Press (2010).

66. Tordella, J. P., "Fracture in the extrusion of amorphous polymers through capillaries," J. Appl. Phys., 27(5), 454-458(1956)..

67. Agassant, J. F., Arda, D. R., Combeaud, C., Merten, A., Muenstedt, H., Mackley, M. R., Vergnes, B., "Polymer processing extrusion instabilities and methods for their elimination or minimization," Int. Polym. Proc., 21(3), 239-255(2006).

68. Doelder, D. C., *Design and implementation of polymer melt fracture models*, Doctoral dissertation, Technische Universiteit Eindhoven(1999).

69. Combeaud, C., Demay, Y., Vergnes, B., "Experimental study of the volume defects in polystyrene extrusion," J. Non-Newtonian Fluid Mech., 121(2), 175-185(2004).

70. Tordella, J.P., "Melt fracture-extrudate roughness in plastic extrusion," SPE J., 36-40 (1956).

71. Cogswell, F. N. "Stretching flow instabilities at the exits of extrusion dies J. Non-Newtonian Fluid Mech., 2(1), 37-47(1977).

72. Gogos, C. G., Maxell, B., "Velocity profiles of the exit region of molten polyethylene extrudates," Polym. Eng. Sci., 6(4), 353-358(1966).

73. Wang, S. Q., Drda, P. A., "Superfluid-like stick-slip transition in capillary flow of linear polyethylene melts. 1. General features," Macromolecules, 29(7), 2627-2632(1996).

74. Barone, J. R., Plucktaveesak, N., Wang, S. Q., "Interfacial molecular instability mechanism for sharkskin phenomenon in capillary extrusion of linear polyethylenes," J. Rheo. 42(4), 813-832(1998).

75. Hatzikiriakos, S. G., Stewart, C. W., Dealy, J. M., "Effect of surface coatings on wall slip of LLDPE," Int. Polym. Proc., 8(1), 30-35(1993).

76. Bartos, O. "Fracture of polymer melts at high shear stress," J. Appl. Phys., 35(9), 2767-2775(1964).

77. Ui, J., Ishimaru, Y., Murakami, H., Fukushima, N., Mori, Y., "Study of flow properties of polymer melt with the screw extruder," Polym. Eng. Sci., *4*(4), 295-305(1964).

78. Ballenger, T. F., Chen, I. J., Crowder, J. W., Hagler, G. E., Bogue, D. C., White, J. L., "Polymer melt flow instabilities in extrusion: investigation of the mechanism and material and geometric variables," T.Sco.Rheol., 15(2), 195-215(1971).

79. Honerkamp, J., Weese, J. "A nonlinear regularization method for the calculation of relaxation spectra," Rheol. Acta, 32(1), 65-73(1993).

80. Amintowlieh, Y, *Rheological Modification of Polypropylene by Incorporation of Long Chain Branches Using UV Radiation*, PhD. thesis, University of Waterloo (2014).

81. Amintowlieh, Y., Tzoganakis, C., Hatzikiriakos, S.G., Penlidis, A. "Effects of processing variables on Polypropylene degradation and long chain branching with UV irradiation,' Polym. Deg. and Stab., 104, 1-10(2014).

82. Amintowlieh, Y., Tzoganakis, C., Penlidis, A. "The effect of depth and duration of UV radiation on polypropylene modification via photoinitiation," J. Appl. Polym. Sci., 131, 41021-41032(2014).